www.directivepublications.org

The Journal of Anatomy

ISSN 2995-6552

Research Article

The Cardiac Fulcrum.

Jorge C. Trainini, Mario A. Beraudo, Mario Wernicke, Alejandro Trainini.

Affiliations

1. *Formed Head of the Cardiovascular Surgery Service and Director of the Presidente Perón Hospital, Avellaneda, Buenos Aires, Argentina. Honorary Professor, National University of Avellaneda (UNDAV), Buenos Aires, Argentina. Formed President of the Argentina College of Cardiovascular Surgeons.*
2. *Cardiovascular surgeon. Clínica Güemes, Luján, Buenos Aires, Argentina.*
3. *Pathologist, Clínica Güemes, Luján, Buenos Aires, Argentina.*
4. *Cardiovascular surgeon. Hospital Presidente Perón , Avellaneda, Buenos Aires, Argentina. Hospital Posadas, Haedo, Buenos Aires, Argentina.*

Abstract

Objective: The cardiac muscle cannot be anatomically free in the thorax and without a support to fulfill its hemodynamic function. Therefore, the possibility of the existence of a support point acting as a lever was analyzed.
Material and methods: A total of 77 hearts from the morgue and slaughterhouses were used:
a. 56 from two-year-old bovids weighing between 1300-1900 g (average 1650 g);
b. 17 human (three from 8-, 16-, and 23-week gestation embryos, respectively; four from 30- and 36-day, and 10 and 27-week infants; two from 4-year-old and 10-year- old children; and eight from adults with an average weight of 300 g);
c. 4 from pigs (400 g).
Anatomical, histological, histochemical and radiological studies were carried out. The heart was fixed in 10% buffered formalin. Histological studies were done using hematoxylin-eosin and Masson's trichrome staining techniques and four-micron sections. Immunomarking (s100-neurofilaments) was also performed.
The myocardial band was unwound completely. The myocardial band was uncoiled in its entirety. The extracted pieces were analyzed for anatomy and histology. The investigation was completed with simple radiographic imaging studies, magnetic resonance imaging and computed tomography.
Results: In anatomical investigations we have found in all human and bovine hearts studied a nucleus underlying the right trigone of bone-chondroid-tendinous histological structure. Microscopic analysis revealed in bovine hearts a trabecular osteochondral matrix [fulcrum]. In all human hearts the fulcrum was found to be formed by chondroid tissue. In this structure, not described by other authors, the origin and end of the myocardial fibers have muscular insertion. Imaging techniques confirmed its existence.
Conclusions: The cardiac fulcrum found in the anatomical investigation of human and bovine hearts would clarify about the necessary fulcrum of the myocardial muscle to complete its twisting movements.

Keywords: heart; cardiac anatomy; myocardium; myocardial support; cardiac anatomy; myocardium; myocardial support

CHAPTER 1

THE CARDIAC FULCRUM, SUPPORT OF THE MYOCARDIUM

a.The crucial question

The inevitable question arose from the beginning of the investigation. (80). In order to twist, the muscular segments constituting the myocardial helicoid and forming the ventricular chambers should twist on a point of support in the same way as a skeletal muscle does on a firm insertion; is there any in the heart? If this support is real, how does the myocardium insert into this structure? This topic became an essential concern in our reflections. It was logical to speculate that its helical disposition and the remarkable physiological characteristics of the myocardium requires it to have a point of support in order to fulfill its function as an ejection (torsion) and suction (detorsion) pump. The heart has a size equivalent to a human fist and an average weight of 270 grams; it propels a quantity of blood that ranges from 4 to 6 liters/minute at a speed of 200 cm/s. It also has a consumption of only 10 watts, works continuously for 80 years without maintenance and almost without noise, producing 100 000 beats per day. Its task is equivalent to extracting from a depth of 1 m 1 ton of water per day with a mechanical efficiency (work/energy ratio) of 50%, not attained by man-made machines, which

***Corresponding Author:** **Jorge C. Trainini,** Formed Head of the Cardiovascular Surgery Service and Director of the Presidente Perón Hospital, Avellaneda, Buenos Aires, Argentina. Honorary Professor, National University of Avellaneda (UNDAV), Buenos Aires, Argentina. Formed President of the Argentina College of Cardiovascular Surgeons, Argentina. **Email:** jctrainini@hotmail.com.
Received: 07-January-2026, Manuscript No. TJOA - 5359 **; Editor Assigned:** 09-January-2026 **; Reviewed:** 02-February-2026, QC No. TJOA - 5359 **;**
Published: 28-February-2026, **DOI:** 10.52338/tjoa.2026.5359.
Citation: Jorge C. Trainini. The Cardiac Fulcrum. The Journal of Anatomy. 2026 February; 15(1). doi: 10.52338/tjoa.2026.5359.
Copyright © 2026 **Jorge C. Trainini.** This is an open access article distributed under the Creative Commons Attribution License, which permits unrestricted use, distribution, and reproduction in any medium, provided the original work is properly cited.

reach 30%. Its efficiency allows 70% of the left ventricular content to be ejected with only 12% shortening of its contractile unit, the sarcomere.

We finally achieved our objective by finding in all the dissected bovine, porcine and human hearts, a solid structure whose histological conformation is different according to the specimens analyzed, presenting itself as bone or chondroid tissue. We also observed that both the muscle fibers of the right segment (initial insertion) and those of the ascending segment (final insertion) are tethered to this myocardial support. Thus, the ventricular myocardium is made up of a set of muscle fibers twisted around themselves, resembling a rope (cord model), flattened into a "band." This, by spiraling twice, defines a helix that delimits the two ventricles and determines their functionality (**Figure 1**) (16,84), holding the myocardium at its origin and end at the *cardiac fulcrum*.

Figure 1. Helical myocardium in the cord model that simplifies the spatial structure.

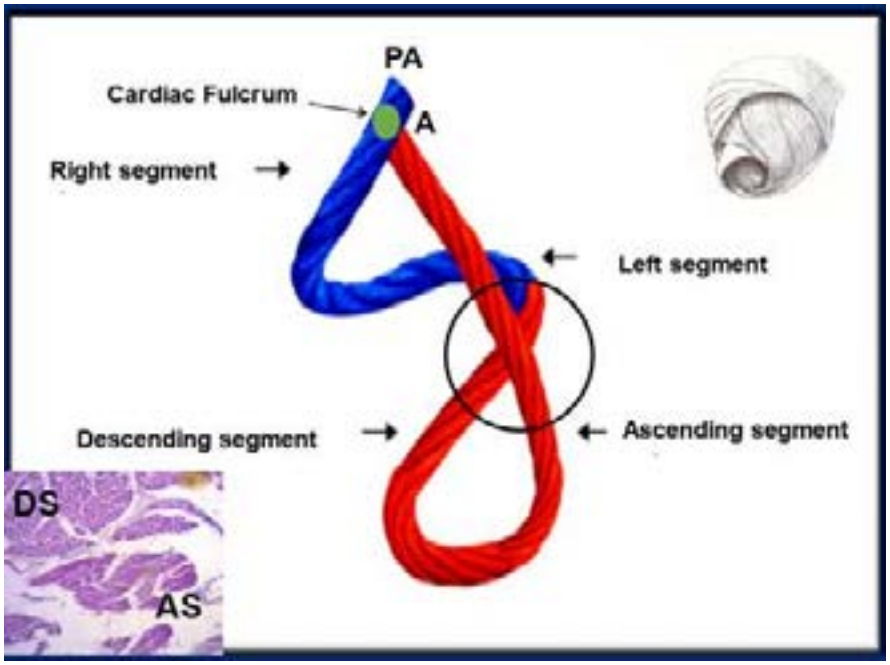

The figure shows the different segments forming it. In blue: basal loop. In red: apical loop. PA: location of the pulmonary artery; A: location of the aorta. The location of the heart's support, called the fulcrum, is shown. The figure in the right angle illustrates the three- dimensional arrangement of the continuous myocardium. Histology (left inset) details the different orientation of the longitudinal fibers (ascending segment, AS) in relation to the descending fibers (transverse fibers, DS). Given the different orientations of the fibers, the area marked with the black circle corresponds to the beginning of the opposite helical movement that produces myocardial torsion.

Cardiac anatomo-functionality in classical concepts entails an organizational deficit in the location and physiology of its integrating components. Consequently, the description in the real spatial dimension of the heart, definitely formed by a helical myocardium, solves not only the three- dimensional morphological aspect, but also the cardiomechanics and the diagnostic and therapeutic perspectives of the heart. For this task, it was necessary to establish complex links between medical concepts and other disciplines, especially mechanics, in order to elucidate the natural phenomena of the central organ of circulation, clearly a hydraulic pump.

We are aware that this research journey is subject to reflections that lead to new therapeutic possibilities. As expressed in the prologue by Prof. Miguel Angel Garcia Fernandez of the Faculty of Medicine of the Complutense University of Madrid, in the last installment of this research, published under the name "*Anatomy and Organization of the Helical Heart*" (73) in 2023 and presented in Madrid and London, this project is similar to the ascent of a peak, not yet climbed, which is unknown and steep. Therefore, on too many occasions it is not unusual for us to have found ourselves lost, disoriented, but always ready to return to the path to continue the ascent in the understanding of the findings that we were painstakingly achieving.

It was necessary to understand that medical knowledge, like all science, is a cultural production. This determines that the imposition of changes that attempt to transcend the prevailing situation is a difficult process. Alfred Whitehead (1861-1947) forcefully denounced this difficulty in the evolution of ideas. That is why he expressed: "*In its plenitude, every system is a triumphant success; in its decadence, it is a hindrance*".(89) Therefore, a theory needs the idea, the project, the language and finally the politics as an element of power and resources to materialize and spread its hypothesis. Faced with this human reality, we have always been convinced that between the external phenomenon and the sensation that reaches the consciousness there is always a delay, a waiting time to understand the non-objective reality that science has.

The true secret of cardiac mechanics lies deep within the myocardium. The cardiac muscle at first glance does not show its most hidden treasure. Only with proper dissection the mystery is revealed and the *cardiac fulcrum*, that is, the support of the myocardium, emerges from within the muscle fibers (64,79). It is an osteochondral anatomical piece that links the continuous myocardium at its ends and allows it to perform its work of strength and maintain its spiral arrangement (64). It is a stabilizer of cardiac function, a support that allows it to perform torsion/detorsion, helical movements, and a point of support with the lever functionality that every muscle needs. This myocardium with its helical structure explains a large part of cardiac pathophysiology. The beginning of this mystery led us to delve into more complex paths and evaluate a heart with three energetic times, the third being an intermediate stage between systole and diastole (**Figure 2**), the protodiastolic phase of myocardial contraction (PPMC), which is followed by the passive filling phase (diastole) (85,87). The path in search of the cardiac support was full of foreseen and random circumstances. In truth, it was difficult for us to accept what had been found, despite our obsessive search for it, and even more so to encourage us to spread it (72,74-76). We always kept in mind the words of Anaximander of Miletus (6th century B.C.): "*From where the beginning of things comes, there also lies the cause of their dissolution, for by virtue of a necessary law they must reciprocally pay and expiate the guilt and the penalty of injustice in the order of time*".(83).

Figure 2. Left ventricular ejection and suction phases. ISP: isovolumetric systolic phase; P+: positive pressure; P-: negative pressure; PPMC: protodiastolic phase of myocardial contraction.

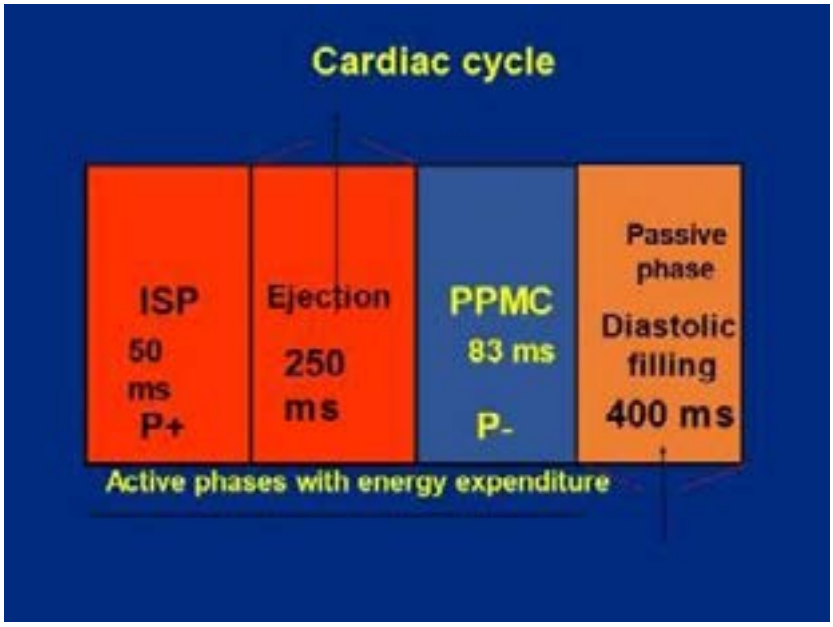

b.Anatomic dissection of the myocardium

Material and Methods

A total of 77 hearts from the morgue and slaughterhouses were used:

a. 56 from two-year-old bovids weighing between 1300-1900 g (average 1650 g);
b. 17 human (three from 8-, 16-, and 23-week gestation embryos, respectively; four from 30- and 36-day, and 10 and 27-week infants; two from 4-year-old and 10-year-old children; and eight from adults with an average weight of 300 g);
c. 4 from pigs (400 g).

Anatomical, histological, histochemical and radiological studies were carried out. The heart was fixed in 10% buffered formalin. Histological studies were done using hematoxylin-eosin and Masson's trichrome staining techniques and four-micron sections. Immunomarking (s100- neurofilaments) was also performed (22).

Dissection technique

The heart to be dissected was boiled in water with acetic acid (15 cc per liter) for two hours. This step allowed the myocardium to be free of fatty deposits, making dissection easier and more detailed. Then the aorta and pulmonary artery were cut about three centimeters from their origin separating the attachment between them and, subsequently, a longitudinal incision was done at the level of the anterior interventricular sulcus, on the superficial fibers extending transversally along the anterior wall of the ventricles (interband or aberrant fibers) (**Figure 3**) (40,46,50). Between the atria and the ventricles there is simply connective tissue, which implied the easy separation of these chambers given the denaturation produced by heat. This assertion coincides with Claudius Galen's theory in the II century AD. (83) stating that the atria can be detached from the ventricles without any incision, simply separating them from their respective ventricles. This fact is understandable since in the evolutionary

process, the horizontal arrangement of the atria (dependence chambers of the venous semicircle) became attached to the ventricular muscle component (chambers dependent on the arterial semicircle), their origins therefore being different. Thus, the single atrium in fish became the right atrium in mammals, while the single ventricle became the left atrium. Both atria then represent strategic vestiges of the venous segment in the primitive circulatory duct of fishes.

Figure 3. Interband fibers (IBF). PA: pulmonary artery; RM: Right margin; LM: Left margin; AIS: Anterior interventricular sulcus. Interband fibers are shown as they pass from the left ventricle to the right ventricle.

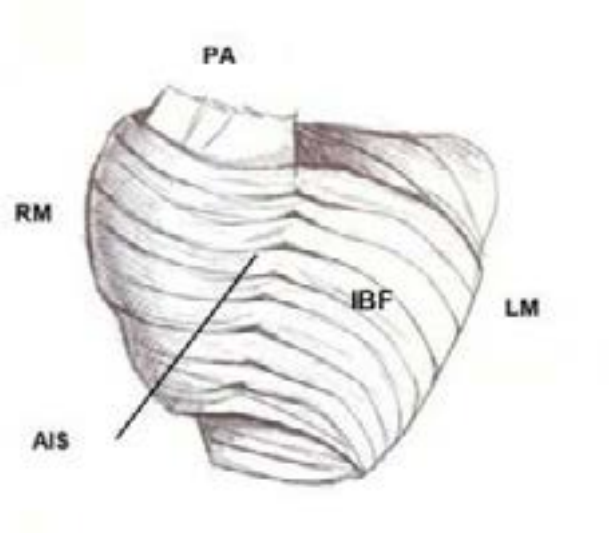

There is a fundamental fact at the beginning of the unfolding, since any attempt not to respect the axes where the myocardium folds during dissection causes a rupture of the cardiac mass.

It must be understood that the overlapping segments are intimately attached to each other in order to establish high performance behavior. This situation, without knowledge of the helical structure of the heart, had already been observed by Andreas Vesalius in his 1543 publication "*De Humanis Corporis Fabrica*" (83).

The key maneuver to unfold the myocardium consists in entering the anterior interventricular sulcus (**Figure 4**) with a blunt instrument, leaving on the left side of the operator the end of the myocardium corresponding to the pulmonary artery and its continuity with the right ventricular free wall (right segment). The upper portion of the right ventricular cavity is lined by the pulmo-tricuspid cord, which allows the pulmonary artery to be positioned anteriorly and to the left of the aorta in order to form the helix. The pulmonary tricuspid cord should be considered a band between the pulmonary ring and the tricuspid valve, parallel to the aortic ring, and is constituted by a crossing of the muscle fibers between the anterior septal band and the septal band (also called the bridge), belonging to the right ventricle (**Figure 5**).

Figure 4. Cleavage plane (red line) to initiate ventricular unfolding (bovine heart)

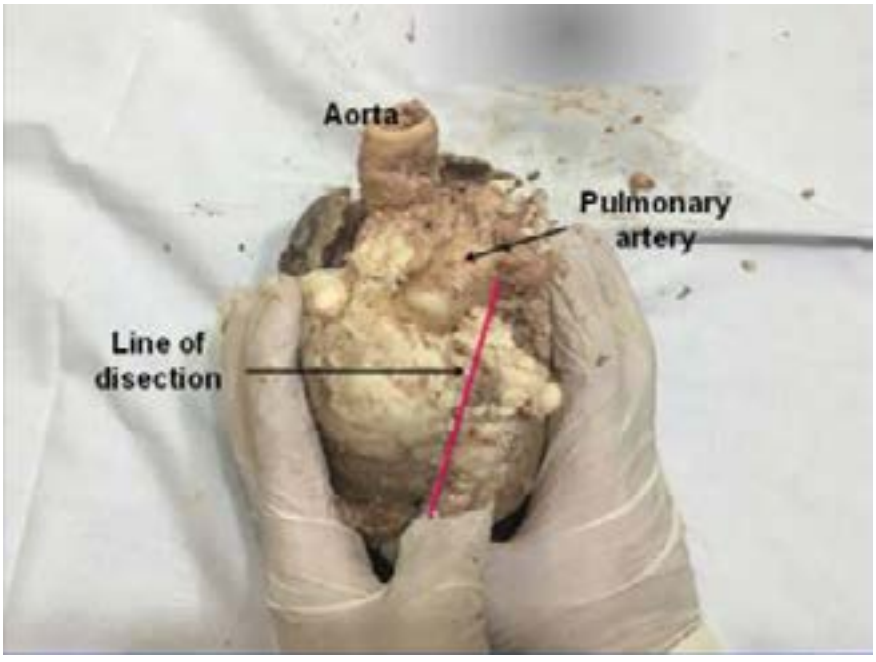

Figure 5. The pulmo-tricuspid cord (ptc) between the tricuspid orifice (TO) and the pulmonary artery (PA) is seen in detail. The circle marks the site of the cardiac fulcrum (CF) that is visualized when the pulmonary artery and the pulmo-tricuspid cord are removed from their apposition at the beginning of unfolding. The right coronary artery (rca) has been sectioned to show the course of the pulmo-tricuspid cord. A: aorta (bovine heart).

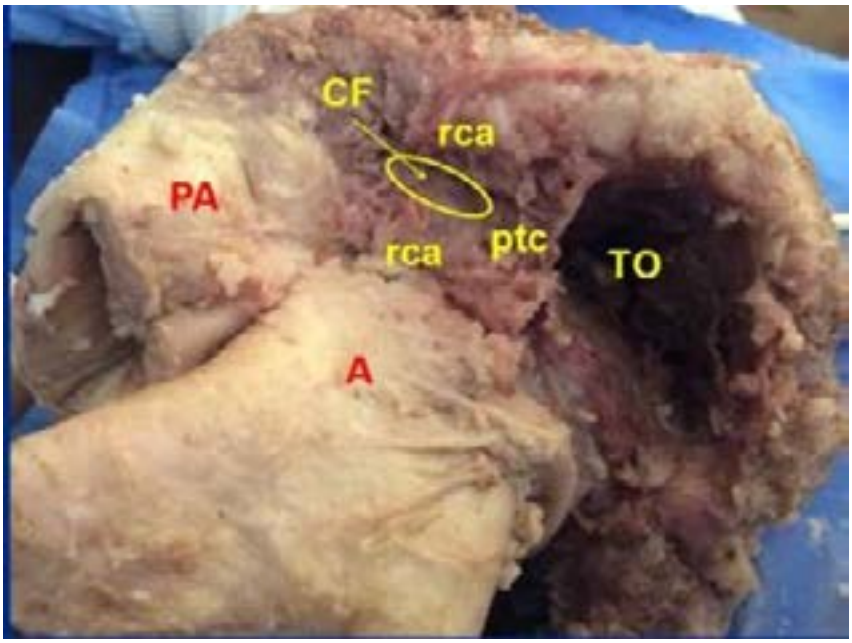

Next, traction is applied towards the same left side, completely releasing the pulmonary artery from the rest of the myocardium (**Figures 6 and 7**). This myocardial dissection reveals the cardiac fulcrum below and in front of the aorta, in a separate location from the right trigone and in an inferior plane to the origin of the right coronary artery, without continuity with the aortic valve and inserted as a complementary element between the aorta and the myocardium (56,65). This structure, point of attachment of the origin and end of the cardiac muscle, constitutes the insertion of the myocardium in a manner analogous to a skeletal muscle.

Figure 6. This figure shows the continuous myocardium arrangement at the beginning of its unfolding. The pulmonary artery and the right segment have been separated from the fulcrum in order to indicate its intermediate location between the right segment (anterior location) and the ascending segment (posterior location). A: Macroscopic view of the fulcrum in an adult human heart. B: Microscopic view of the human fulcrum. Note the myocardial fibers (m) inserting into the tendinous fulcrum matrix (f).

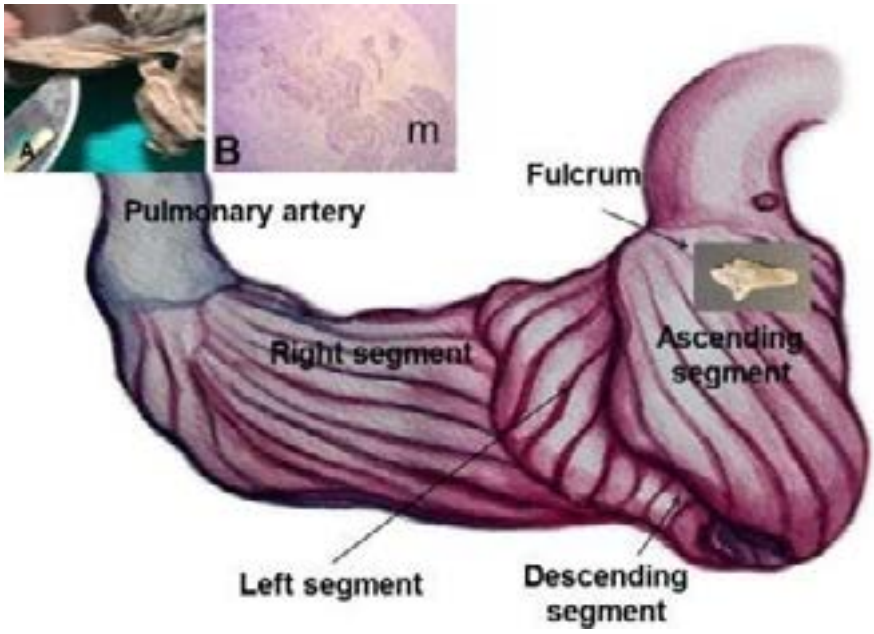

Figure 7. Cardiac fulcrum (CF) in a bovine heart.

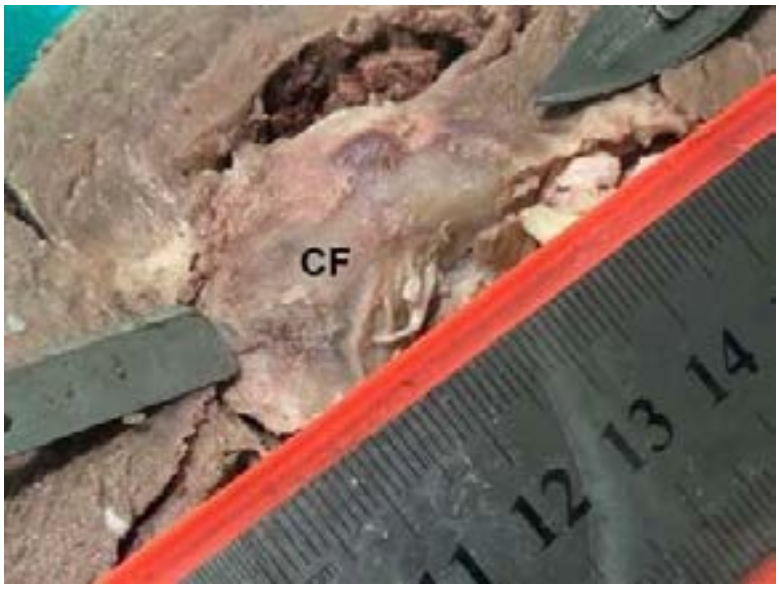

It should be understood that as the myocardium is unfolded, separating the pulmonary artery and the pulmonary-tricuspid cord (anterior) from the ascending segment (posterior), the view of the anatomical homogeneous and functional integrity of the heart is lost. This concurrence of the beginning and end of the cardiac muscle in the cardiac fulcrum constitutes a meeting point between the right segment and the ascending segment, origin and end of the myocardium. Thus, both ends are situated at the same point, with the origin of the myocardial fibers placed anteriorly to their end.

The progression of myocardial dissection implies finding the whole extent of the right segment, the beginning of the left segment, and at the posterior margin of the right ventricular chamber the dihedral angle formed by the interventricular septum and the free wall of the right ventricle (right segment). (**Figures 8A and B**). The next step (the most delicate one) consists in entering the aforementioned dihedral angle between the right ventricular and intraseptal fibers. This separation from the right ventricle allows entering into the ventral part of the septum (**Figure 8C**). Then, the dorsal part of the septum is dissected between the posterior septal band (right ventricle) and the descending segment to detach and separate the aorta.

Finally, the trajectories of the muscle planes belonging to the descending segment are separated in a blunt manner from those of the ascending segment leading to the cardiac fulcrum contiguous with the aorta, to the right of the operator, allowing by rotating its ends to extend and align the continuous myocardium in all its length (**Figure 8D and 9**). Being able to unfold the myocardium with a similar thickness in all its extension proves that it is unique and continuous and not a heuristic construction. (**Figure 10**). The diagram in **figures 11, 12** and chart 1, details the different segments that constitute it, as well as the final insertions composing the origin and end of the myocardium, very close to each other in the intact helical heart, prior to unfolding.

Figure 8. Unfolding of the continuous myocardium

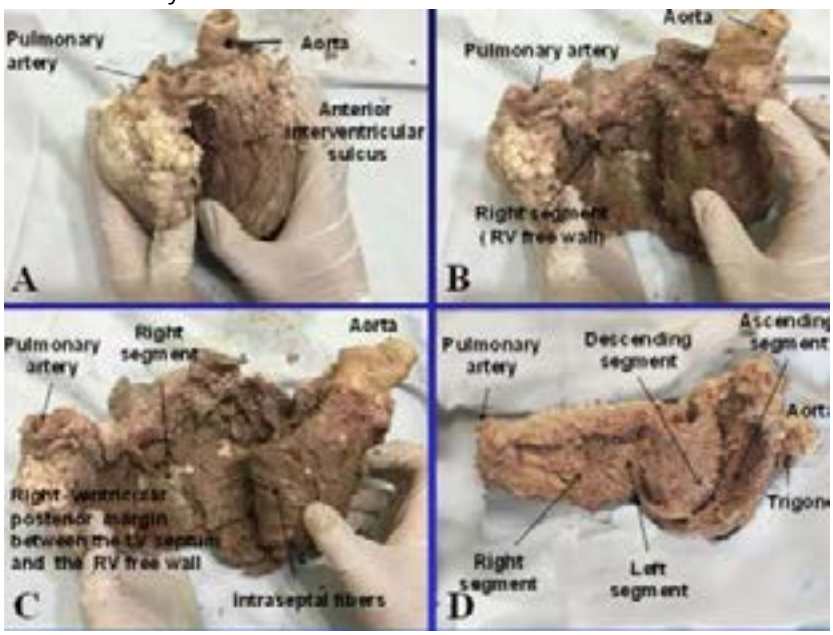

Figure 9. A shows torsion (black circle), B unfolding, and C the torque (black circle) produced in the second rtwist of the myocardium.

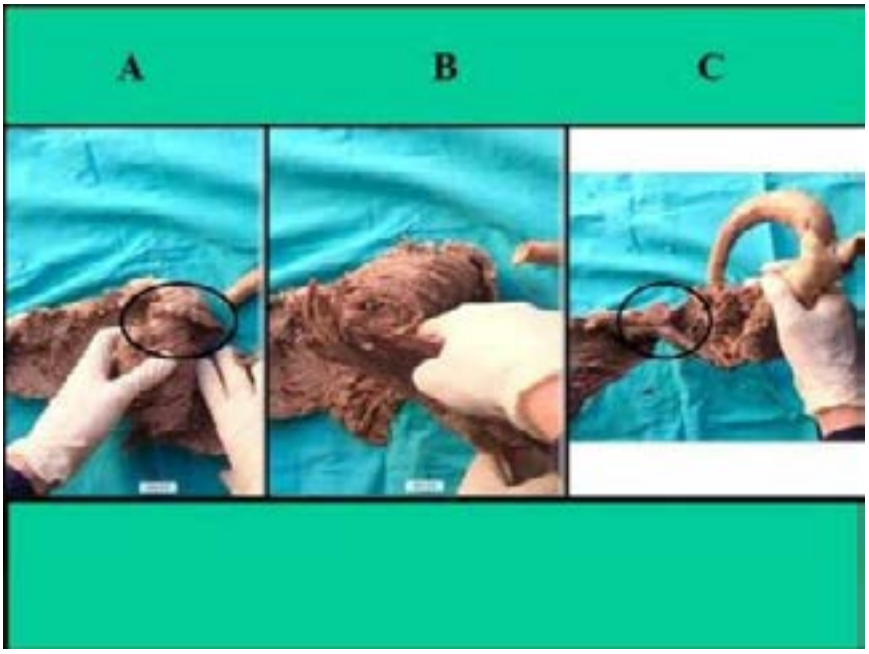

Figure 10. Myocardium unfolded in its entirety showing the segments that compose it. The yellow circles indicate the sites where the three twists of the continuous myocardium form a helicoid. PA: pulmonary artery; RS: right segment; LS: left segment; DS: descending segment; AS: ascending segment; A: aorta

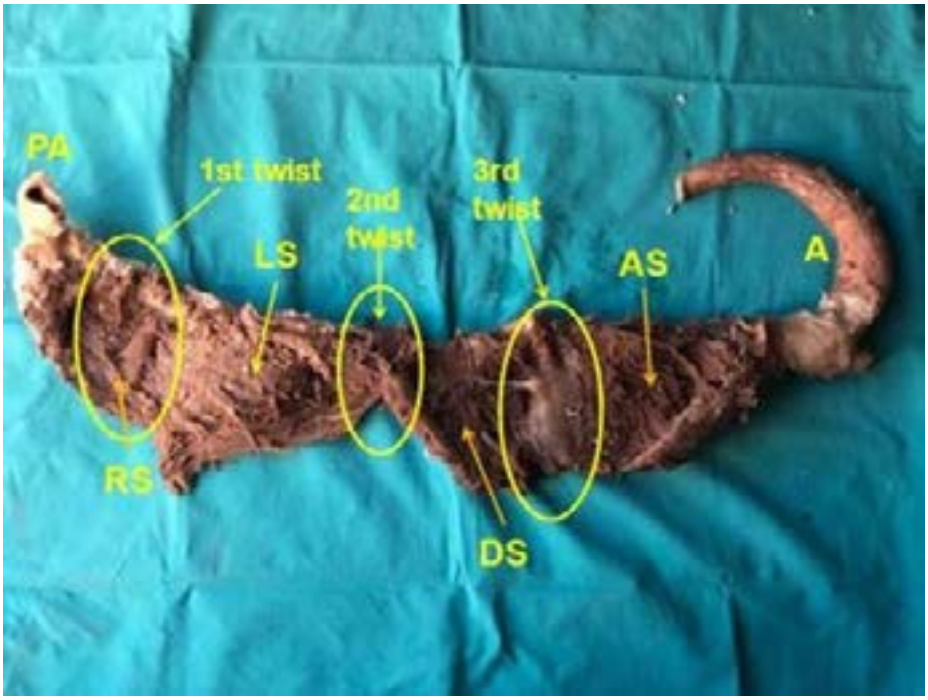

Figure 11. Helical myocardium in the rope model created by modeling that simplifies the spatial structure with its three turns. The different segments that comprise it are shown. rs: right segment; ls: left segment; DS: descending segment; AS: ascending segment. PA: location of the pulmonary artery; A: location of the aorta. The three turns (red circles) are located, which determine that the continuous myocardium becomes helical, with the consequent alignment of the ventricles to perform their torsion/untorsion function. In the lower right corner, the ascending segment of the adult human heart is observed inserting into the cardiac fulcrum. Above is a photograph of the fulcrum where the myocardium is tethered.

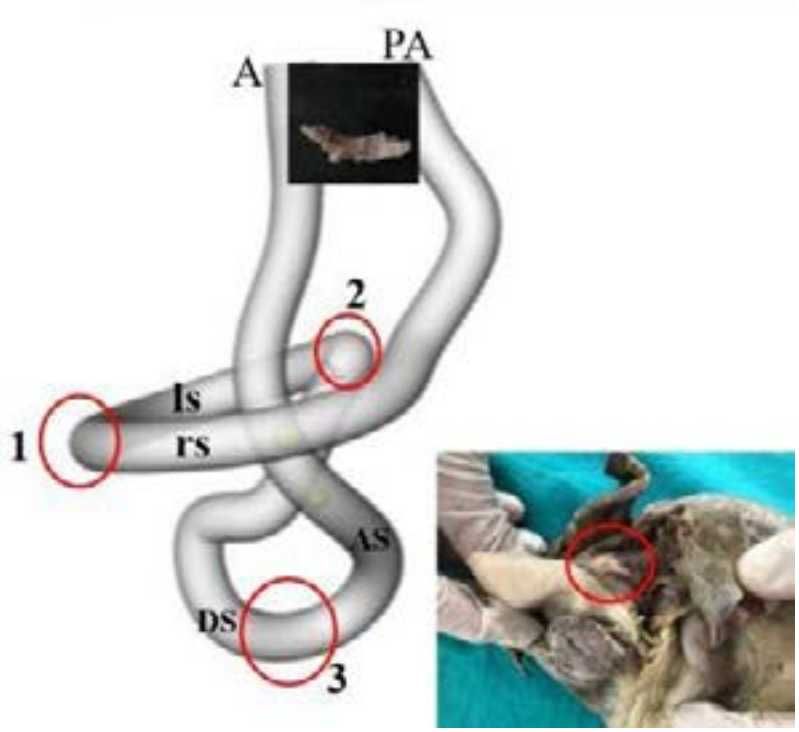

Figure 12. Descriptive diagram of the continuous myocardium segments. A: aorta; PA: pulmonary artery; RS: right segment; LS: left segment; DS: descending segment; AS: ascending segment; ptc: pulmo-tricuspid cord; tr: trigones; apm: anterior papillary muscle; ppm: posterior papillary muscle.

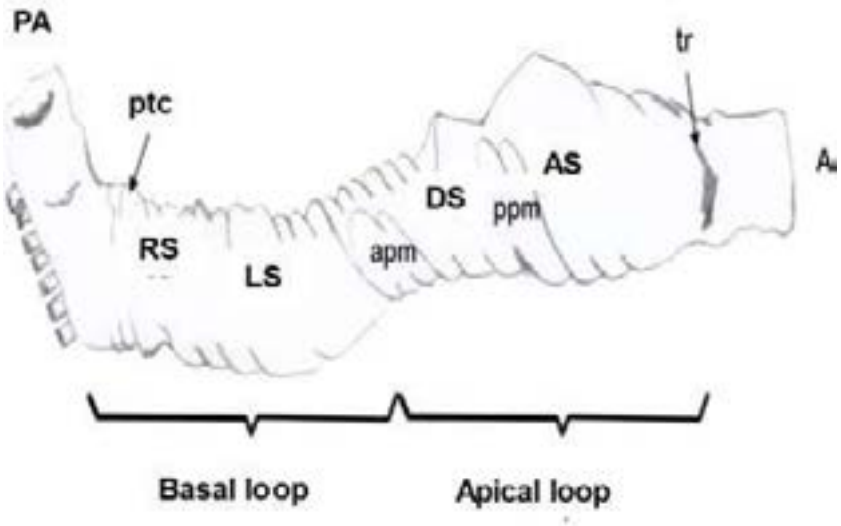

Chart 1.

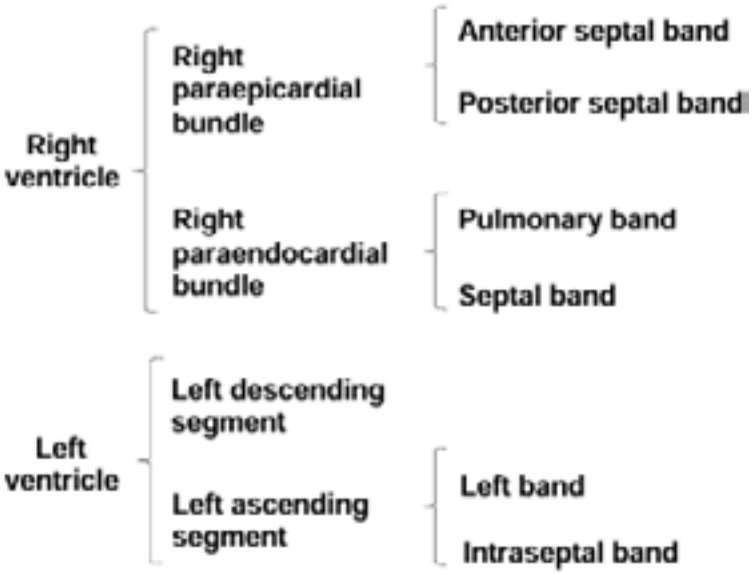

c.Topography of the cardiac fulcrum

This site of myocardial insertion, which we have called the cardiac fulcrum, is located in the vicinity of the tricuspid valve (right), the aorta (superior) and the pulmo-tricuspid cord (anterior) (**Figure 13**). In order to find it, it is necessary to move the pulmonary artery and the right segment to the left of the observer, baring the root of the aorta. This action reveals the fulcrum below the aorta and inferior to the right trigone, without any continuity with it, below the origin of the right coronary artery, detached from the aortic valve continuity, which rests on the upper surface of the fulcrum (**Figures 14 and 15**) (86). From this point, on the lateral wall of the aorta, its direction is towards the free wall of the right ventricle below the tricuspid valve.

Figure 13. The location of the cardiac fulcrum is demonstrated. References: LCA: left coronary artery; RCA: right coronary artery. Note the atrioventricular (AV) node contiguous to the cardiac fulcrum.

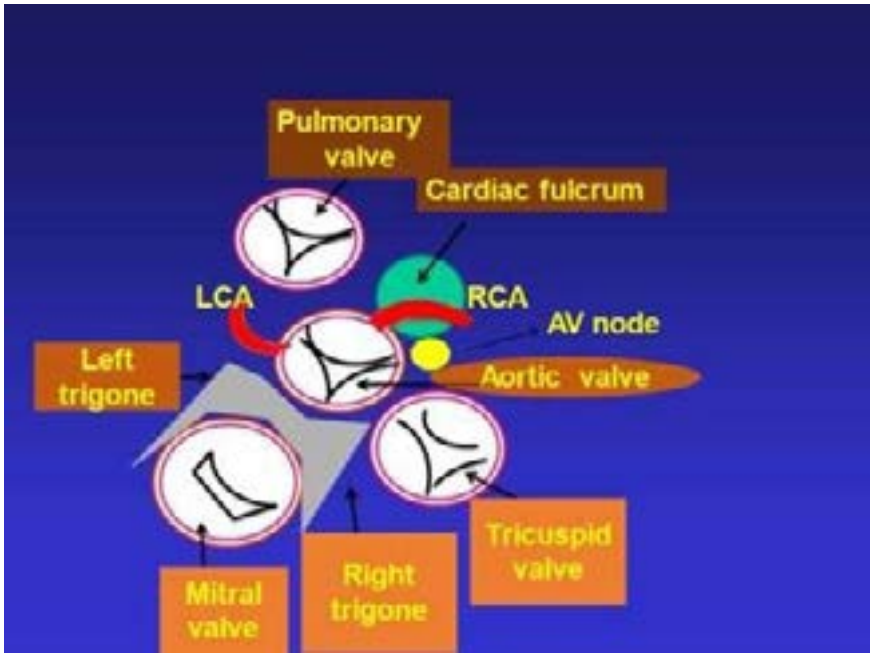

The important fact of the fulcrum functionality comes from the macroscopic and microscopic observation that demonstrates the tethering of the myocardial fibers to this solid, consistent nucleus. Its conformation was corroborated by histology. This structure, origin and end of the continuous helical myocardium, was called cardiac fulcrum in a parallelism and homage to the designation of the point of support to exert a lever expressed by Archimedes of Syracuse (Greece,288 BC-212 BC) with the words “Give me a point of support and I will lift the world”, historical slogan that reached our days through Plutarch’s text “Parallel Lives” and that corresponds to a letter sent by Archimedes to King Hieron of Syracuse (73).

It should be noted that in order to visualize the cardiac fulcrum in its anatomical situation and to establish its relationships, it is necessary to unfold the helical myocardium. Figure 1 shows the location of the cardiac fulcrum in the cord model, supported by Torrent Guasp (19312005), which simplifies the understanding of the helical myocardium (17).
In bovids, its size, corroborated by dissection and imaging studies (computed tomography, magnetic resonance imaging, ultrasound), is approximately 37 mm long, 45 mm wide, and 15 mm thick, with a triangular shape (**Figures 14 to 16**). In humans, it has the same morphology, but its size is 50% that of the bovine fulcrum in each of its dimensions (**Figures 17 and 18**). In pigs, it also has the same shape (**Figure 19**).

Figure 14. The size of the cardiac fulcrum obtained from bovine hearts is shown in its three dimensions.



Figure 15. The para-aortic surface of the fulcrum contacting the aorta is seen on the left image. The right image shows the torsion angle shaped by cardiac movements (bovine heart).

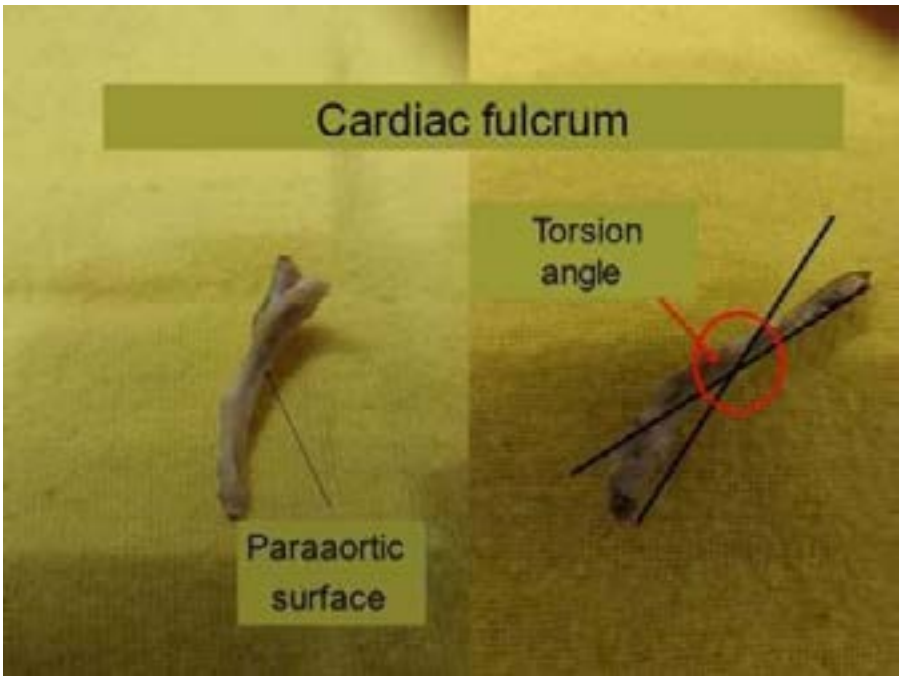

Figure 16. Cardiac fulcrum of a bovine heart. Profile views.



Figure 17. Cardiac fulcrum of a dissected bovine (A) and adult human (57 years old) (B).



A B

Figure 18. Cardiac fulcrum of a human heart (22 years).



Figure 19. Cardiac fulcrum of a pig heart.

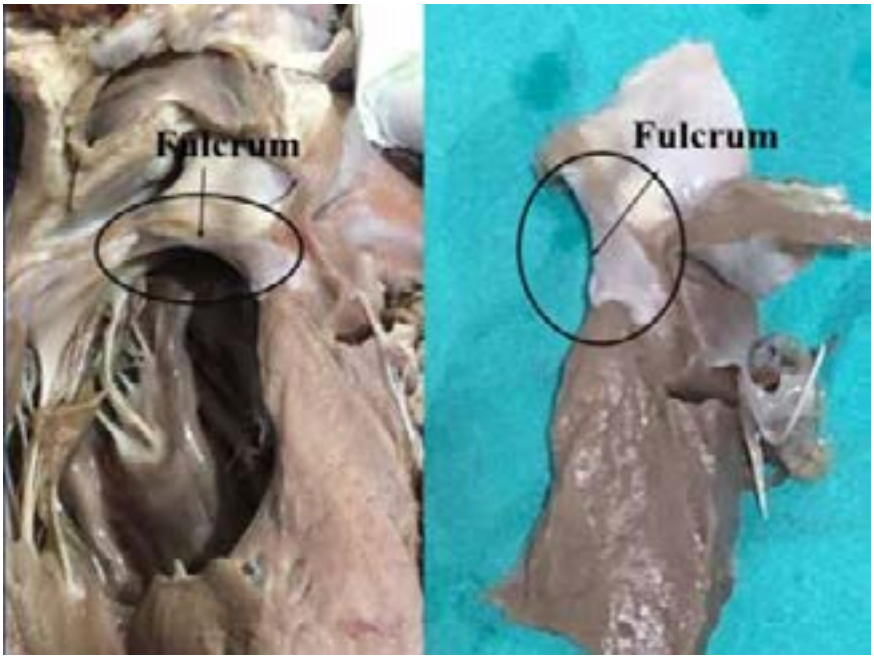

Its triangle-like shape has a bifid character at its right end (insertion of the right segment) and ends in a point at the opposite end (attachment of the ascending segment). **Figure 20** shows these details, as well as the articular surface with the aorta and its location in the heart.

Figure 20. Bovine cardiac fulcrum located in its anatomical position in a silicone cardiac model (copy of a biological heart).

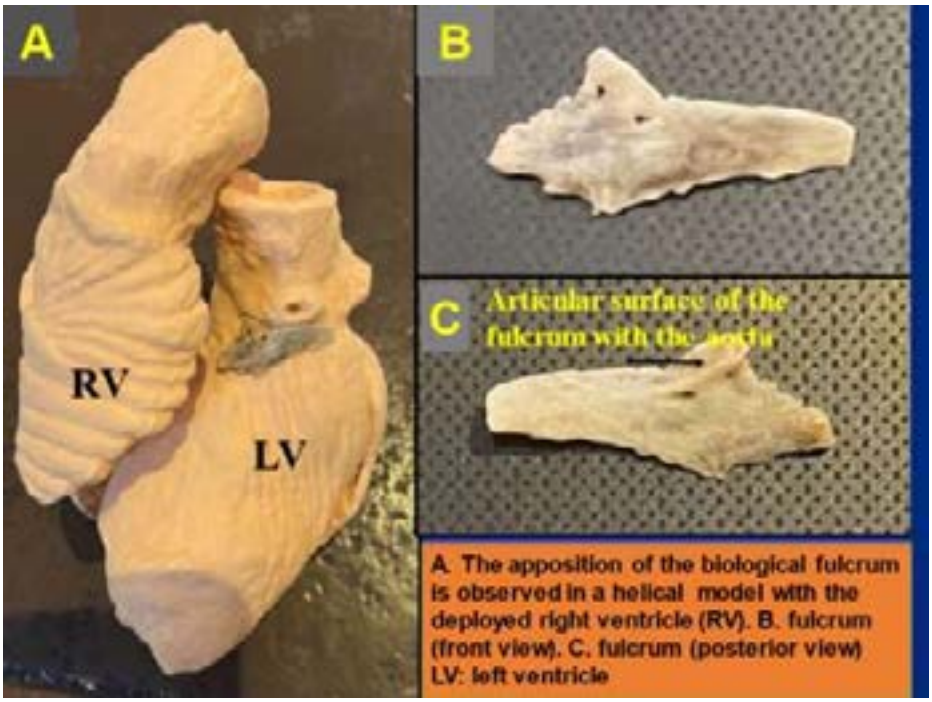

d.Histological análisis of the cardiac fulcrum. Myocardial insertion

During the dissection of the myocardium, the finding in this research of the cardiac fulcrum as a structure where the myocardium is inserted led us to further inquiries: What are its characteristics? Where is it located? What is its histology? Is its presence analogous in different species? How is the myocardial muscle inserted into this structure that we have called the cardiac fulcrum? What properties does it have? Does the fulcrum have any functional relationship with the AV node, which is located between it and the septal leaflet of the tricuspid valve?

The existence of a bony formation called “os cordis” in mammals (bovine, buffalo, sheep, goat, antelope, deer, giraffe, camel, dog, cat, pig, sea lion, horse, elephant, and chimpanzee) is a well-known fact in veterinary science (**Figure 21**). Beyond mere mention, until our research, no function or meaning was ever assigned to its presence, nor was it described in humans (8,56) The article we published in 2021 entitled “Myocardial torsion and cardiac fulcrum (Torsion myocardique et pivot cardiaque)“ involved the first human observation of the cardiac fulcrum and its importance (65).

Figure 21. Cardiac fulcrum below the aorta (bovine heart). The insert shows the resected piece.

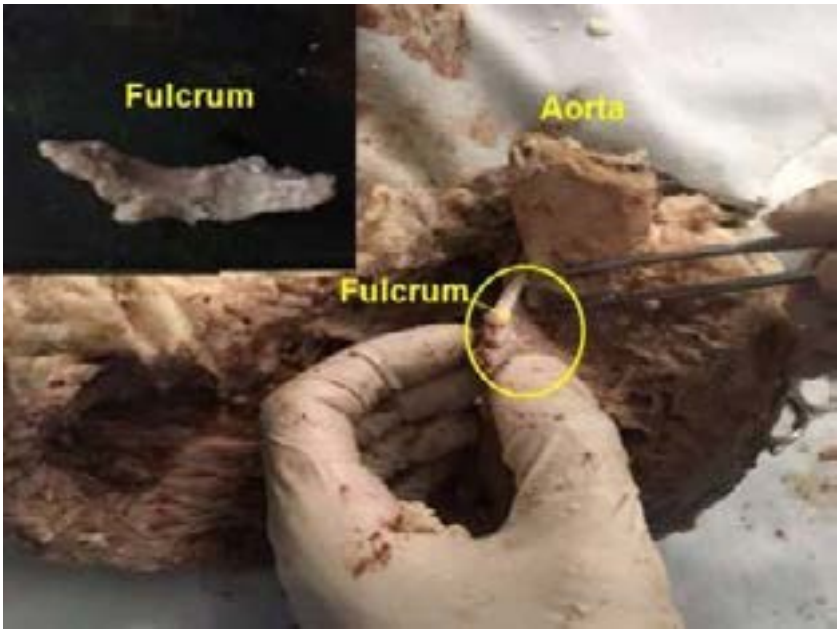

In bovids, the bone-like consistency of the cardiac fulcrum (**Figure 22**) has been confirmed by histology (**Figures 23 to 25**). Microscopic analysis of the bovine cardiac fulcrum shows a trabecular osteochondral matrix with segmental lines. Its general structure resembles the metaphyseal growth of long bones. At higher magnification, bone trabeculae with osteoblasts and segmental lines secondary to bone apposition can be observed. In young bovine hearts the fulcrum tends to be cartilaginous, developing into a bony structure with increasing body weight of the animal. The same histological findings have been found in chimpanzees (25). The sequential insertion of myocardial fibers into the bovine fulcrum can be seen in **figures 26 to 29**.

Figure 22. Cardiac fulcrum in a bovine heart. The microscopic image of the myocardium insertion into the bone matrix can be seen in the right-hand corner.

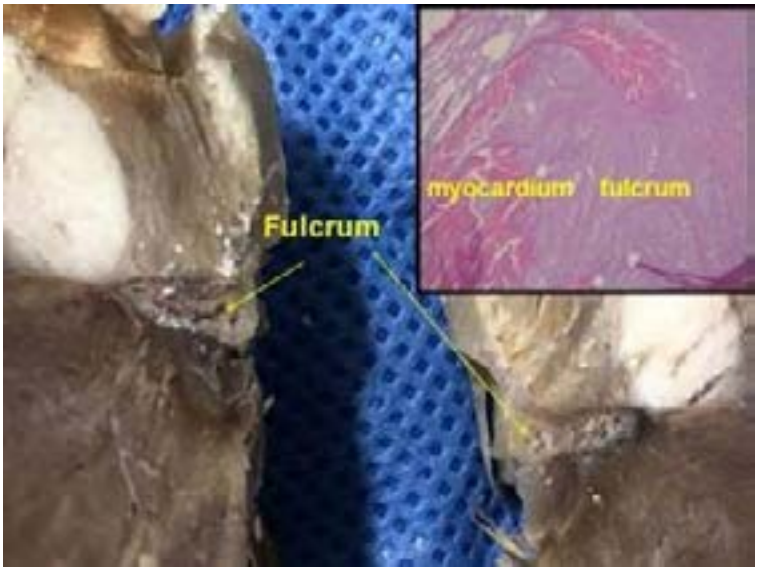

Figure 23. The histological section shows trabecular bone tissue with osteological segmentation lines corresponding to the cardiac fulcrum (bovine heart). H&E technique (40x).

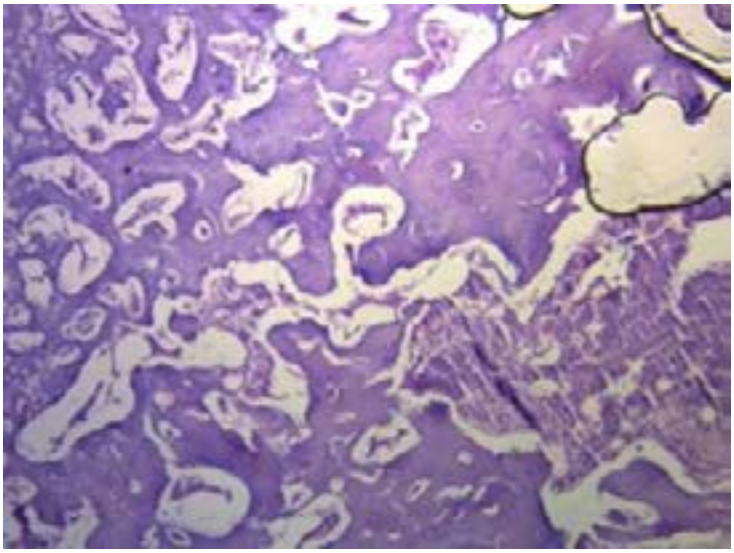

Figure 24. Mature bone trabeculae that make up the tissue of the cardiac fulcrum (bovine heart). H&E technique (10x).

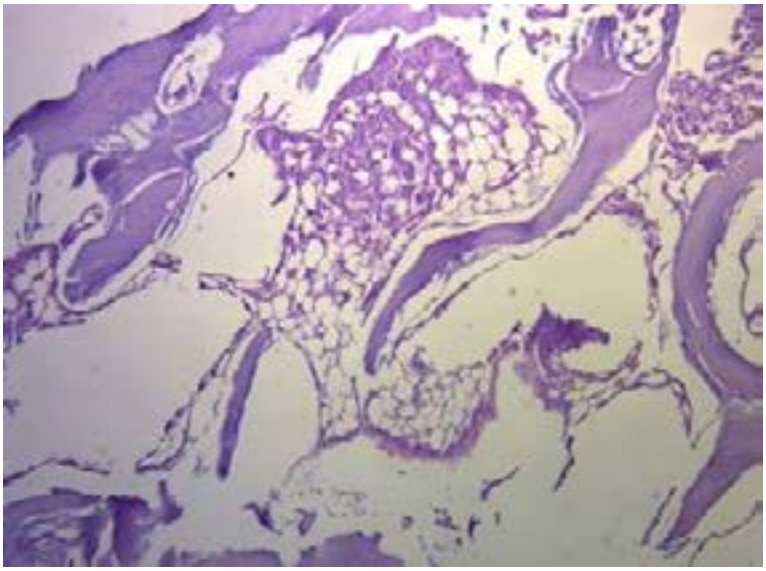

Figure 25. H&E staining of the cardiac fulcrum at high magnification (40x). Bone trabeculae with osteoblasts and segmental lines can be seen. The structure forms the scaffolding of trabecular bone tissue similar to the metaphyseal growth zones of long bones. Bone trabeculae with osteoblasts and segmental lines secondary to bone apposition (bovine heart).

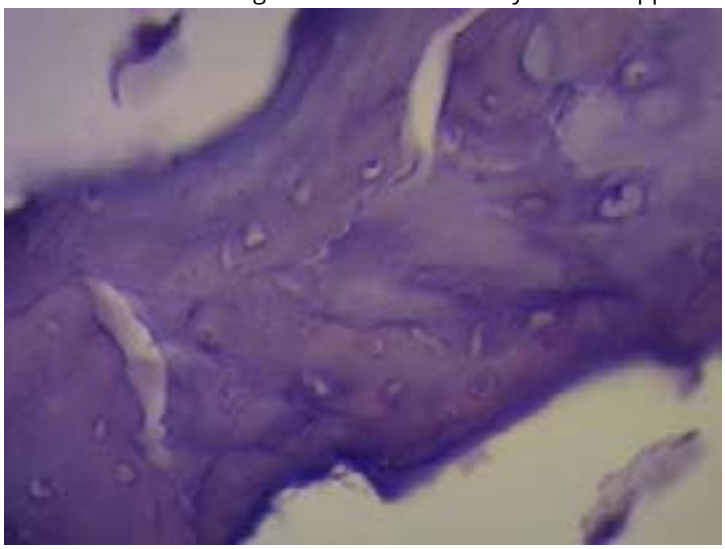

Figure 26. Bovine heart. Myocardial fibers can be seen at the insertion line in the cardiac fulcrum.

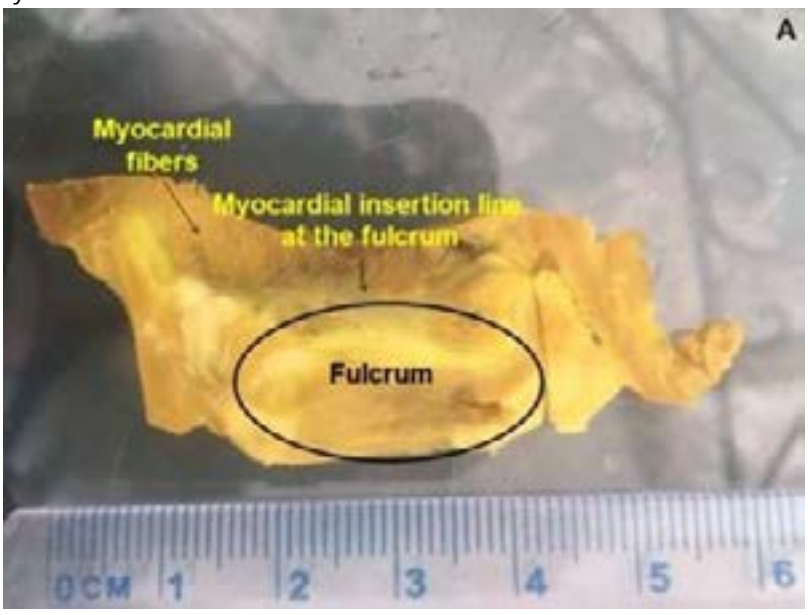

Figure 27. Insertion of the myocardium into the cardiac fulcrum (bovine heart). References: 1. Myocardial fibers and myxoid stroma; 2. Myocardial bands in a chondroid stroma (insertion); 3. Cortical bone tissue of the fulcrum.4. bone tissue H&E technique (15x).

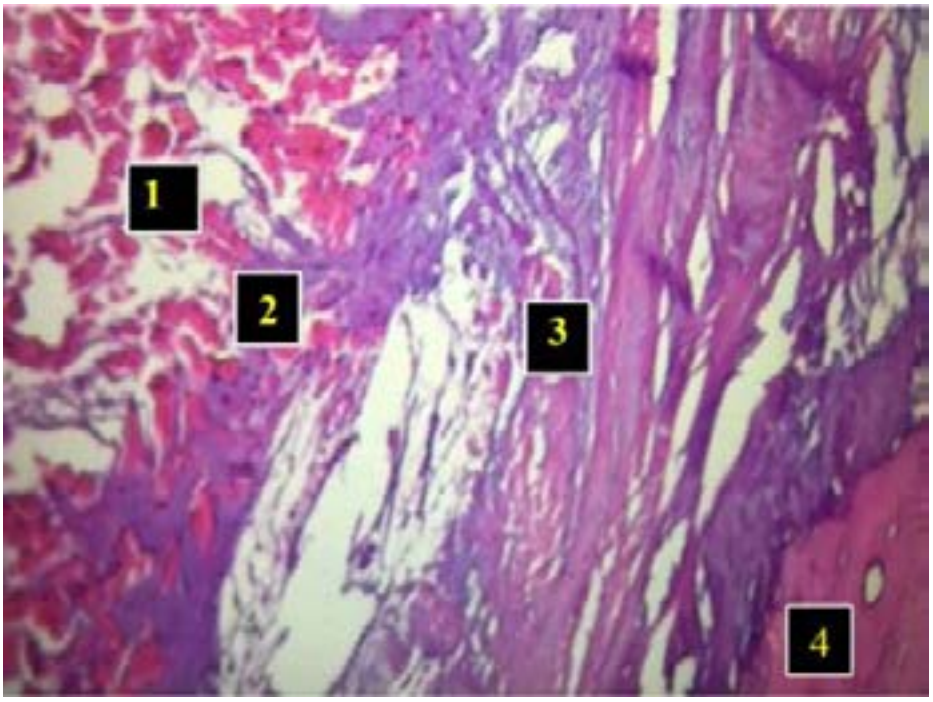

Figure 28. Insertion of myocardial fibers into chondroid tissue (fulcrum) in a bovine heart. H&E technique (40x).

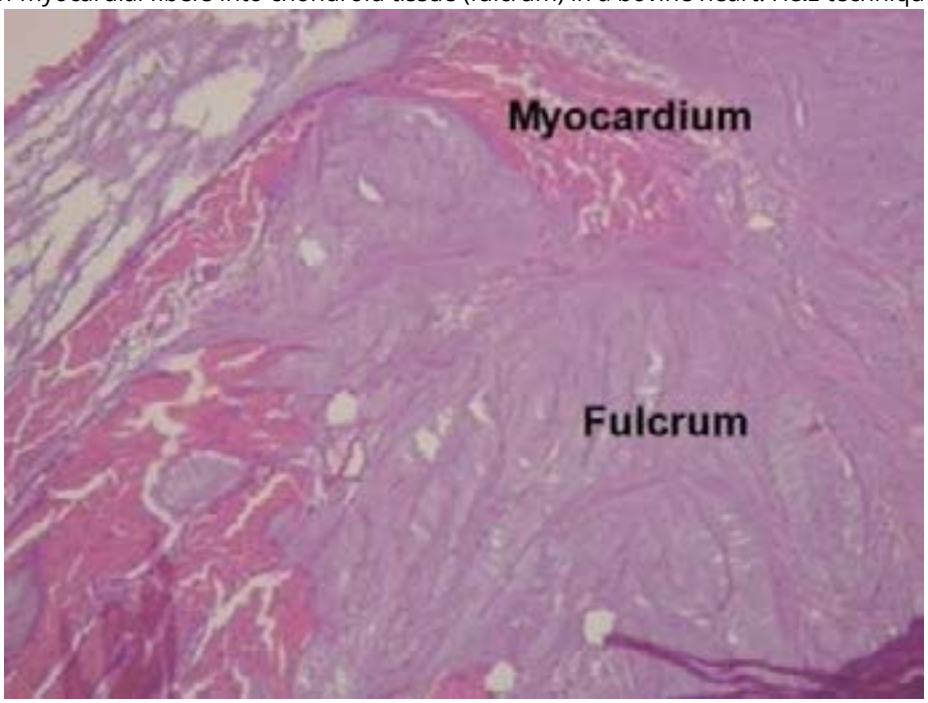

Figure 29. Cardiomyocytes from the right segment are observed in the middle of the fulcrum in a bovine heart. H&E technique (40x).

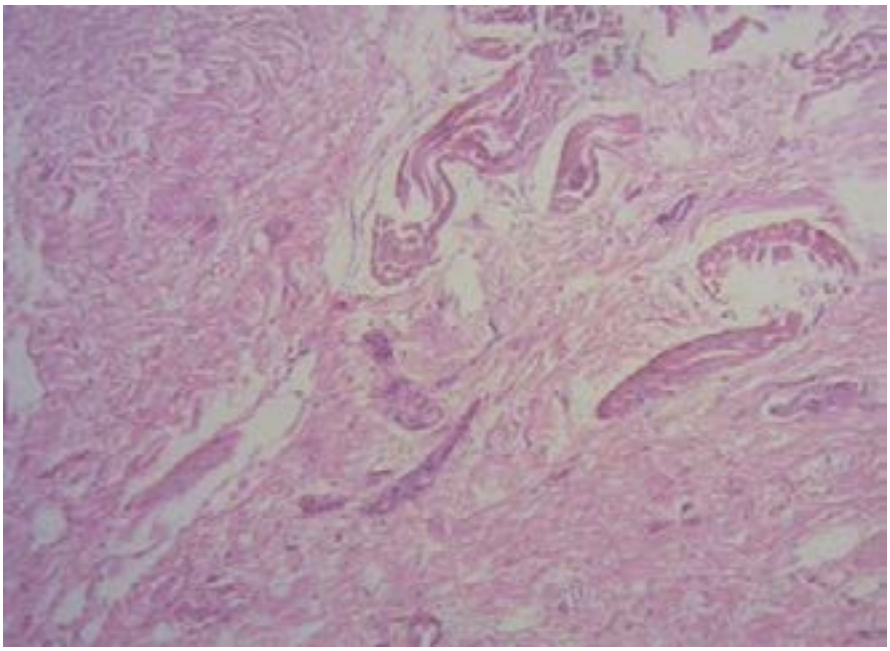

In the 10-year-old human heart, the histological description of the cardiac fulcrum is related to that early age, as the sample shows a central area of the fulcrum formed by chondroid tissue. Given the age, it is logical that the size is smaller and characterized by more chondroid than bone tissue (**Figures 30 and 31**). This finding was repeated in the 23-week-old human fetus with characteristic bluish precondroid areas in a myxoid stroma (**Figures 32 to 34**).

Figure 30. Cardiac fulcrum in a ten-year-old human heart (explant).

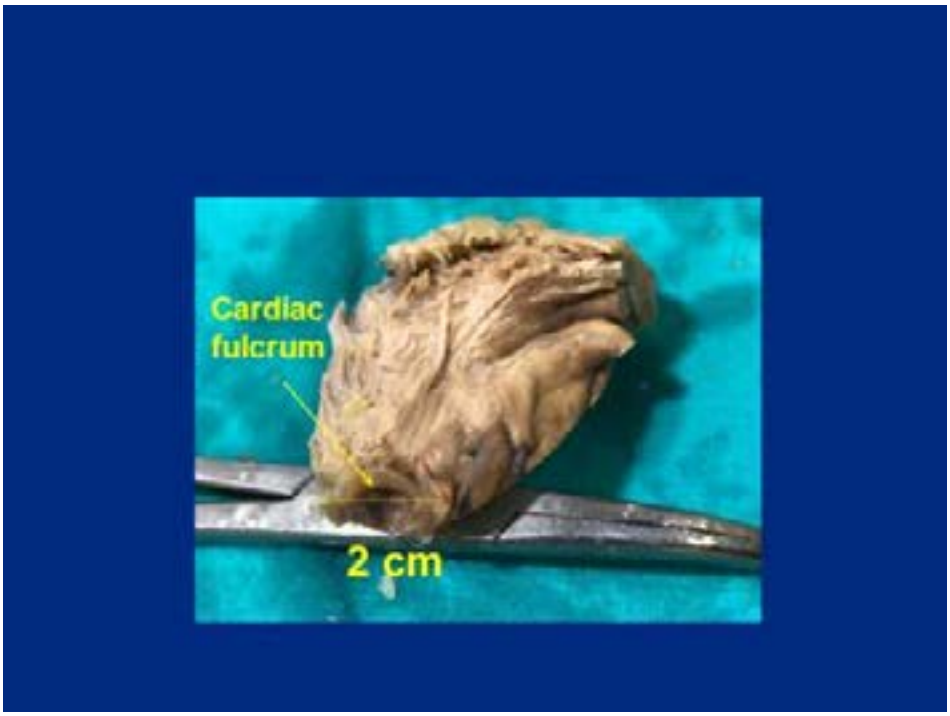

Figure 31. Ten-year-old human heart. H&E technique (15x). Central area of the fulcrum formed by chondroid tissue.

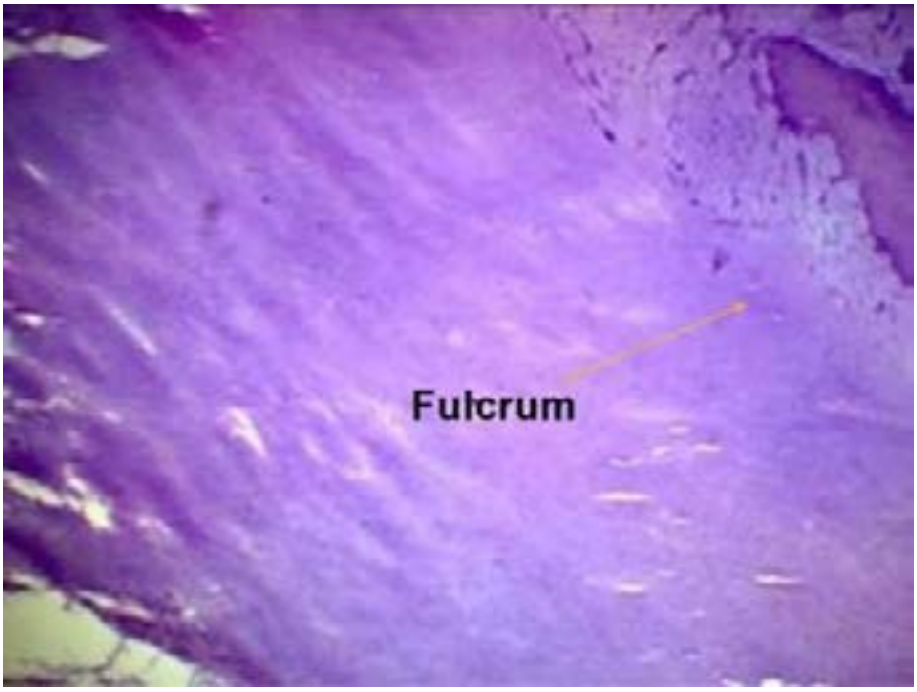

Figure 32. Human embryo heart. Section line (23-week gestation).



Figure 33. Human embryo heart. Cardiac fulcrum in the human embryo heart from the previous figure, after being sectioned (23-week gestation). References: A: Aorta; PA: Pulmonary artery, VT: Tricuspid valve.



Figure 34. Bluish precondroid areas in a myxoid stroma of a 23-week-old fetus cardiac fulcrum. Masson's trichrome technique (15x).

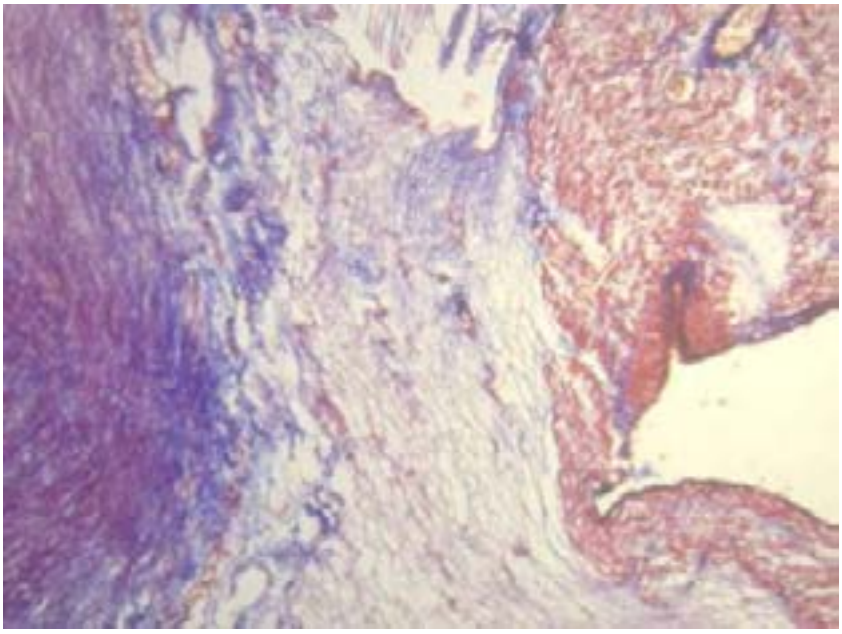

However, histological analysis of the fulcrum in adult human hearts (approximately 25 mm long and 15 mm wide) revealed a chondroid-tendinous matrix, which requires further clarification (**Figures 35 to 37**). In principle, there is similar evidence in the detection, location, and morphology of the fulcrum in all the hearts analyzed. They present insertion of the myocardium into the rigid structure of the fulcrum, integrating a cardiomyocyte-matrix unit, regardless of its bone, cartilage, or tendinous nature in the different specimens studied. This point of attachment implies that, as in all muscles, it acts as a lever and also as a bearing, preventing the ventricular rotational force, due to torque or torsional stress, from extending to the large vessels, thus dissipating the energy produced by the movement of the muscular helix. In this way, the energy of the myocardial torsion-detorsion movements is absorbed by the cardiac fulcrum, which is shaped to take on the morphological characteristics of a helix (Figure 59).

Figura 35. Fulcrum in adult human heart.



Figure 36. Fulcrum in adult human heart (detail of figure 35).

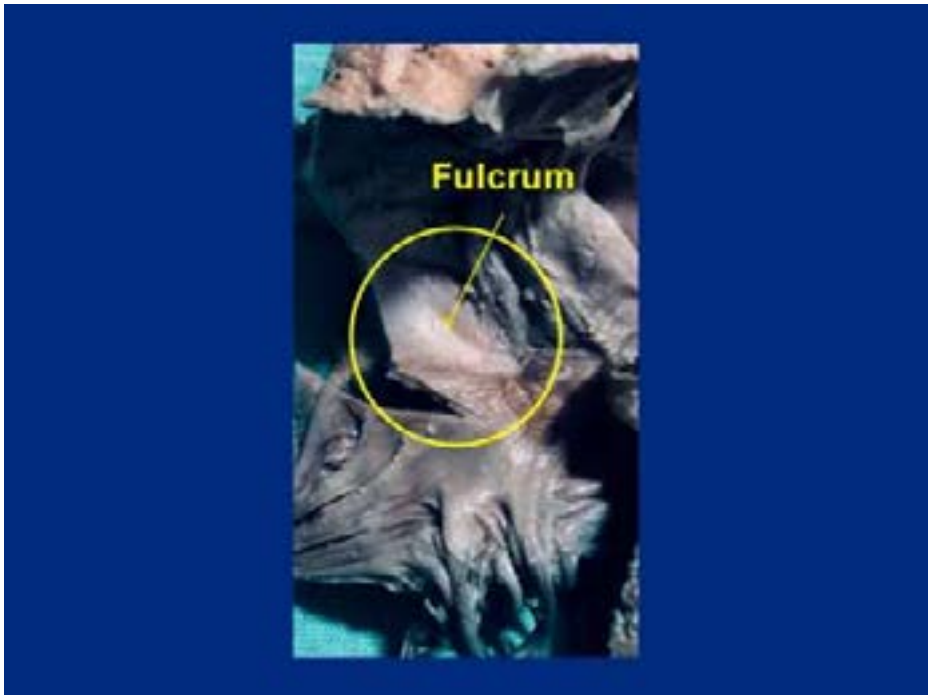

Figure 37. Adult human heart. The ascending segment is seen inserting into the cardiac fulcrum. References: LA: Left atrium; RA: Right atrium; PA: Pulmonary artery; RV: Right ventricle.

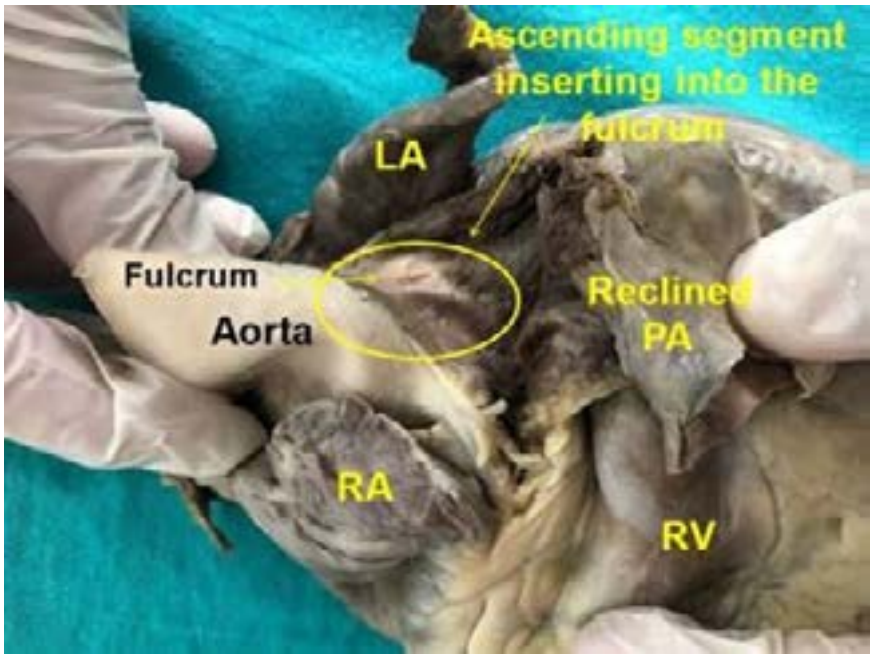

The discovery of a bone structure in the bovine os cordis and its relationship with the myxoid-chondroid consistency in human hearts, even in embryos, is consistent with the interpretative analysis. This difference corresponds to the different evolution given by age from chondroid to osteoid material and by the greater power of bovids, requiring a more rigid support. In fact, it is not the same to anchor a heavy and powerful myocardium, such as that of a bovine heart, than that of a human heart, which weighs only 270 grams. The former requires a very strong buoy, such as bone. In contrast, a cartilaginous-myxoid support is sufficient for humans.

Thus, histological analysis of the fulcrum in adult human hearts revealed a chondroid- tendinous collagen matrix, which needs further clarification. The fact that it has been found in humans and different species implies that, from a functional point of view, its presence is indication of the myocardium insertion, a circumstance that we have corroborated in all the histology analyzed, constituting a solid point of reasoning to fulfill its biomechanical action. And we found this demonstration when we directed the histological analysis to the point of insertion of the myocardium with the cardiac fulcrum, whether osseous, chondroid or tendinous. In all the hearts analyzed, we found this myocardial attachment, which we can symbolize as “ivy to stone”, in the rigid structure of the fulcrum integrating a cardiomyocyte-matrix unit, even if this was osseous, cartilaginous or tendinous, according to the studies we have carried out in this investigation (**Figures 38 to 48**). In this concept there is an analogy between skeletal muscle and myocardium. The former performs its contraction between a fixed and a mobile support point. This situation is found in the anatomical dissection material of the continuous myocardium, since there is greater solidity in the insertion between the fulcrum and the ascending segment in relation to the tethering of the right segment in this support.

Figure 38. Scalloped cardiomyocytes penetrating a fibrocollagenous matrix (cardiac fulcrum). 1. Scalloped cardiomyocytes; 2. Frayed cardiomyocytes; 3. Atrophic cardiomyocytes; 4. Fibrocollagenous matrix (adult human heart). H&E technique (15x).

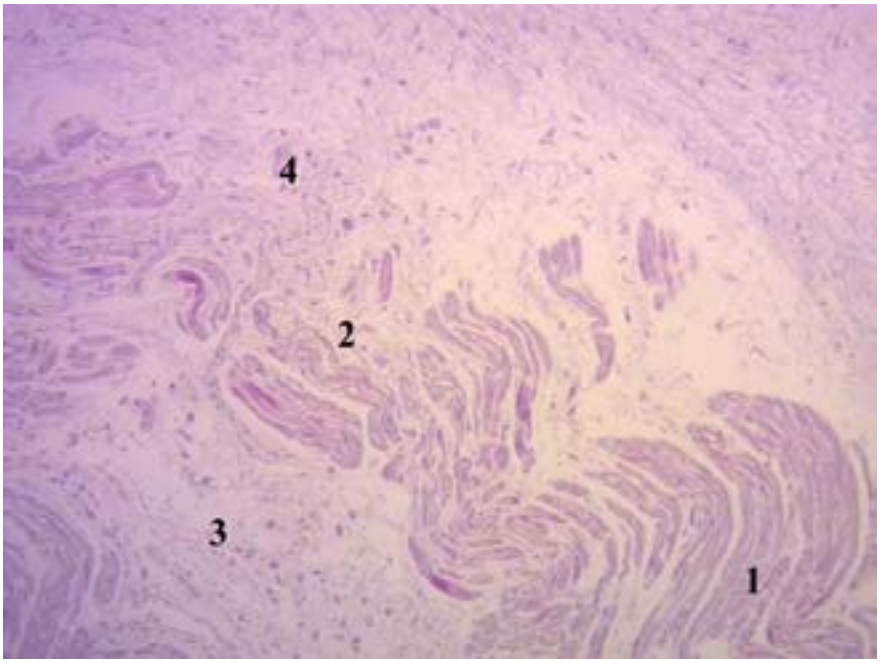

Figure 39. Scalloping collagenous fibers integrating the fibrotendinous matrix of the fulcrum (adult human heart) Reference. 1. Rests of atrophied cardiomyocytes. 2. Fibrotendinous matrix. H&E technique (15x).

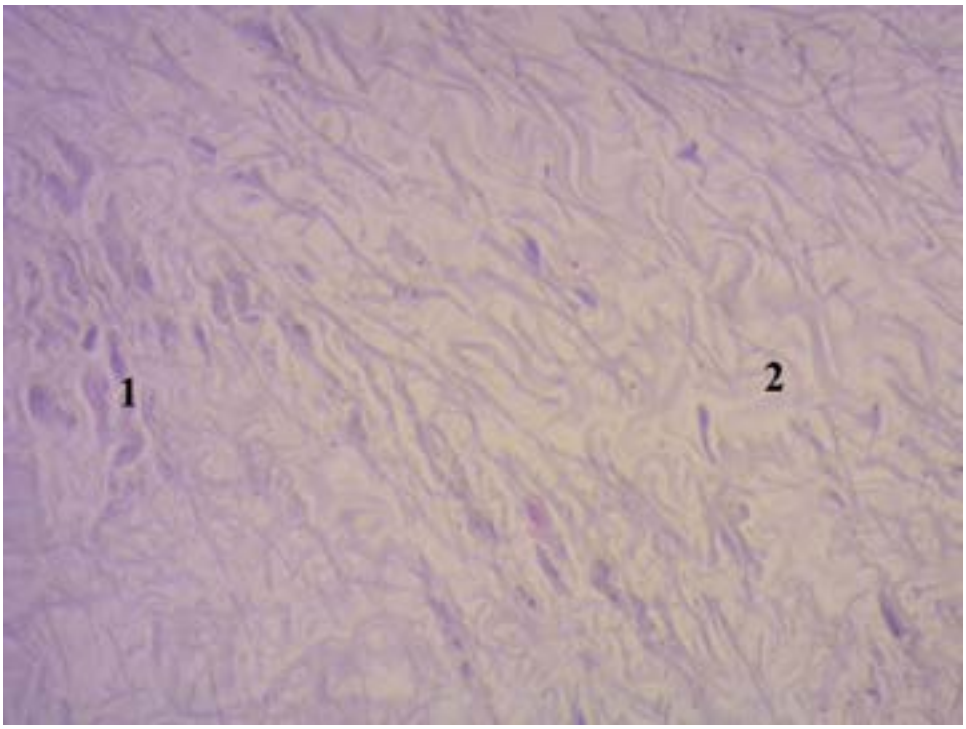

Figure 40. Adult human heart. Cardiomyocytes penetrating the fibrocollagenous tissue of the cardiac fulcrum. References: 1. Cardiomyocytes; 2. Fibrocollagenous matrix (adult human heart). The insertion site is detailed in the circle. H&E technique (15x).

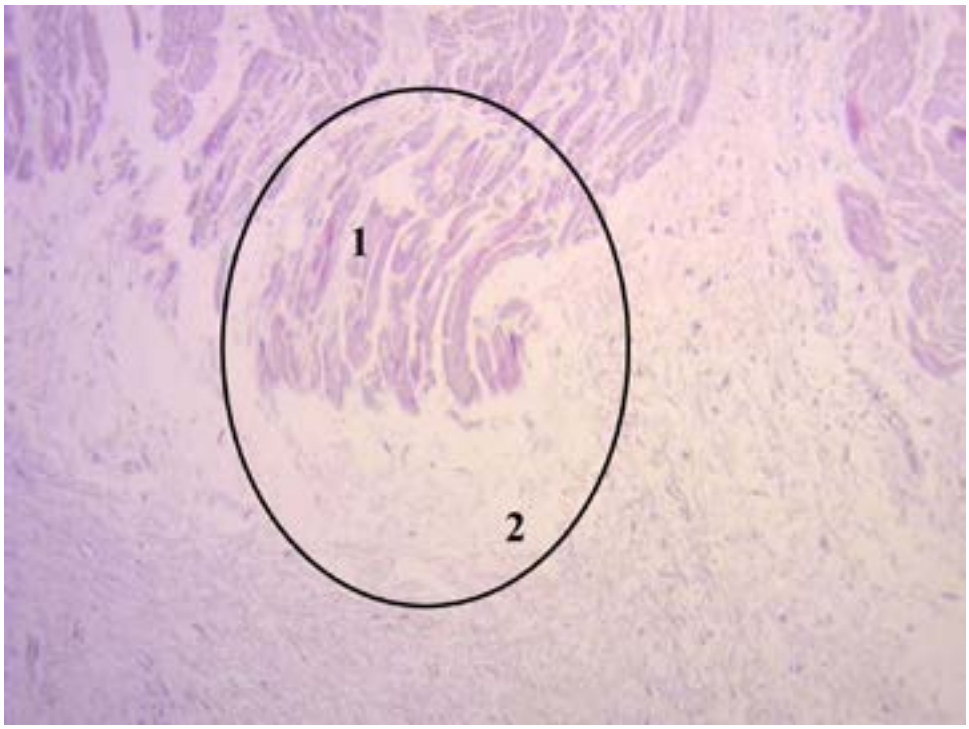

Figure 41. Adult human heart. Transition zone, cardiomyocytes inserting into fibrous tissue in an adult human heart.

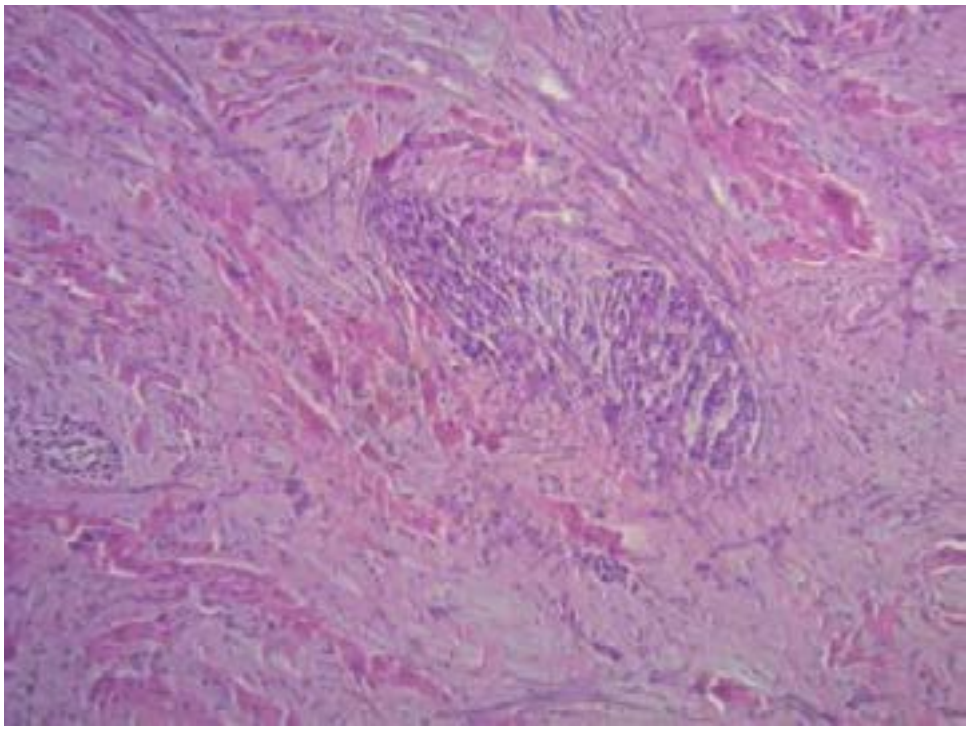

Figure 42. Adult human heart. Ascending segment of the continuous myocardium before entering the cardiac fulcrum. Scant prechondroid tissue. Adipose tissue is observed. H&E technique (15x).

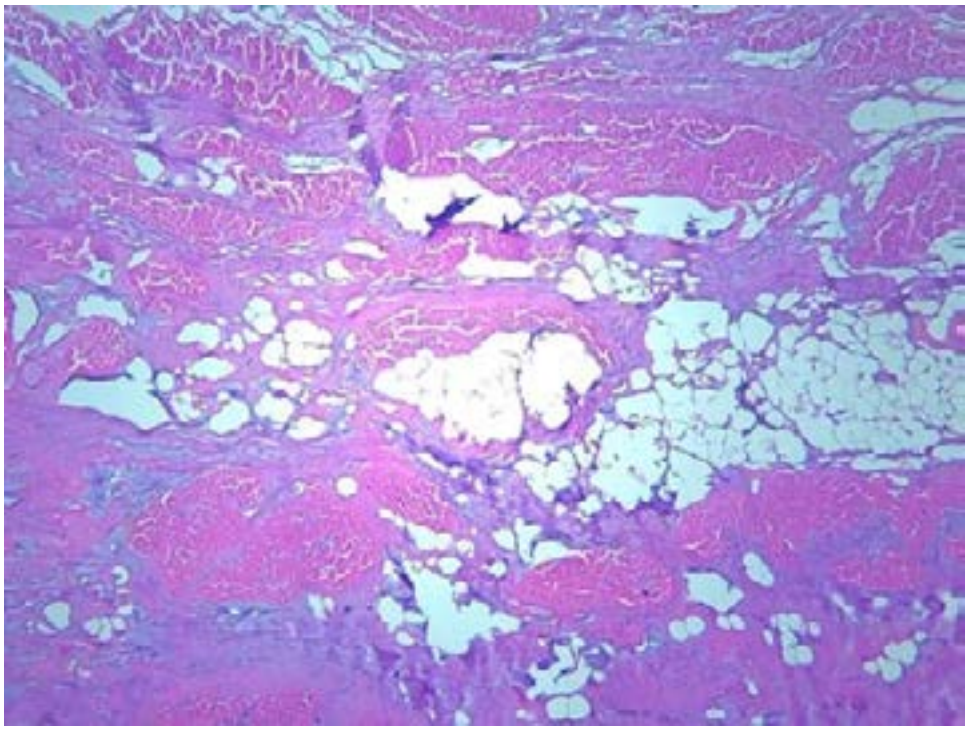

Figure 43. Adult human heart. The same segment of the previous figure entering the fulcrum. Still scarce prechondroid tissue. H&E technique (15x).

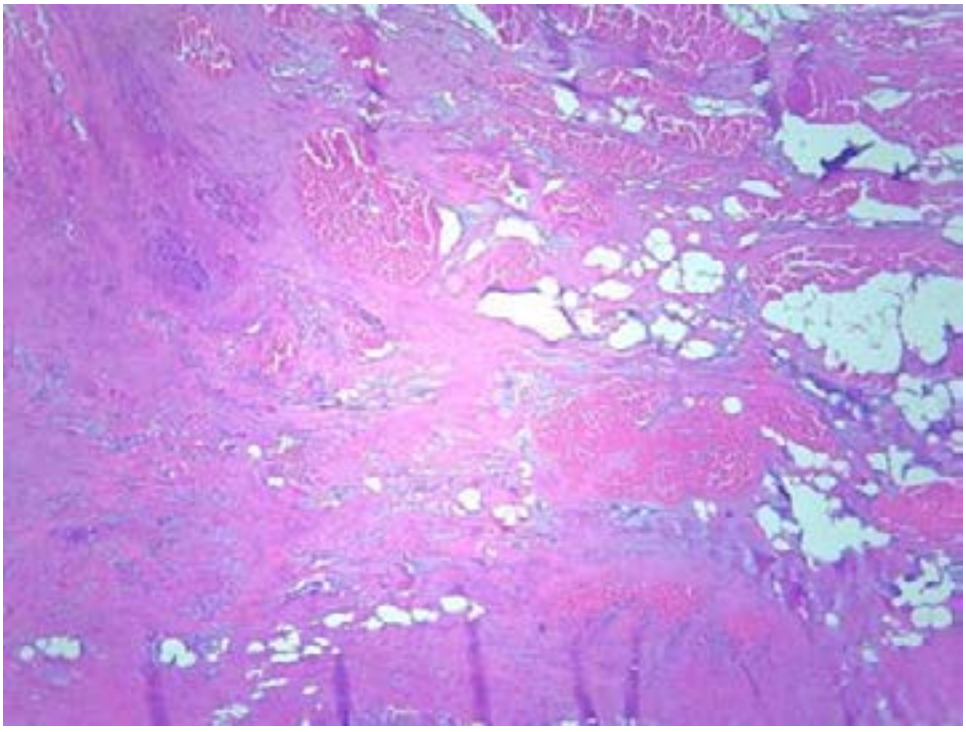

Figure 44. Adult human heart. Ascending segment of the previous figure in the middle of the fulcrum. The fibers are already surrounded by prechondroid stroma. H&E technique (15x).

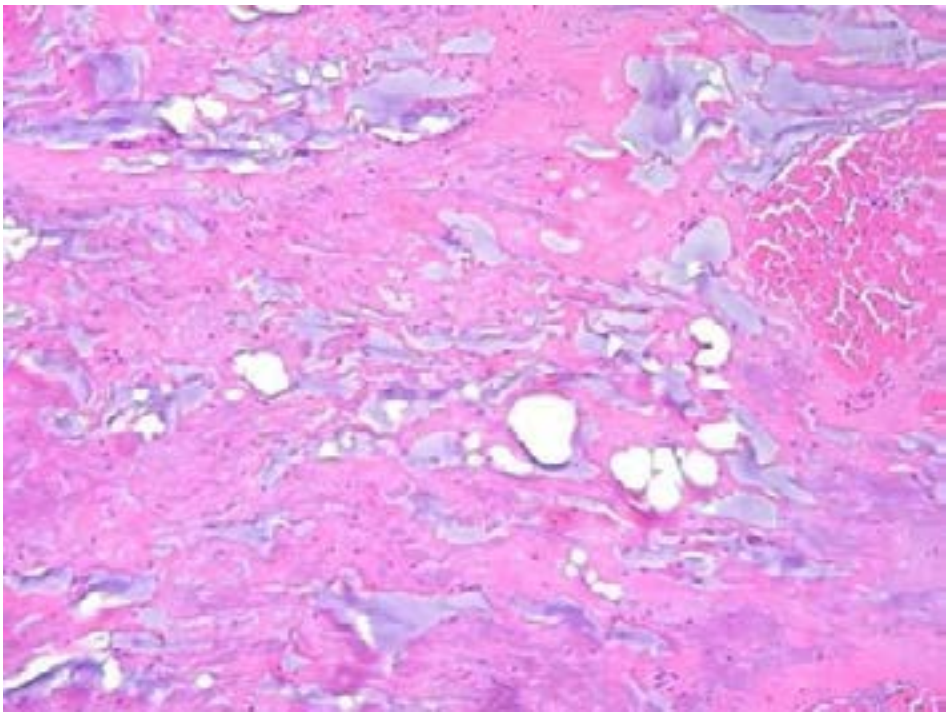

Figure 45. Adult human heart. Cardiomyocytes surrounded by chondroid material at the insertion point in the fulcrum, H&E (25x).

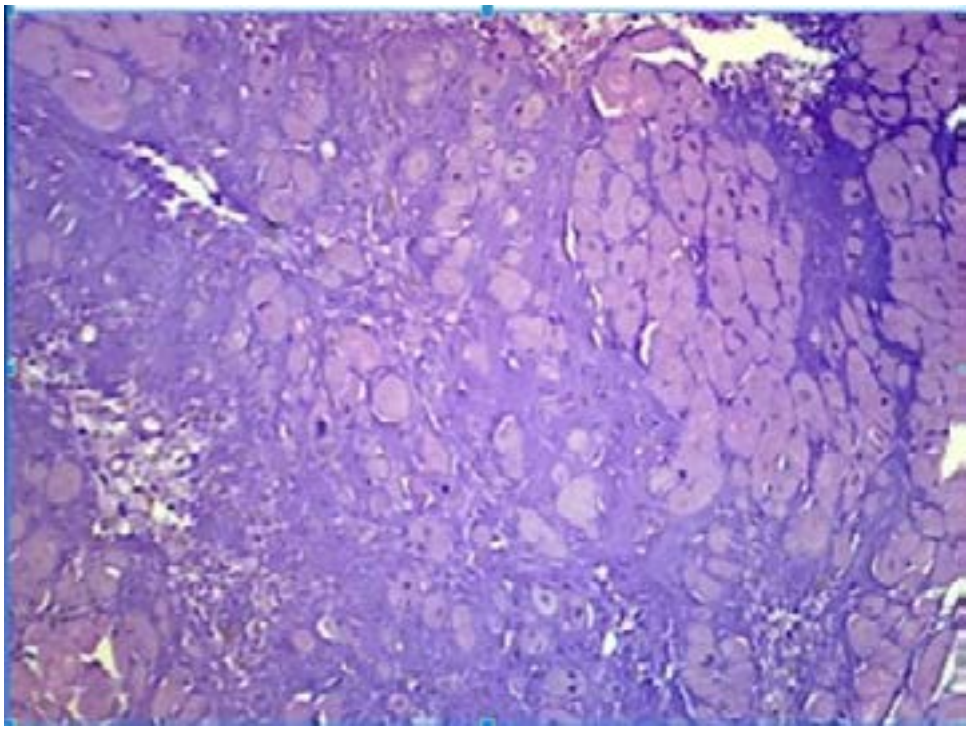

Figure 46. Fulcrum in adult human heart. Right segment in the fulcrum. The chondroid stroma remodels to collagenous tissue adopting a tendinous structure. Thinner and scalloped cardiomyocytes are seen surrounded by collagen tissue, H&E (25x).

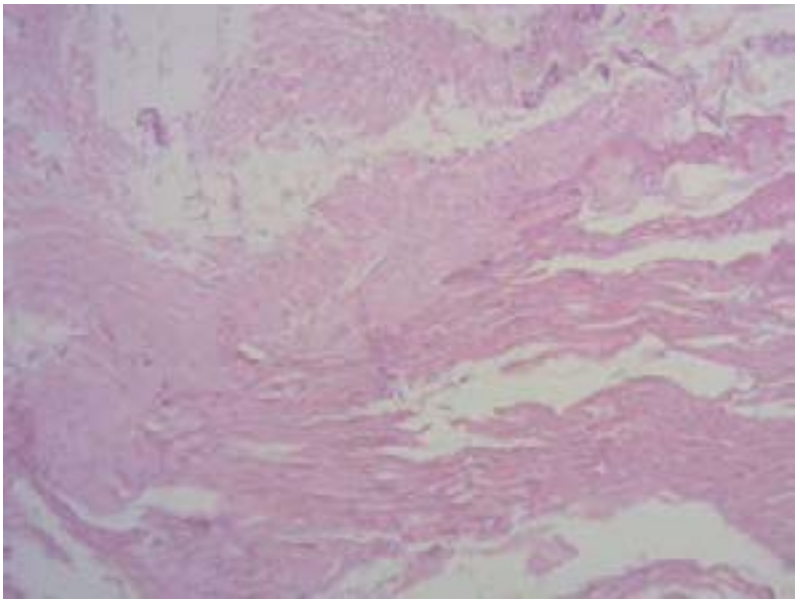

Figure 47. Insertion of cardiomyocytes in a human heart fulcrum, H&E (40x).

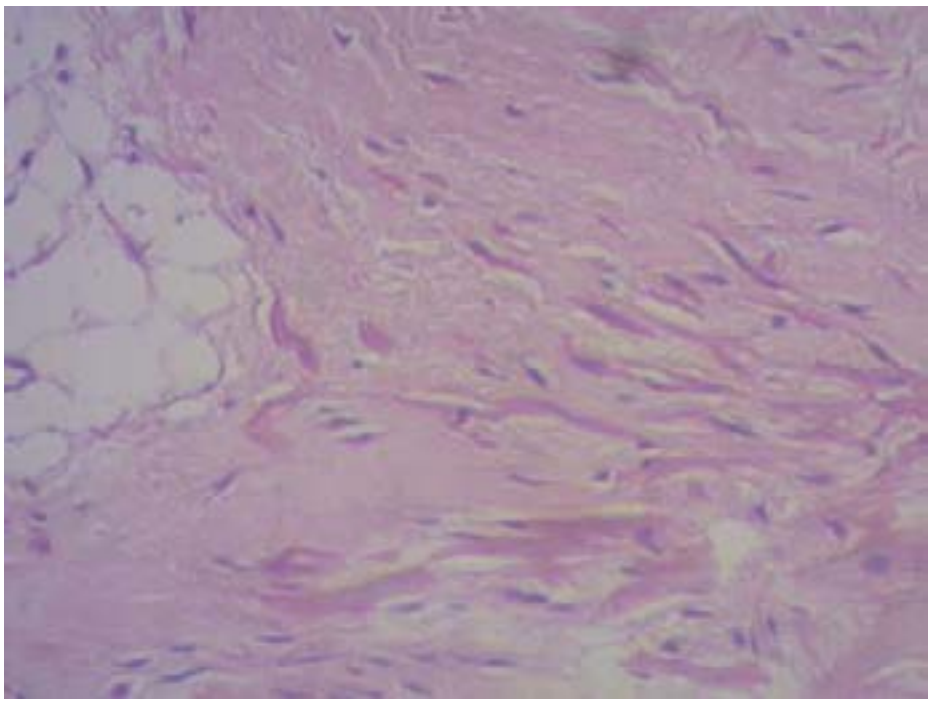

Figure 48. Central area of a human heart fulcrum. Fibrous tendon and cardiomyocytes, H&E (25x).

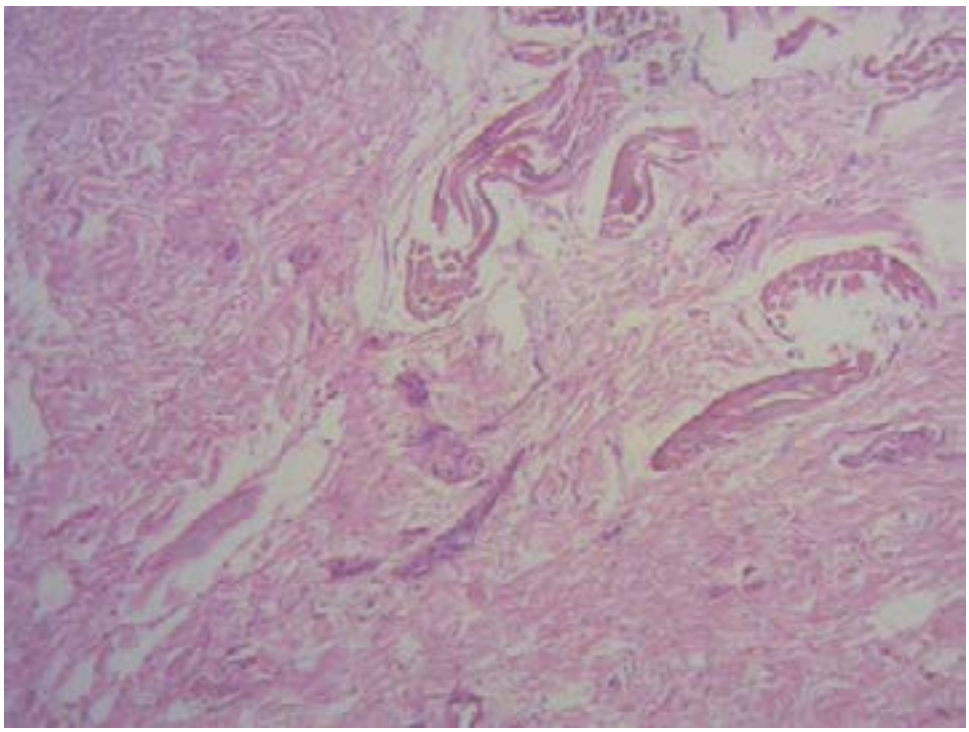

In this development, fundamental questions arose: why have we found that the cardiac fulcrum in adult human hearts has characteristics similar to a tendon, beyond the fact that it fulfills the same function of tethering the helical myocardium that other species have? Why does it not have the same structure as that found in the human gestational heart or in the child?
The interpretation we have is that the cardiac fulcrum of cartilaginous-osseous characteristic is a vestigial organ characteristic of the evolution of mammals. A vestigial structure should be understood as the retention during the process of evolution of genetically determined attributes that have lost part or all of their ancestral function in a given species (21). Due to this fact we find it in the initial process of human gestation, but then its osteo-cartilaginous histology disappears, remaining as a tendinous matrix sufficient to achieve the insertion of the myocardium in order to comply with a muscular power far below that of larger mammals.
It should be remembered that in bovines the *fulcrum* is bony in nature. **Figure 49** shows a histological section of the fulcrum and its relationships in a porcine heart.

Figure 49. Porcine heart. Relationships of the fulcrum. 1: fulcrum; 2: ascending segment inserting into the left end of the fulcrum; 3: right loop segment; 4: interatrial septum; 5: AV node (cardiomyocytes of the right segment intermingle with the neurofilaments).

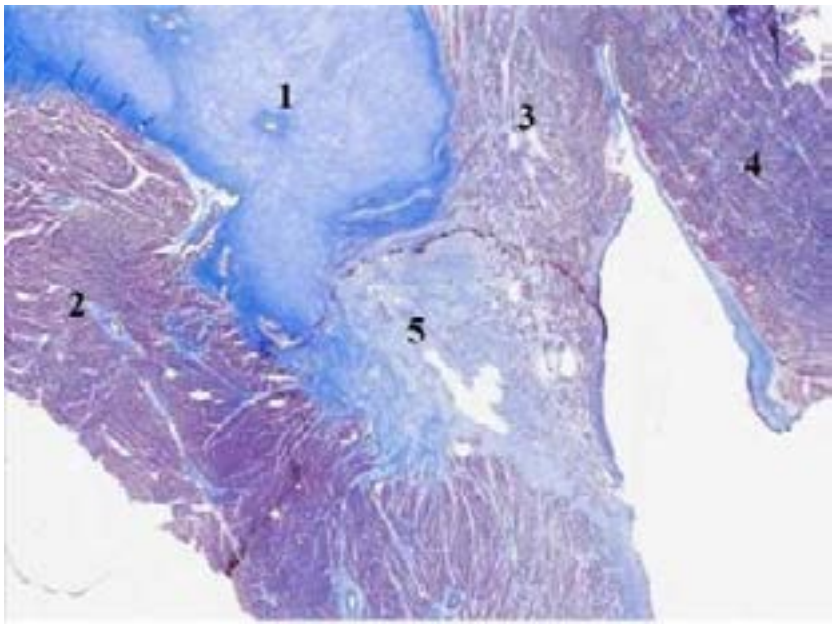

To faithfully establish the identity of the cardiac fulcrum, a histological analysis was also performed on the trigones in an attempt to find cardiomyocytes in them, as a possible insertion of the cardiac muscle in these structures. In our investigation only collagen tissue without cardiomyocytes was observed in the trigones, confirming that the fulcrum is the support of the myocardium, both at its beginning and at its end (**Figure 50**).

Figure 50. Trigones. Scalloped collagenous tissue and elastoid interstitial tissue are observed. No inclusion of cardiomyocytes is found. H&E technique (15x).

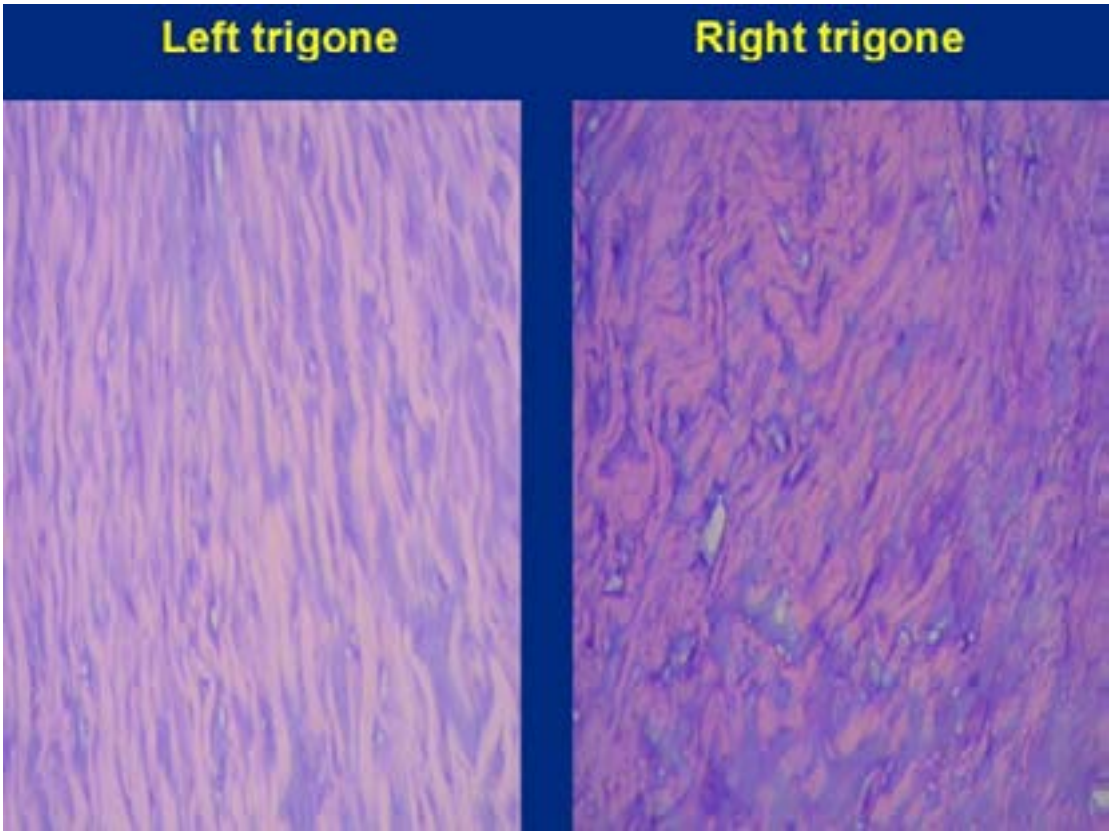

e- Images of the cardiac fulcrum

The bovine hearts, studied with computed tomography (**Figures 51 to 53**), magnetic resonance imaging (**Figures 54 and 55**) and simple radiology (**Figure 56**) evidenced the osteochondral structure found in the dissection, showing the same morphology and analogous size. In human computed tomography we have found, in the analysis of the region where the cardiac fulcrum is located in the dissections performed, the presence of intensity above 110 Hounsfield units (HU), while the adjacent muscle has units below 80 HU. Thus, in the image, the fulcrum structure reaches an average of 132 ± 4.5 HU. In the adjacent areas, corresponding to the myocardial muscle, this value was between 47.96 ± 12.5 and 77.59 ± 21.64 HU (**Figure 57**).

By means of echocardiography, recent and still unpublished works reveal the visualization of the cardiac fulcrum having as references for its location the septum, the right coronary leaflet and the tricuspid septal leaflet (**Figure 58**). The favored views have been: modified 3-chamber parasternal long axis view, modified apical 3-chamber view and parasternal and subxiphoid intermediate short axes views (between the great vessels and short axis at the level of the AV valves). The intermediate apical 2-chamber view (between 4 chambers and pure 2 chambers) allows longitudinal insonation of the fulcrum. Moreover, Sosa Olavarría et al (39) found the cardiac fulcrum with echocardiography, which they published under the title "Trainini's cardiac fulcrum in the fetal heart" (2023). They studied 50 simple human pregnancies with 18- and 37- week gestation fetuses. By means of fetal cardiac ultrasonography, 2D, color and three-dimensional Doppler, STIC, HD Flow and speckle tracking modalities were obtained.

Figure 51. Computed tomography. There is evidence of a hyperdense image in the topography of the interventricular septum adjacent to the root of the aorta, 3.7 cm long and a density of 298 HU (bovine heart).

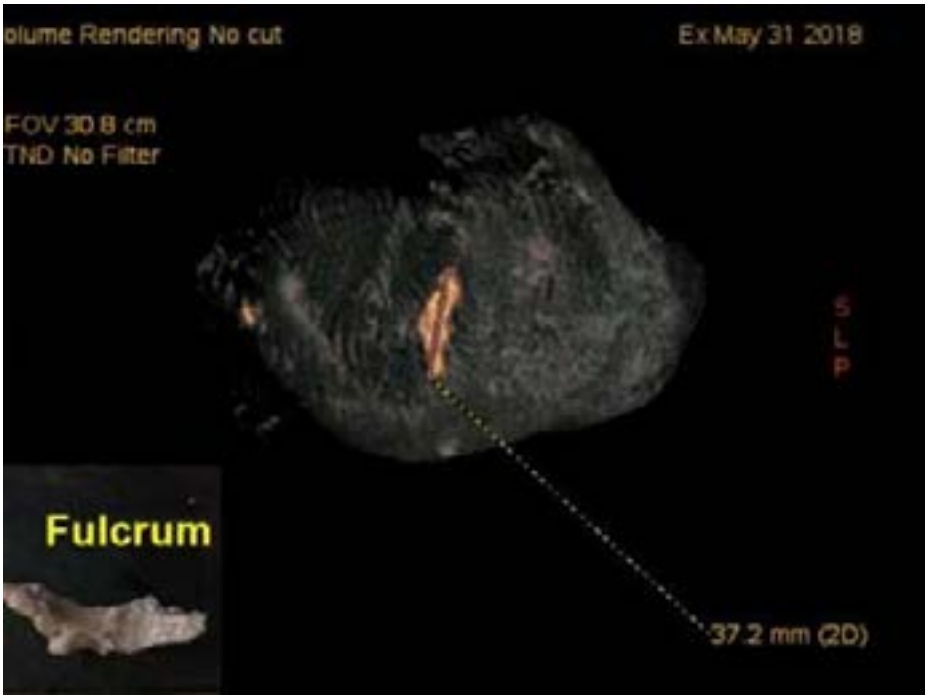

Figure 52. Cardiac fulcrum in computed tomography (bovine heart). The inset shows the resected fulcrum.

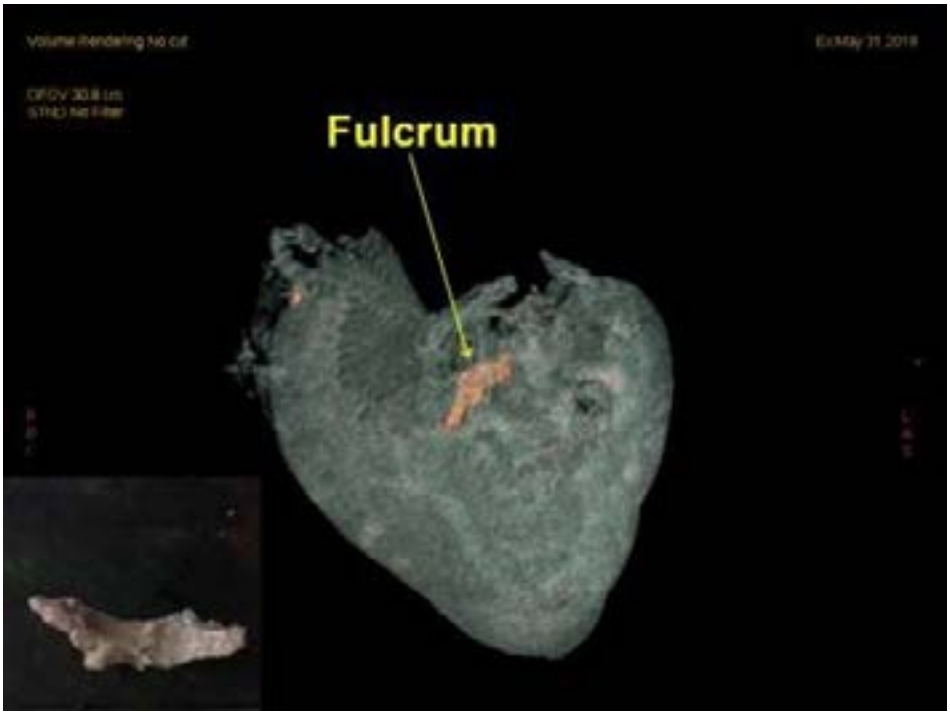

Figure 53. Computed tomography. The area marked with the arrow shows an image adjacent to the aortic root over the interventricular septum (bovine heart).

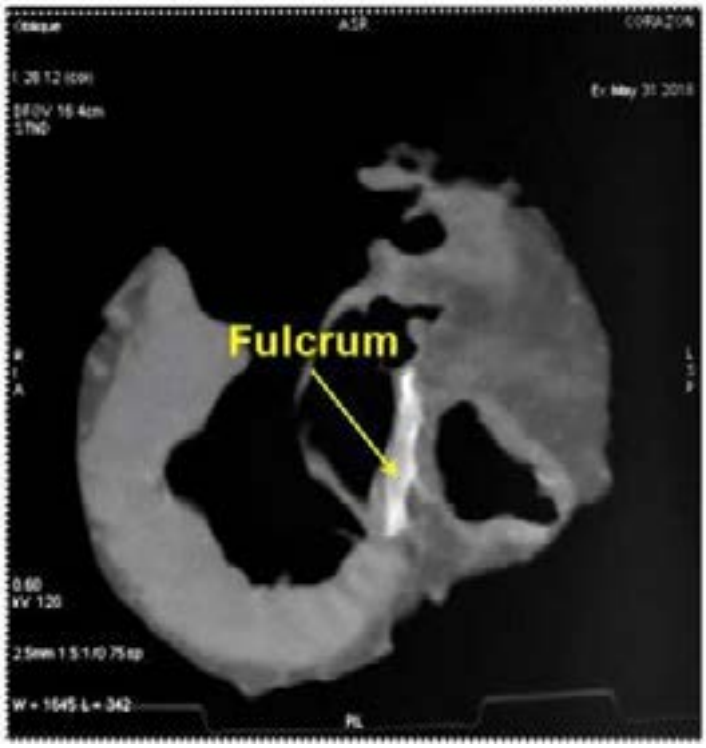

Figure 54. Magnetic resonance imaging in bovine heart.

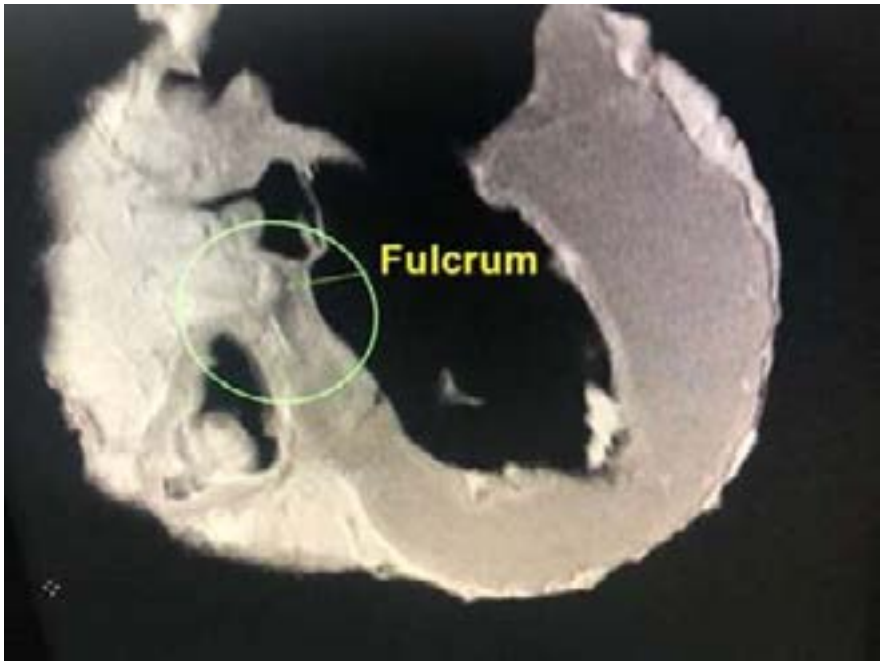

Figure 55. Magnetic resonance imaging in bovine heart.

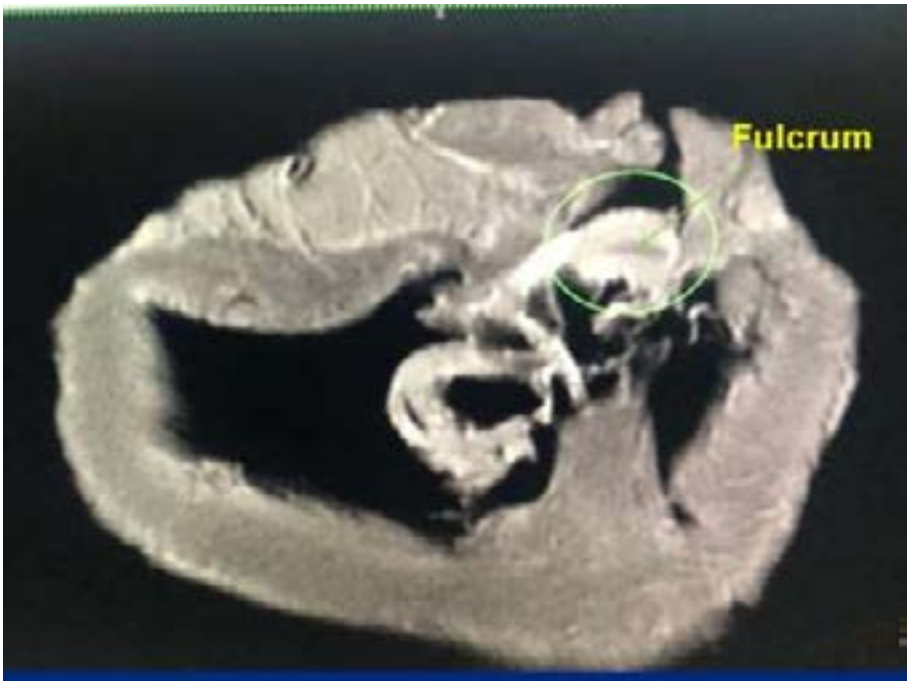

Figure 56. The cardiac fulcrum is observed in a radiological image with mammography technique in bovine heart.

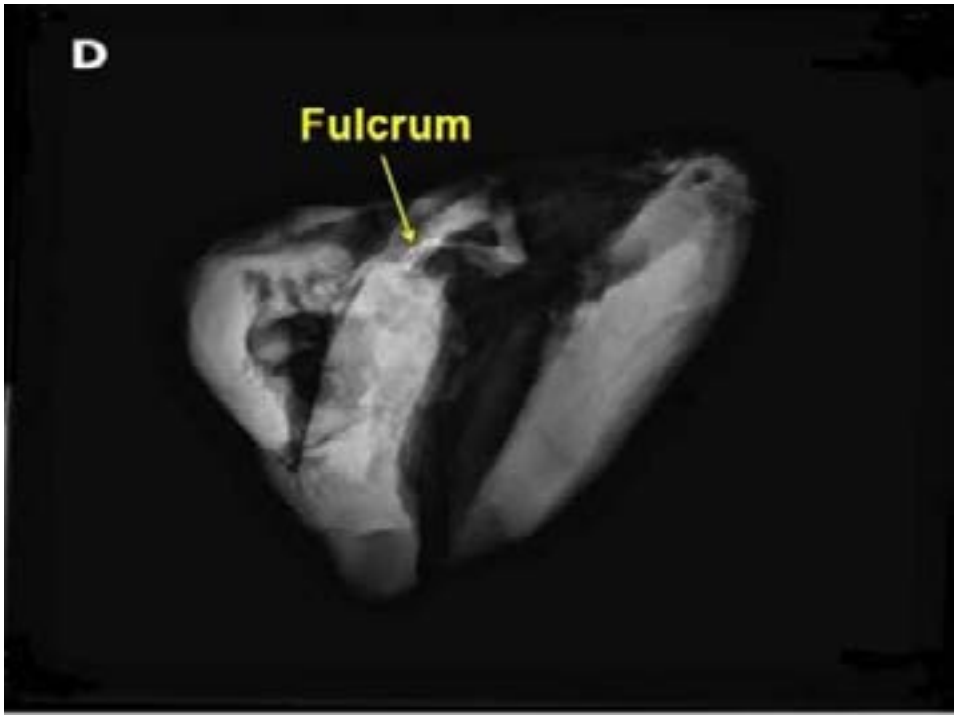

Figure 57. Computed tomography in a patient with evidence of cardiac fulcrum. PA: pulmonary artery; RV: right ventricle; LV: left ventricle; LA: left atrium

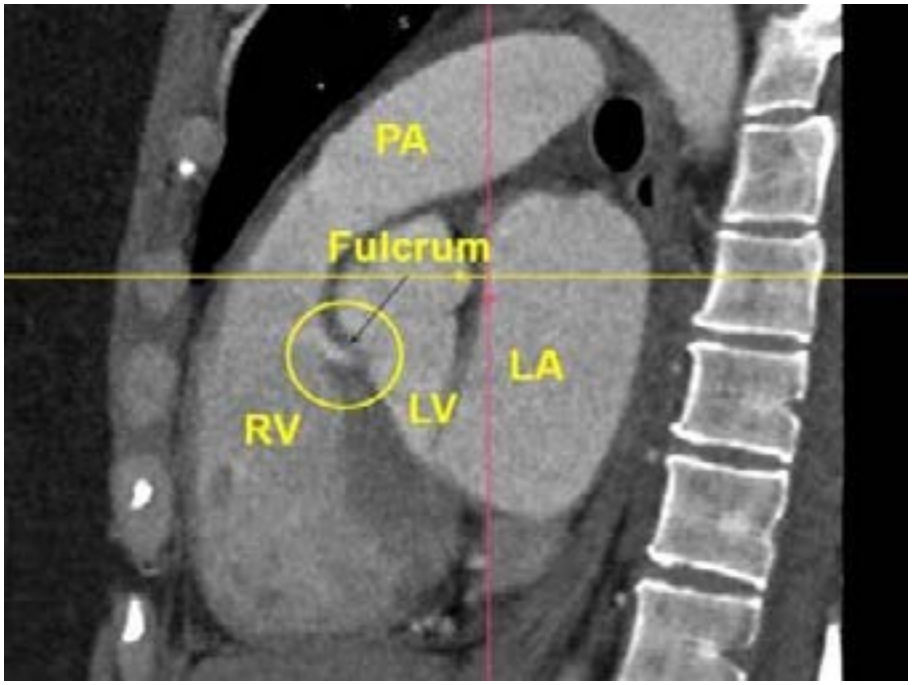

Figure 58. Echocardiographic 4-chamber view (left) with zoom on the septum (right) (human heart). RV: right ventricle; RA: right atrium; LV: left ventricle; LA: left atrium; AS: ascending segment entering the fulcrum (green arrow, yellow circle); red arrow: septal leaflet of the tricuspid valve. (Courtesy of Dr Efraín Herrero).

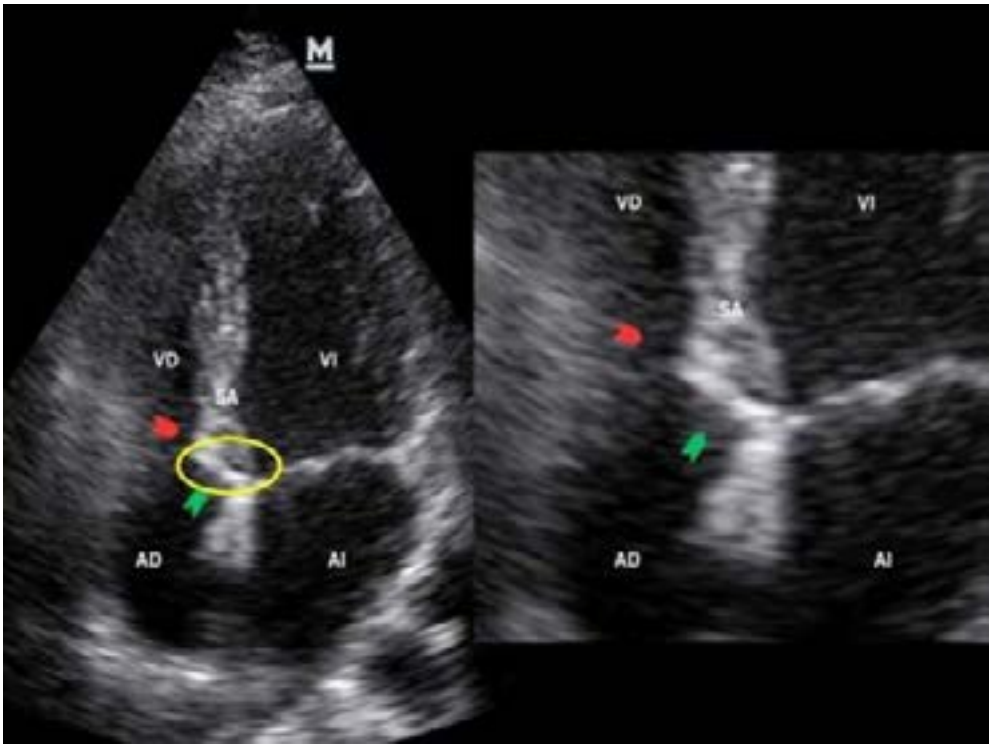

f. Kinetics of the Cardiac Fulcrum

The contraction and recoil of myocardial muscle fibers, whose ends must rest on some "fixed point" to have mechanical effect, would not be effective without the existence of the cardiac fulcrum. The fulcrum is located at the center of gravity of the lever, which ensures its functionality in the cardiac system, allowing the forces to be equally distributed. For this mechanism to be subjected to tractions in a magnitude of one hundred thousand times a day, it must meet certain conditions: a) stability; b) resistance; c) heterogeneity; d) anisotropy; e) elasticity; and f) plasticity. These faculties allow it to reach a certain level of stress when subjected to loads and then recover its shape when the loads are removed (81).

As can be seen in **figure 59**, if only a force (F1) is applied to the fulcrum at a point (P1) on the left insertion line, the fulcrum would move in that direction, since it is a semi-floating body. But if a force (F2) equal and opposite to (F1) is applied at the insertion point (P2), opposite to (P1), on the right insertion line, the fulcrum would not move. As both forces are produced by the same muscle fiber of the myocardium, which originates at (P1) and ends at (P2), both forces are equal (similar to those of an elastic band). The same can be applied to the totality of myocardial muscle fibers inserted in the myocardium along the lines of insertion (**Figure 59**). Therefore, to maintain the equilibrium of a system of forces applied on both sides, these forces must be equal and opposite (80).

Figure 59. The yellow arrows show the orientation of the cardiac fulcrum movements during systole, and the black arrows during suction (protodiastolic phase of myocardial contraction PPMC). The inset shows that if only one force is applied to the fulcrum, it will move. On the contrary, if a force (F2) equal and opposite to F1 is applied at the insertion point P2, opposite end to P1, the fulcrum will not destabilize.

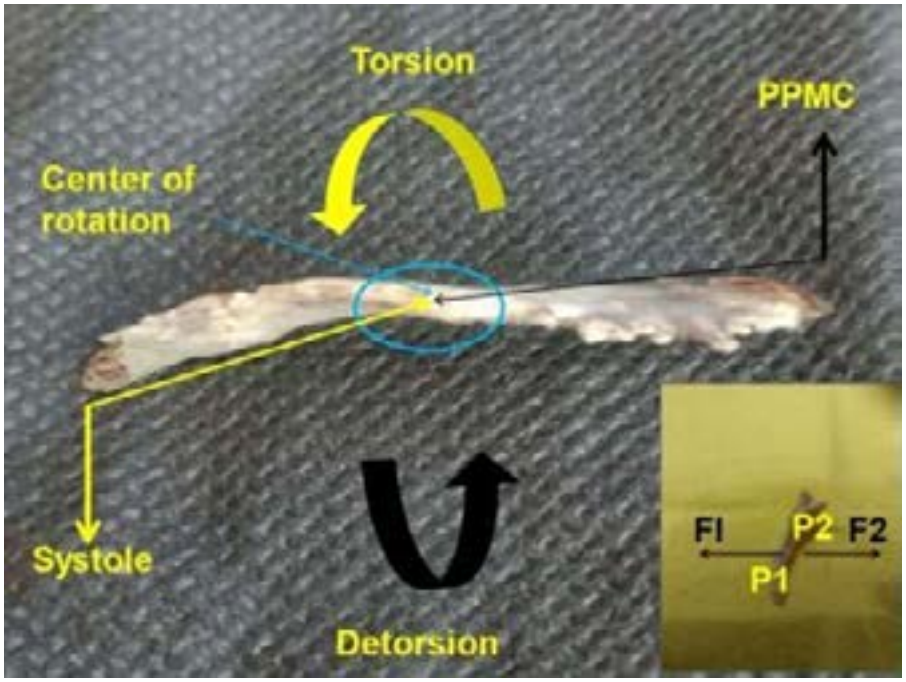

The *fulcrum* acts like a seesaw during cardiac movements. During systole, it approaches the apex, primarily at its right end, where the continuous myocardium originates, while the opposite end, where the fibers of the ascending segment insert, rises. During the beginning of diastole, in its first 80-100 ms, there is muscle activation with energy expenditure. This phase, classically called the isovolumic diastolic phase, in light of these findings in our research, we have named it the protodiastolic phase of myocardial contraction (PPMC). At this point in the cardiac cycle, the fulcrum undergoes movements opposite to those previously described, thus performing the movements of a seesaw. In turn, the fulcrum's torque is molded by twisting and detwisting movements, alternately during systolic ejection and PPMC. During diastole, it returns to its initial resting position. To achieve this hysteresis, reformulation requires external (electrical) stimulation; hence, it is called extrinsic hysteresis, as opposed to hysteresis achieved through endogenous factors (intrinsic hysteresis, e.g., rubber). In the sequential movements of the myocardium, each segment, through its action, favors the other (**Figure 60**).

Figure 60. A: in systole the descending (DS) and ascending (AS) segments contract in opposite directions generating myocardial torsion. B: In the active LV Protodiastolic Phase of Myocardial Contraction (LVPPMC), the DS relaxes and the AS remains contracted, this interplay allowing to keep the atrioventricular valves closed with isometric myocardial deformation to generate an intraventricular pressure drop. C: Diagram showing the phases of the cardiac cycle and the duration of DS and AS contraction.

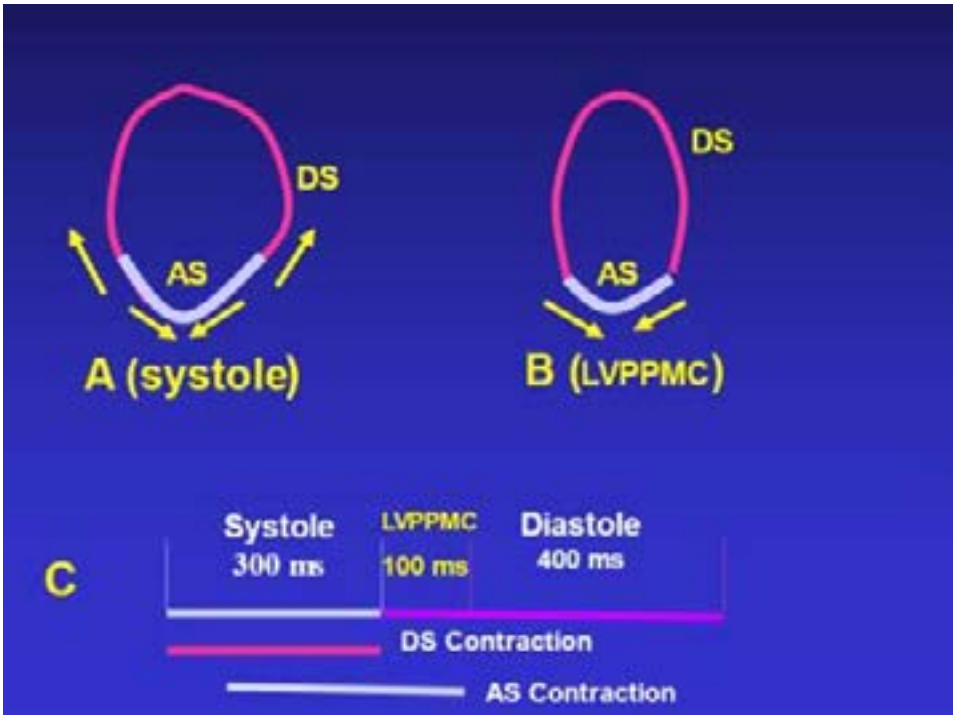

As the *fulcrum* is subjected to the forces of the myocardial segments attached to its structure, it obviously registers modifications in the space that even lead it to model its morphology. This concept is explained by the fact that the myocardial movements are sequential and superimposed on the myocardial segments, determining tensions that act as a lever arm with epicenter at the point of support, i.e. the *fulcrum* (81).

During systole, the different segments contract sequentially and synchronously according to the stimulation pattern we have investigated. This begins in the right segment, tethered to the right and anterior sector of the *cardiac fulcrum*, with continuation in the left, descending and ascending segments. The fundamental peculiarity of this activation is that although at its origin it is unidirectional, upon reaching the junction of the descending and ascending bands, simultaneity is produced -by transverse activation- in both, generating a helical movement essential for the myocardium to eject the ventricular content at a speed of 200 cm/s (Figure 1) (43-46). This systolic activation produces longitudinal shortening of the myocardium with circular narrowing and the muscular torsion that characterizes its helical conformation, which implies that the fulcrum undergoes a downward displacement, accompanied by a torque from its right end toward the opposite end due to torsion (Figure 59).

When the ejection period ends, the ascending segment remains in an active process of contraction in its terminal part, that is, in its attachment to the *cardiac fulcrum*, occurring mainly in its antero-inferior portion and posterior surface. This phase occupies about 80-100 ms and is intermediate between systole and diastole. We have called it the Protodiastolic Phase of Myocardial Contraction (PPMC) and it is caused by the process of generating negative intracavitary ventricular pressure, which, upon opening of the atrioventricular valves, will precipitate the entry of blood into the ventricles by a suction mechanism. During this phase the myocardium lengthens, narrows and untwists (11,82).

Under these stresses the fulcrum undergoes an upward displacement and generates a torque opposite to that during systole. Obviously, this continuous torque in coupling models the fulcrum with a torsion that is well observed in a profile view (Figure 59). The torque is a demonstration of the opposing forces that stress the fulcrum; thus, the ascent-descent of the continuous myocardium together with torsion-detorsion models its morphology.

The section of the *fulcrum* is not axisymmetric in relation to its axis, therefore the torsion- detorsion it undergoes in each cardiac cycle determines deformations at each point of its structure. Thus, the torque (twisting force) (**Figure 61**) applied at each of its ends during the cardiac cycle causes the free ends of the bar to rotate at an angle Φ, which is called the twisting angle or twist. In this deformation the maximum shear strain is produced in the middle of the fulcrum surfaces and around the axis at which it rotates. When this system of

forces is applied, a rotation effect is produced, without achieving a manifest shift. In the fulcrum we would be in the presence of two couplings (a system of parallel forces of equal intensity but opposite directions, with resultant equal to 0) meeting at point 0. In synthesis, the continuous myocardium meeting at its origin and end with the fulcrum develops a moment of force (torque) which determines its rotation in opposite directions that are equalized at point 0 (center of rotation). When these two forces counteract each other, the sum is zero.

Figure 61. Torque of the cardiac fulcrum.

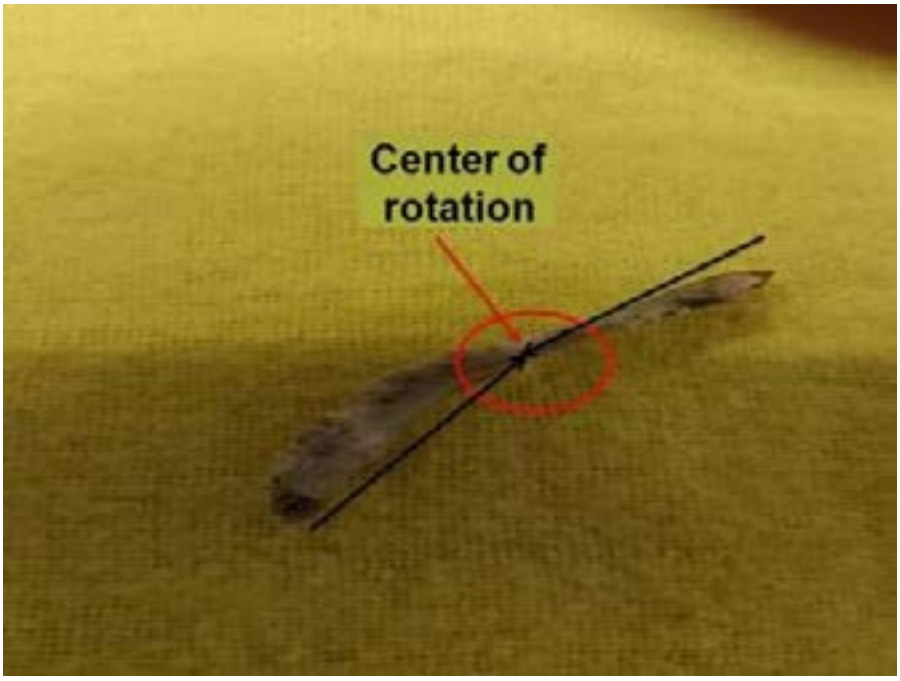

It was also possible to document the *fulcrum* during movement. We have observed *fulcrum* displacements in adult humans during the phases of the cardiac cycle in resonance magnetic, which implies possibilities of knowledge of cardiac mechanics and also of pathological situations. In systole (**Figure 62**) the *cardiac fulcrum* descends horizontally due to the concomitant myocardial shortening and torsion (clockwise rotation), which allows the image to be outlined. During PPMC (**Figure 63**), when the terminal end of the ascending segment contracts, the heart undergoes elongation accompanied by detorsion (counterclockwise rotation). In this phase of the cardiac cycle the *fulcrum* is observed with a certain pause in the movement according to PPMC, without volumetric changes in the ventricular chambers and with geometric deformation of the myocardium. In diastole the *fulcrum* is shown in its full magnitude with its characteristic morphology (**Figure 64**).

Figure 62. Systole (myocardial shortening and torsion). Resonance magnetic in adult human.

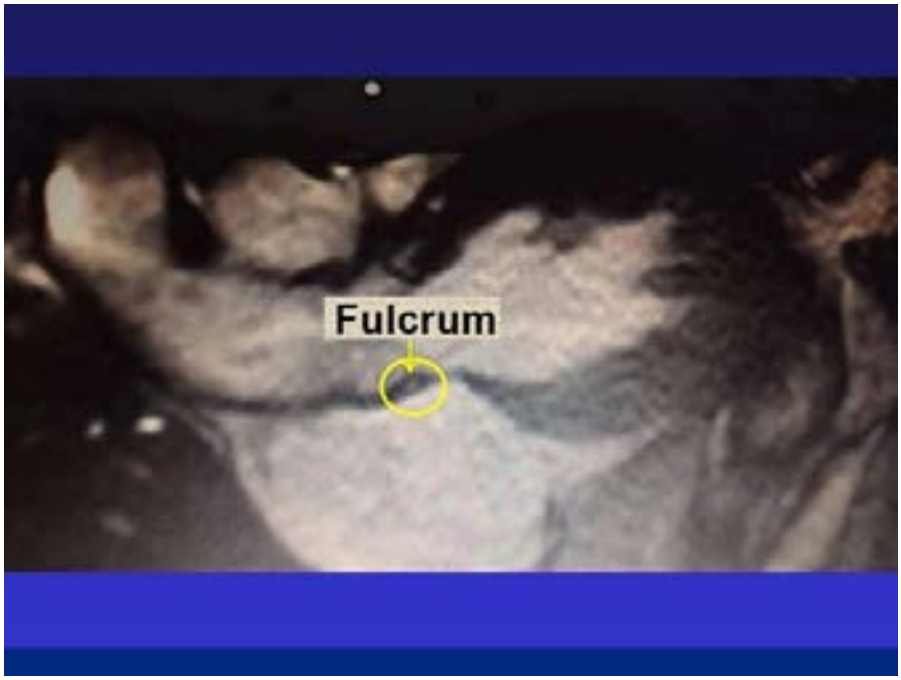

Figure 63. PPMC (myocardial elongation and detorsion). Resonance magnetic in adult human.

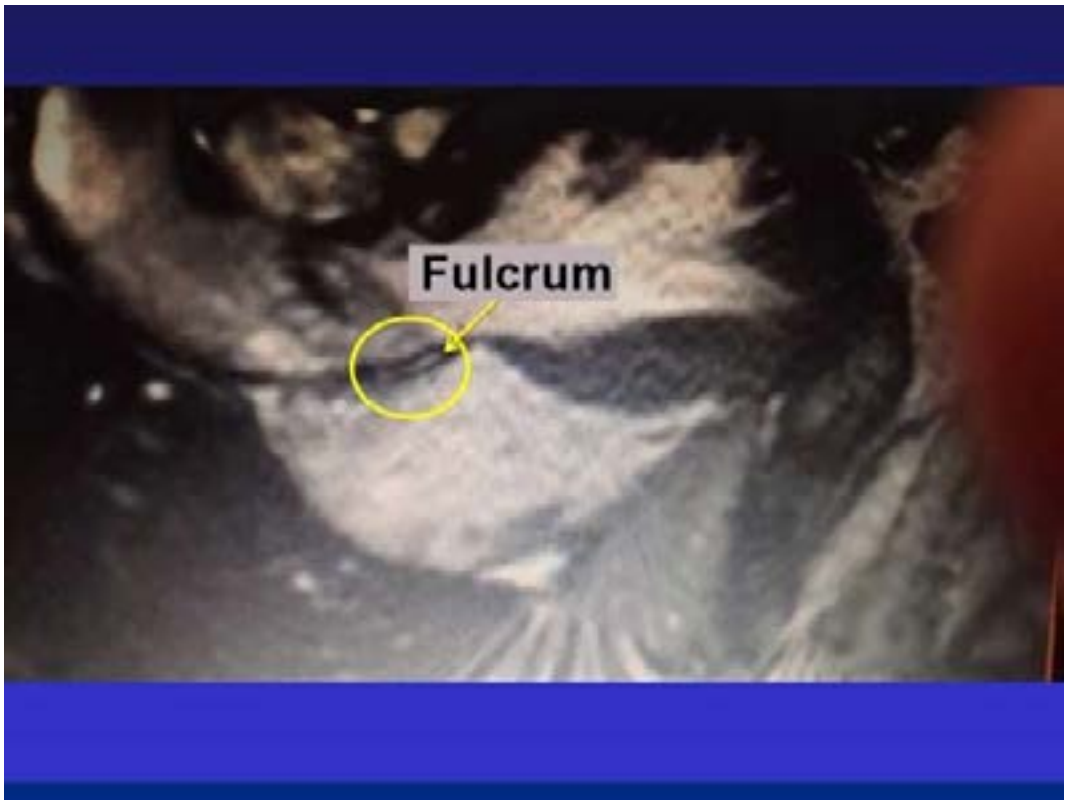

Figure 64. Diastole (myocardial enlargement). Resonance magnetic in adult human.



The *fulcrum* is not only a support for the myocardium. The heart, with its movements, generates tensions that are absorbed by the fulcrum, avoiding their transfer to the aorta. In this way, it prevents the aorta from traction and rotation, which would produce resistance to blood ejection. From the anatomy the *fulcrum* can be confirmed to present on its upper edge a ledge that adapts to the aortic annulus determining a proof of the organization pattern of the helical heart (Figures 14 and 15).

g. Analysis of the continuous helical myocardium and its support: the fulcrum

This study on the anatomy and histology of the myocardium provides evidence that the myocardial fibers constitute a continuous muscle that describes a double helicoid to form both ventricles and that, to fulfill its muscular function, it needs a point of support that we have investigated, found, and called the *cardiac fulcrum*. Thus, the myocardium has the following characteristics derived from the anatomical and histological analysis carried out:

1. It is constituted by a single, continuous, coiled muscle that forms a helicoid with two spirals.
2. The myocardium, as any muscle, is tethered at its origin and its end to a support that we have described and called the *cardiac fulcrum*. The muscle fibers surrounding the atrioventricular annuli have no insertion in them.
3. The spatial helical arrangement forces the muscle to superimpose segments in its spatial conformation.
4. This anatomical arrangement has a profound correspondence with myocardial movements and with the stimulation that runs through its segments.
5. The transverse interconnections between the muscular tracts do not invalidate the concept of continuous myocardium, this situation being understood in its helical conformation, as a result of the evolutionary development with the aim of obtaining solidity in its structure in strict relationship with the potential of its function.
6. The *fulcrum* is contiguous to the AV node, which with its specialized fibers surrounds and invades it.

Therefore, the myocardium can be defined as a single muscle that in its longitudinal continuity adopts a spiralling spatial conformation, inserted at its ends (origin and end) in an osteochondral-tendinous nucleus according to the specimens analyzed, called *cardiac fulcrum*. This arrangement defines the two ventricular chambers (86).

The myocardium as a single muscle coiled in a helix is not reliably represented by the word “band”, a term that has generated discussion from a strictly academic anatomic point of view. The concept of “band” does not correspond to the etymology of the word and to a complete spiralling individuality of its course where it is obliged to superimpose the segments. In contrast to the band concept, some authors have proposed the concept of a “mesh” arrangement of myocardial fibers (73). This term is not acceptable either, since this structure is not related to the functional anatomical organization of the heart. There are solid criteria that support the concept of continuity of the myocardium as a single, continuous, spiral muscle:

1) Muscular homogenization masks the real spiral continuity of the fibers by overlapping its segments to obtain their helical conformation. This implies considering that its compact structure, by being folded as an helicoid, is functionally required in birds and mammals in order for blood to be ejected at a high speed in a limited time, through an organ that must supply two circulations (systemic and pulmonary). The anatomical investigation of the heart through adequate dissection, histological exploration, the analysis of images obtained by radiological and echocardiographic examination, electrophysiological studies carried out with three-dimensional electroanatomical mapping and diffusion tensor cardiac magnetic resonance imaging shows the continuous muscular trajectory circumscribing the two ventricles (**Figure 65**).

Figure 65. Images of myocardial fibers obtained by diffusion tensor imaging, showing their characteristic helical shape.

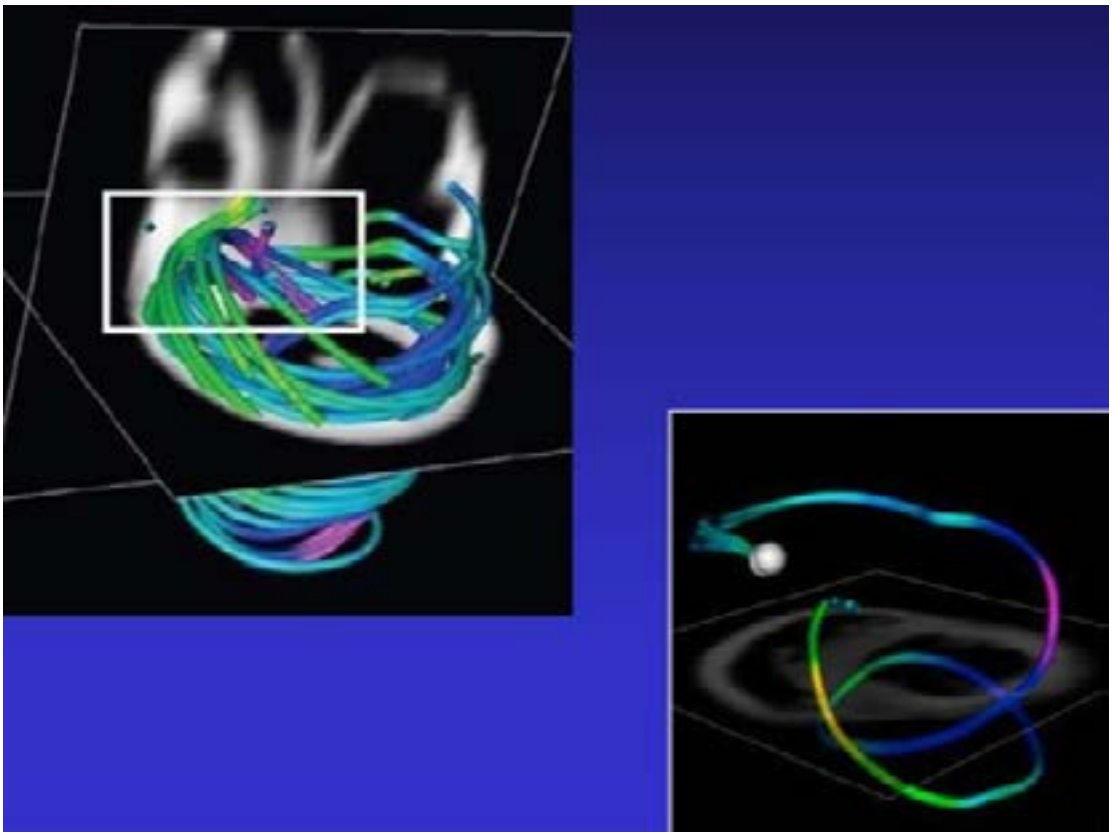

1) When the myocardium is unfolded and a similar thickness is obtained along the entire length of the muscle, it is evident that its continuity is real. When the myocardial muscle is folded, the thickness of the right ventricle is found to be less than that of the left ventricle, since the former is composed of a single segment (right), while the latter has two superimposed segments (descending and ascending).

2) Its function leads it to have a support point as any skeletal muscle, both at its origin and at its end. If the myocardium did not have this spatial helical anatomical conformation, if it did not have an insertion at its ends located in the cardiac base and did not remain free in the apex, that is, pendular in the thorax; and also, if it did not present a stimulation that allows its torsion and detorsion, it could not fulfill its extraordinary muscular power. Echocardiography with speckle- tracking techniques has demonstrated the shortening and lengthening movements during the systolic and suction phases, respectively (6,17.26.27,29). To calculate the twist, the echocardiographers' algorithm performs an algebraic subtraction (adding the value of the positive rotation of the apex to the negative of the base), In our experience it is around +19 ± 9 degrees in normal subjects, always predominating the apical rotation.

The father of biomechanics, Giovanni Borelli (1608-1679), described myocardial torsion by comparing it to the slipping of a rag. Richard Lower in 1669 in your "Tractatus de corde: ítem motu et colore sanguini,et chyli in eum transitu" (14,80) considered that the myocardium was subjected to a torsional movement related with the helical fibers that composed its fibers. He expressed that the heart exerted a movement similar to a "wringing of a linean cloth to squeeze out the water" ("estrujar un paño de lino para exprimir el agua"). This concept was later studied in mice by Henson (18), and verified in humans both in electrophysiological and imaging (echocardiography, magnetic resonance imaging) studies (73). The heart achieves the ejection of its contents by torsion of its walls and the initiation of its filling through detorsion. The torsional movement synchronous with ventricular longitudinal shortening can be explained through the helical arrangement and continuity of the cardiac muscle (24).

3) The trigones do not present cardiomyocyte insertion, which confirms that the only myocardial tether is the fulcrum.

4) Myocardial dissection, histological analysis and cardiac function do not correlate with a mesh conformation.

5) The contiguity of the cardiac fulcrum to the AV node, surrounded by a rich neurofilament plexus, puts us in the anatomical consideration of an electromechanical unit involving stimulation energy and muscle mechanics.

In this investigation, fresh bovine, porcine and human hearts have been used to obtain detailed descriptions to elucidate the true spatial myocardial architecture.

Conclusions

In summary, as expressed above, we find that the orientation and opposite rotational movement of the fibers in the heart, both at the base and at the apex, determine the anatomo-functional model of the continuous helical myocardium. However, the question that arises from the logic of the movement is that, to achieve torsion and consequent detorsion, the muscle segments that form the continuity of the ventricular chambers should perform it on a point of support just as a skeletal muscle does on a firm insertion. This was found in our research and called *cardiac fulcrum*.

The aortic annulus is not continuous. In a sector of its circumference, located between the ends of the trigones, it is interrupted, and it is here where the anterior leaflet of the mitral valve is inserted. The pulmo-tricuspid cord is located in front of an area that surrounds the anterior two thirds of the U-shaped circumference of the aortic annulus, whose open end (posterior) is occupied by the anterior leaflet of the mitral valve. At its ends this tissue has two trigones. The right fibrous trigone (central fibrous body) is the most prominent and is located between the tricuspid (right), aortic (posterior) and pulmo-tricuspid (anterior) orifices. The less prominent left trigone is located between the mitral orifice (left) and the aorta. In the continuity of the aortic orifice with the posterior leaflet of the mitral valve there is no connective tissue, since laterally, the two fibrous bodies are continued by a conjunctive band that surrounds the mitral valve orifice partially and then fades progressively. The septal leaflet of the mitral valve is located as a wedge between the two trigones and can be considered an extension of the atrial endocardium.

With the heart folded we find the *fulcrum* embraced by the pulmo-tricuspid cord and the pulmonary artery on the left side of the aorta. The right ventricle is positioned anteriorly; therefore, the *fulcrum* shows how the bundles that emerge from it, since it is frontal, hide the tethering of the ascending segment to this structure located below this view. When the unfolding of the pulmonary artery and the pulmo-tricuspid cord is started, the insertion of the ascending segment in the *fulcrum* becomes evident (Figure 37).

For three centuries, it has been considered that the myocardial fibers insert into the fibrous skeleton of the heart. The development of the anatomy reported around 1970 by Torrent Guasp (40-42,58) foresaw that the myocardium begins and ends at the base of the great vessels, but that the anchorage of the fibers does not take place in the atrioventricular annuli, but is simply attached, as confirmed by images obtained by diffusion tensor magnetic resonance imaging. Our investigations have demonstrated, in the trajectory of the septal segment of the aortic ring that extends from the left trigone to the right, a structure that we have called *cardiac fulcrum* (below the origin of the right coronary artery), where the continuous myocardium is tethered at its beginning and end, as in all muscles it needs support to fulfill its function. On the other hand, we have not found insertion of cardiomyocytes in the collagen matrix of the trigones, confirming this finding (Figure 50). In all investigations of animal and human hearts, the location of the fulcrum has been found to be contiguous but different from the classic fibrous nucleus (**Figure 66**). The right and left trigones occupy the non-coronary sinus, the posterior half of the left coronary sinus and the posterolateral part of the right coronary sinus. The fulcrum is located in an anterior position, below the right coronary artery.

Torrent Guasp considered that the myocardium lacks a fixed point of support like those of the muscular system to fulfill its function of strength. In this sense, he analyzed that it would function as does the circular musculature of the arteries; thus, it would be supported by the contents of the chamber itself (hemoskeleton). In our research we always considered that there should be a fixed support in the myocardium that would allow it to rotate in helical fashion to fulfill its movements and the fundamental muscular power of shortening-torsion and lengthening-detorsion. The investigation of a support in the continuous myocardium correlates with an organic machine, such as the cardiac one, which, without a solid attachment to a resistant nucleus, would lack the mechanical faculties necessary for its considerable power.

The musculature that forms the right ventricle corresponds to the beginning of the continuous myocardium (right segment) that originates in the cardiac fulcrum. When the right segment separates into two main groups of fibers, forming the paraepicardial and paraendocardial bundles, a raphe is delimited between them called the pulmo-tricuspid cord, located between the pulmonary artery and the tricuspid valve. In relation to the autochthonous muscle bundles that constitute the left ventricle, the ascending segment ends at the base of the aorta. Let us recall that the descending segment is continuous between the left and ascending segments, without any attachment to the fulcrum. Before attaching to it, the ascending segment gathers in a bundle whose outermost fibers form a curvature to reach this attachment. The innermost fibers enter directly without describing any bias. The cardiac fulcrum constitutes a solid point in the attachment of this segment to this structure.

This point of attachment implies, as in all muscles, the function of supporting the muscular lever and also allows it to act as a bearing or pad, preventing the ventricular rotation force, either by torque or torsional effort, from being transferred to the aorta, thus dissipating the energy produced by the movement of the muscular helix and avoiding the artery from being strangled or bent during the period of systolic ejection (56,61,65,66). In the human hearts investigated, the findings are surprising from the interpretation, starting from the basis that it is logical to consider its presence in the entire

evolutionary chain of mammals. It should be considered that this structure, when analyzed in the different specimens, has in common its function of supporting the helical myocardium in order to generate the power required by any muscle, which is different in different mammals. Therefore, its presence is constant in all the hearts studied in both bovids and humans, but its structural characteristic is different. And this difference in the intimate analysis of the cardiac fulcrum is undoubtedly related with the resistance that it must oppose to the energetic action of the myocardium in hearts of different sizes.

Figure 66. On the left, a sectioned bovine heart is seen, and on the right, its echocardiographic counterpart in a human: apical 4-chamber view: both atria and ventricles are observed, in addition to the mitral and tricuspid valves. In the heart cross, in the interatrioventricular septum, a bright image is seen. This is the fibrous skeleton of the heart. Within the fibrous skeleton of the heart, there is a structure where the helical myocardium begins and ends: the cardiac fulcrum. In this image, note how the ascending segment of the apical loop enters this hyperrefrigerant zone we described. Ad: right atrium. Ai: left atrium. SA: ascending segment. RV: right ventricle. LV: left ventricle. Red arrow: septal leaflet of the tricuspid valve. Green circle: cardiac fulcrum

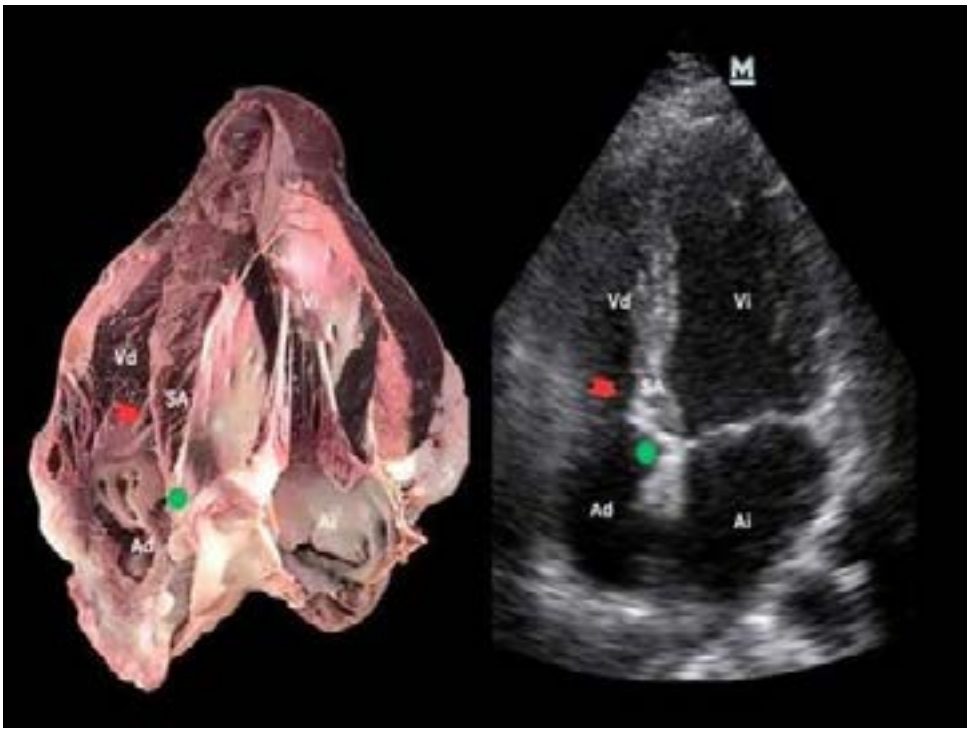

It should be considered that what makes the concept of the fulcrum (support) important is the interweaving between the myocardial fibers and this chondroma. It is the functional element that gives value to this structure.

The fulcrum should not be considered as a nucleus with clear and rigid borders. The insertion of the myocardium in a structure of such characteristics would be inconvenient, since it would generate at that point a sudden tension to movement with tears in the insertion, given the force exerted by the myocardial band to eject the ventricular content. In addition, between bovids and humans, its consistency decreases because the force to be exerted is different according to the body weight.

What we have found in both macroscopy and histology of bovine and human hearts (gestation, infant and adult) is a structure that grows in density towards a more solid center. In this staggering from lower to higher density of the fulcrum, the fibers are inserted as in a tendon matrix (equivalent to what would be the insertion of the tendons of skeletal muscle in the bone). This should be understood as a need to dissipate energy gradually with the least possible traction (bearing mechanism), avoiding an abrupt and repetitive action and reaction principle, and also preventing the aorta from being dragged in the helical movement performed by the band.

We consider that the worth of a structure lies in its function. The fulcrum is important for its function of supporting the myocardium. Without this insertion, it is impossible to surmise the movements and energy of the myocardial band to support the necessary circulatory physiology.

Finally, regarding this important topic, we would like to quote what was published in 2022 in “Anatomy, Histology, Embryiology”, by Best Adam et al (8) supporting the priority of our finding referred to the cardiac fulcrum:

In human cardiac anatomy, in addition to trigones and atrioventricular rings, the heart has a cardiac fulcrum (Figure 1). Works by Trainini and coauthores elucidated the value of this structure in humans and proposed its function and importance once they

had observed the attachment of the continuous myocardium to the fulcrum and naming the structure the 'cardiac fulcrum' (Trainini et al., 2021; Trainini et al., 2022). They proposed that the fulcrum, a thickening at the base of the aorta made up of a collagen matrix, is essential for anchoring the myocardial band allowing the band to contract and relax maintaining efficient cardiovascular blood flow (Trainini et al.2021, Trainini et al., 2022)".

"Anatomy, histology, developmental functions of Ossa cordis. A review".

Best A, Egerbacher M, Swaine S, Pérez W, Alibhai A, Rutland P, Kubale V,. El- Gendy S, Alsafy M, Baiker K, Sturrock C, Catrin R.. University of Nottingham, UK; University of Tirol, Austria, University Collegue Of London, UK; University of Montevideo, Uruguay-Anat, Histol, Embryol 2022; 00:1.13

CHAPTER 2

ANATOMY-PHYSIOLOGY OF THE AV NODE-CARDIAC FULCRUM SYSTEM

In this study, the anatomical and histological relationship between the cardiac fulcrum and the atrioventricular node in human, bovine, and porcine hearts was analyzed, as well as the possible functionality between the two structures. This situation will be analyzed in detail given its importance (**Figure 67**). For this purpose, hearts detailed in Chapter 1, section b of this text ("Anatomical dissection of the helical heart") were used.

The single continuous helical myocardium was deployed according to the technique published in our works (50,73). There is a fundamental concept at the beginning of the unfolding, since any attempt not to respect in the dissection the axes where the myocardium folds as a helicoid, produces a rupture of the cardiac mass. The conjunction between the beginning and end of the cardiac muscle at the cardiac fulcrum constitutes a meeting point between the right segment and the ascending segment, origin and end of the myocardium. Thus, both ends are located in the same place, the origin of the myocardial fibers being in a plane anterior to those of its termination. Samples were taken from the AV node and His bundle in Koch's triangle (**Figure 67**).

Figure 67. 4-year-old human heart: Macroscopy of Koch's triangle, delimited by the septal leaflet of the tricuspid valve, the tendon of Todaro and the coronary sinus. This triangle is a reference to find the AV node.

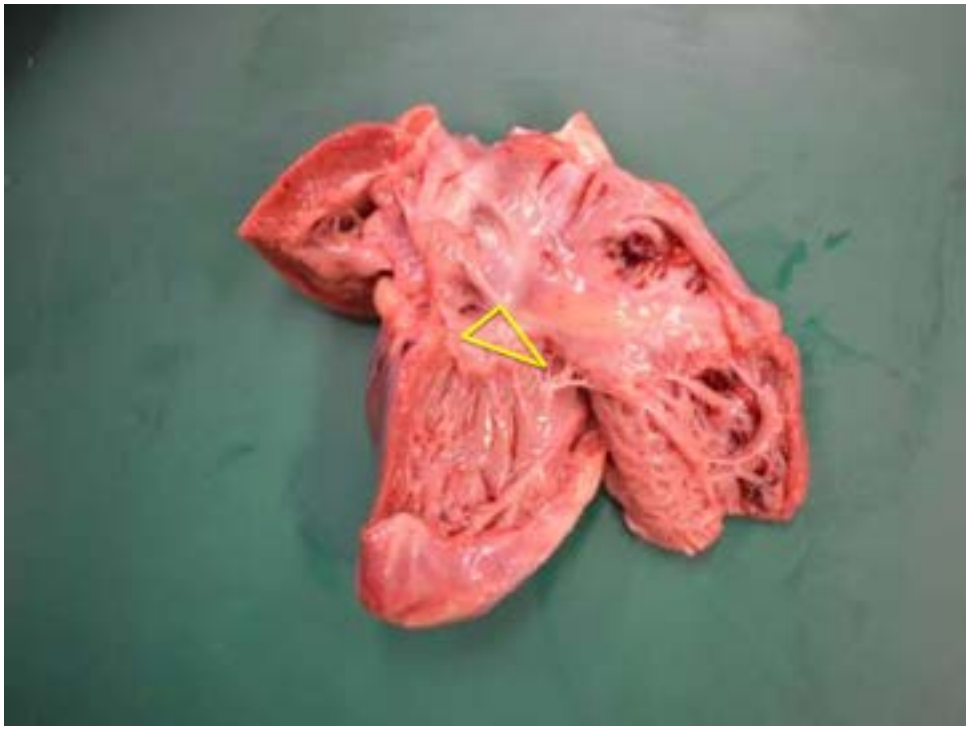

Results

The *fulcrum*, being located in the atrioventricular junction at the insertion of the interventricular septum, below the aorta and pulmonary artery, is adjacent to the Aschoff-Tawara AV node, which is located to its right (**Figures 68 to 71**). The heart support, at its right end, reaches the tricuspid valve ring.The AV node is positioned at the atrioventricular junction, at the base of the muscular septum, below the origin of the great vessels. It is adjacent to the *cardiac fulcrum*, located between it and the implantation of the septal leaflet of the tricuspid valve. It constitutes a conglomerate of cells (specialized myocytes) that

R.F. Rushmer defines as a spherical or bulbous end composed of bundles of fibers (34-36) to transmit electrical impulses to the myocardial mass. In its continuity, it is slightly transformed into the bundle of His, of short extension, sometimes even nonexistent. In humans it is approximately 5 mm long, 3 mm wide and 1 mm thick and is irrigated by a branch of the coronary arteries, generally from the right coronary artery in 90% of cases and from the circumflex artery in the remaining fraction (15).

Figure 68. Human embryo heart showing the relationship between the AV node (2) and the cardiac fulcrum (1).

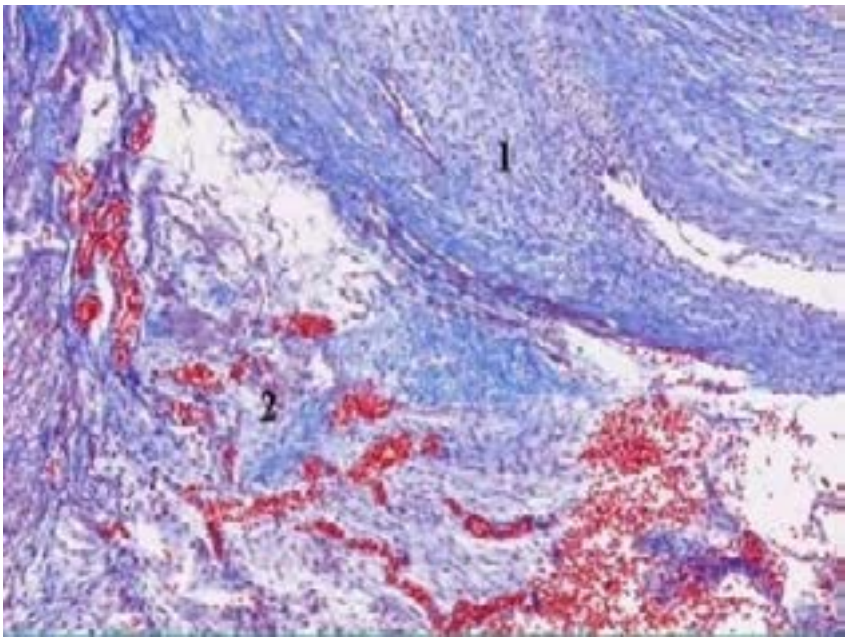

Figure 69. (Bovine heart). Masson's trichrome technique, 25x. Tangential section of the fulcrum, showing bony trabeculae of the fulcrum including plexuses with neurofilaments. 1: bone tissue. 2: terminal plexuses. 3: Fibroconnective tissue.

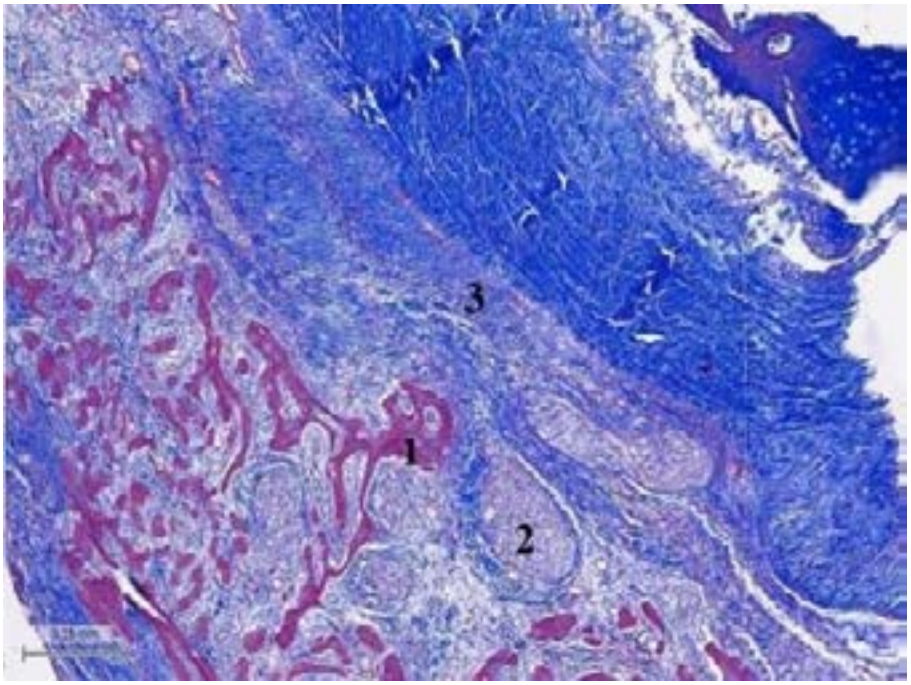

Figure 70. 36-day-old newborn human heart. Magnification 20x. The cardiac fulcrum of cartilaginous matrix is seen with the myocardium and adjacent AV node. AV: Aschoff-Tawara atrioventricular node.

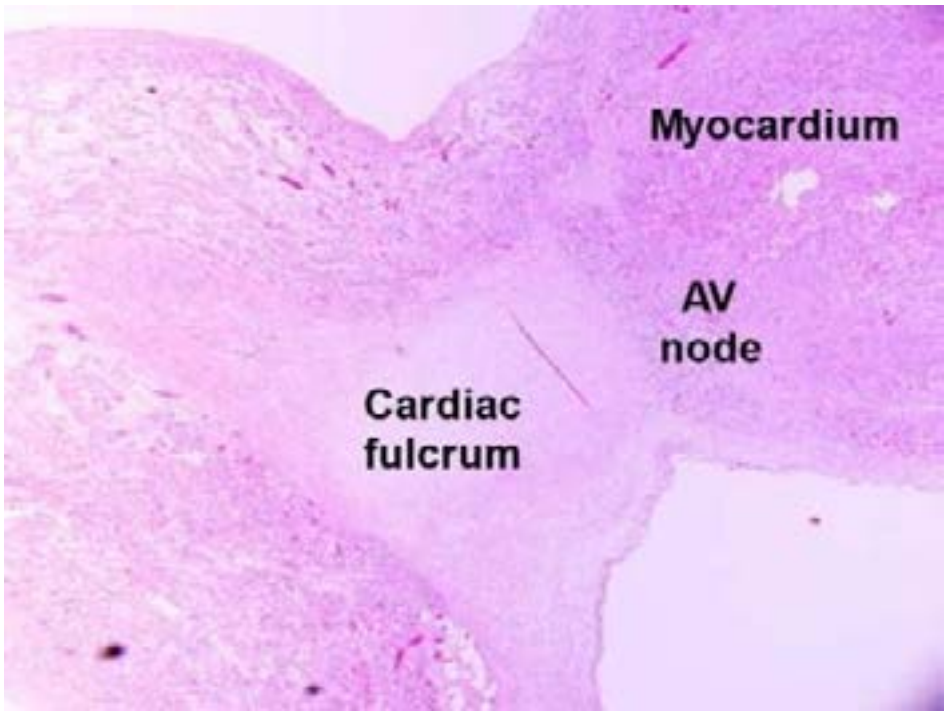

Figure 71. Human embryo heart (20 weeks) showing the relationships between the cardiac fulcrum (1), the tricuspid valve (2), the AV node (3) and ascending segment (4).

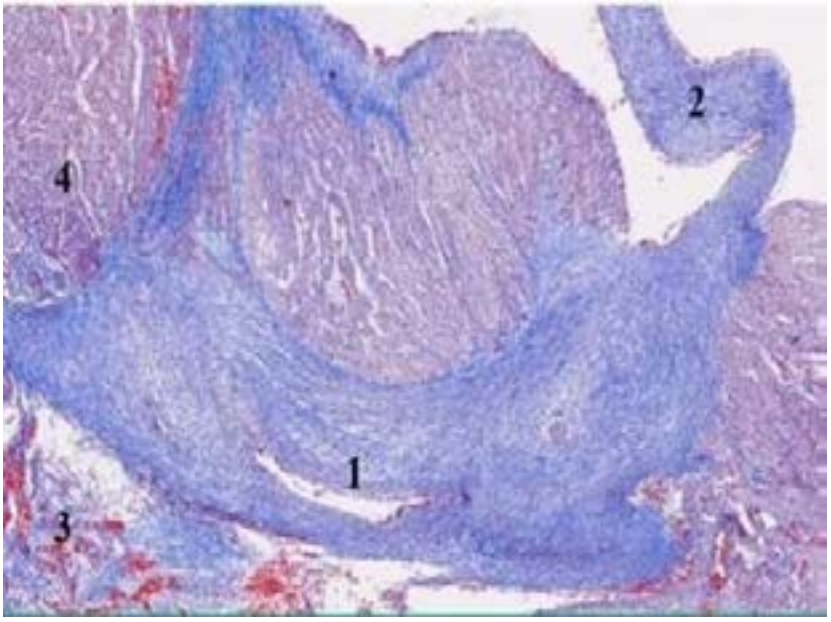

Relationship of the cardiac fulcrum with the AV node

This analysis reveals, in both human and bovine hearts, an issue of importance for cardiac pacing therapeutics (**Figure 72**) (37). In the histological study, the fulcrum was found to be adjacent to the AV node, forming a cellular conglomerate rich in neurofilament plexuses (**Figures 73 to 75**). This contiguity between the two structures is found in all specimens studied, both in bovine and human hearts. Central to the research finding is that neurofilaments are also found within the cardiac fulcrum , upon contact with the muscle fibers that insert into it. Fibroblasts and connective tissue are located in the thickness of the conduction system and between this and the working myocardium, acting as an insulation layer. It is also the connective tissue that constitutes the fibrous ring and the central fibrocartilaginous portion of the fulcrum, thus electrically isolating the atrial and ventricular chambers (**Figures 76 to 79**).

Figure 72. Bovid heart. A longitudinal section of the cardiac fulcrum is observed. Ref. 1: AV node; 2: fulcrum; 3: tricuspid valve.



Figure 73. (Bovine heart). H&E (x25). Plexuses are seen associated with fibrochondroid trabeculae and the myocardium. 1: osseous trabeculae. 2: plexuses. 3: fibroconnective tissue. 4: myocardium.

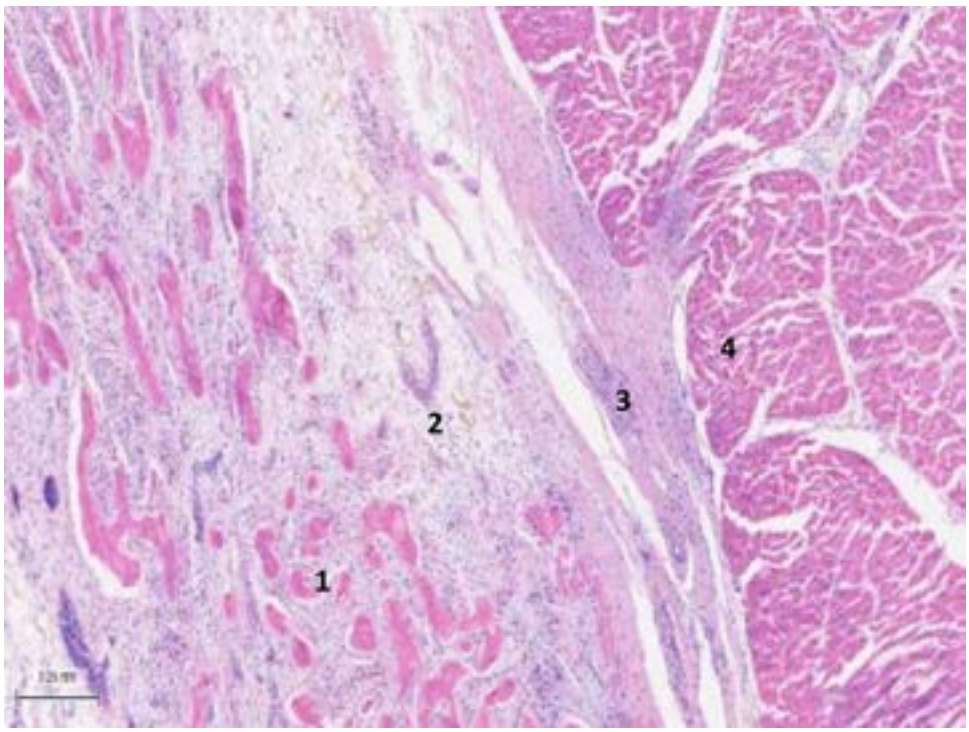

Figure 74. Porcine fulcrum (x20)

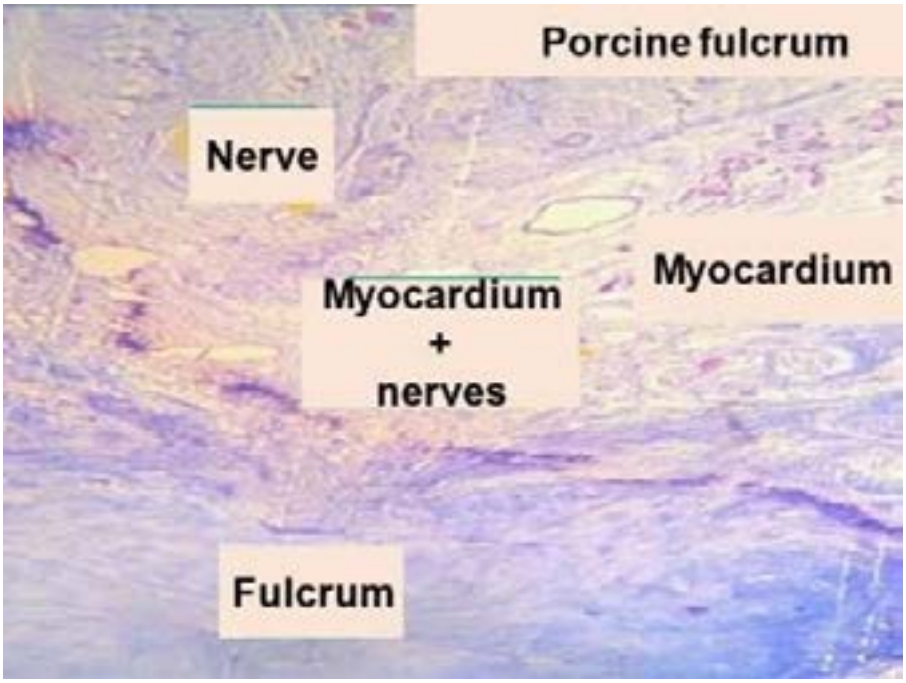

Figure 75. Porcine fulcrum 25x, Masson's staining. 1: Porcine cartilaginous fulcrum. 2: perifulcrum fibrous tissue. 3: septum. 4: intermingled cardiomyocytes of conduction nerves and ganglions can be seen reaching the fulcrum.

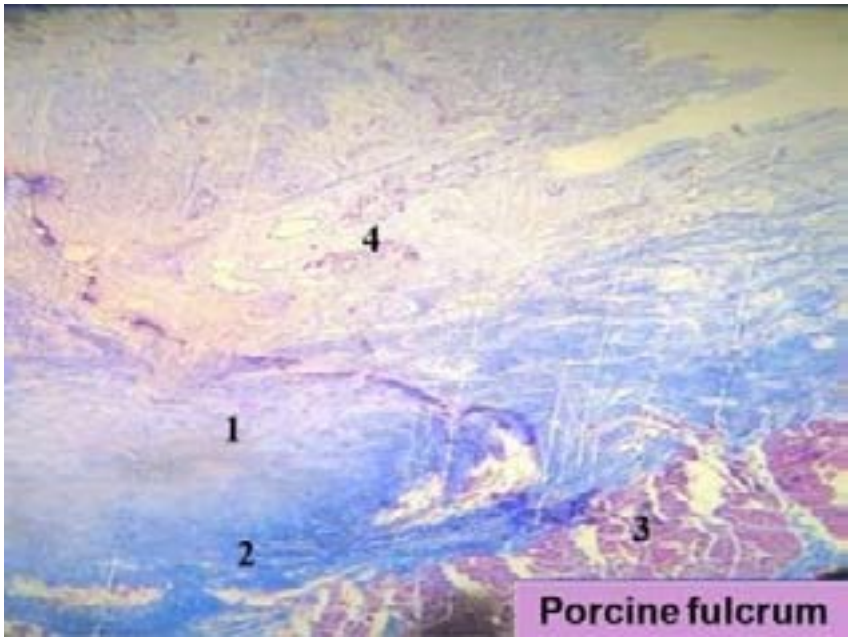

Figure 76. Porcine heart. Relationship of the fulcrum with the AV node. 1: fulcrum; 2: AV node; 3: cardiomyocytes (Purkinje cells) within the AV node.

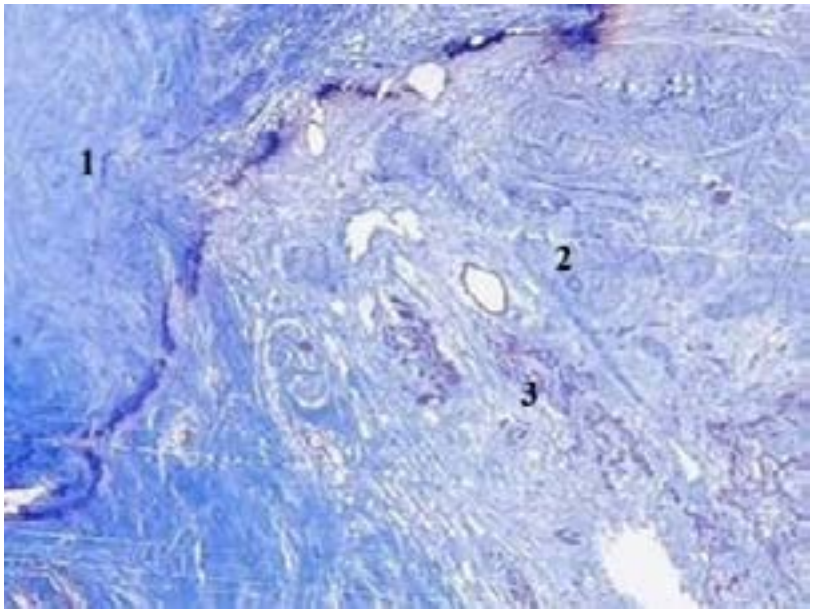

Figure 77. 27-week-old infant heart. Nerve trunk hypertrophy is seen in the cardiac fulcrum (black circles) adjacent to the AV node. HEx200. Inset shows thickened nerve trunk in the cardiac fulcrum confirmed by immunohistochemistry for S-100.

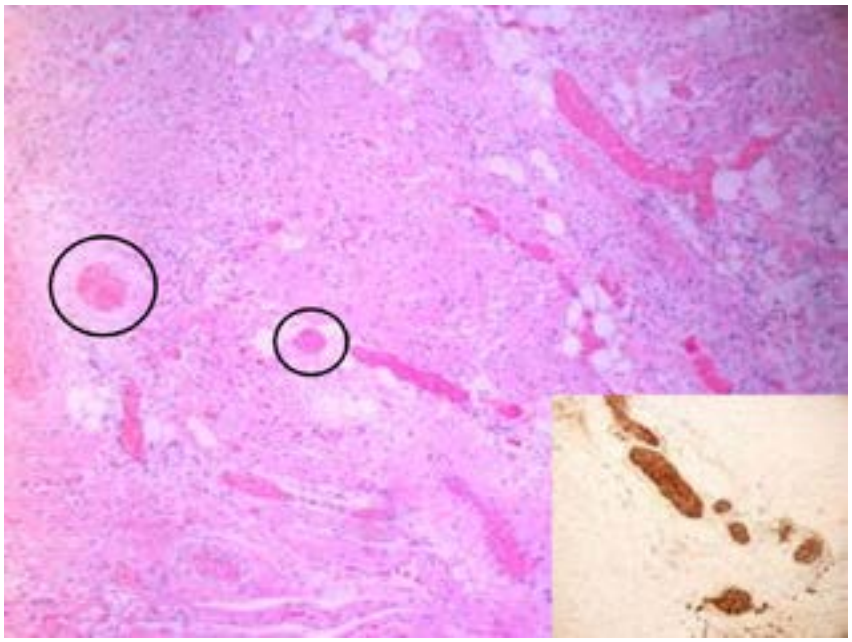

Figure 78. Bovine heart. Immunolabeling technique for neurofilaments (50x). Axons and ganglion cells are observed in the area marked by the circle.

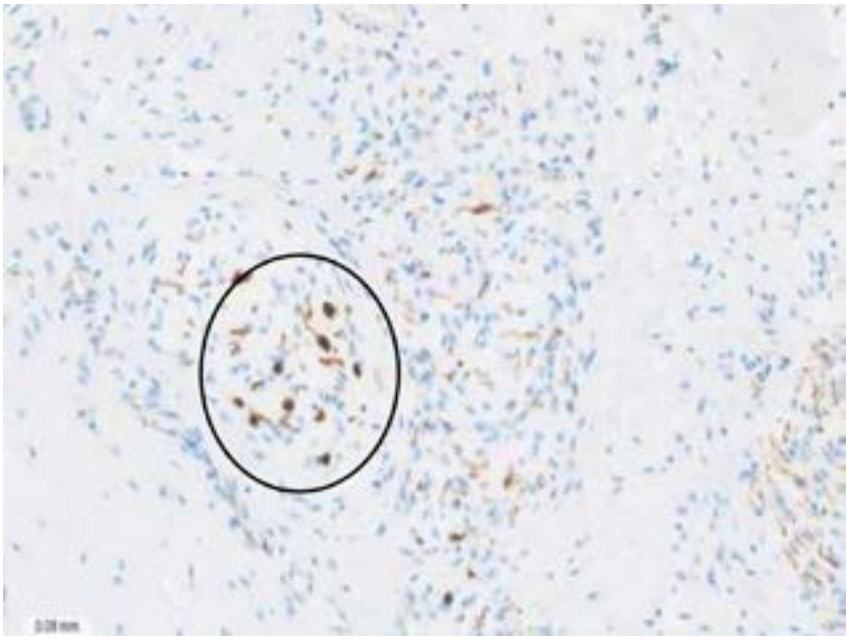

Figure 79. Cross-section of the cartilaginous cardiac fulcrum adjacent to the atrioventricular region (AV node marked with an asterisk). H&E x10.

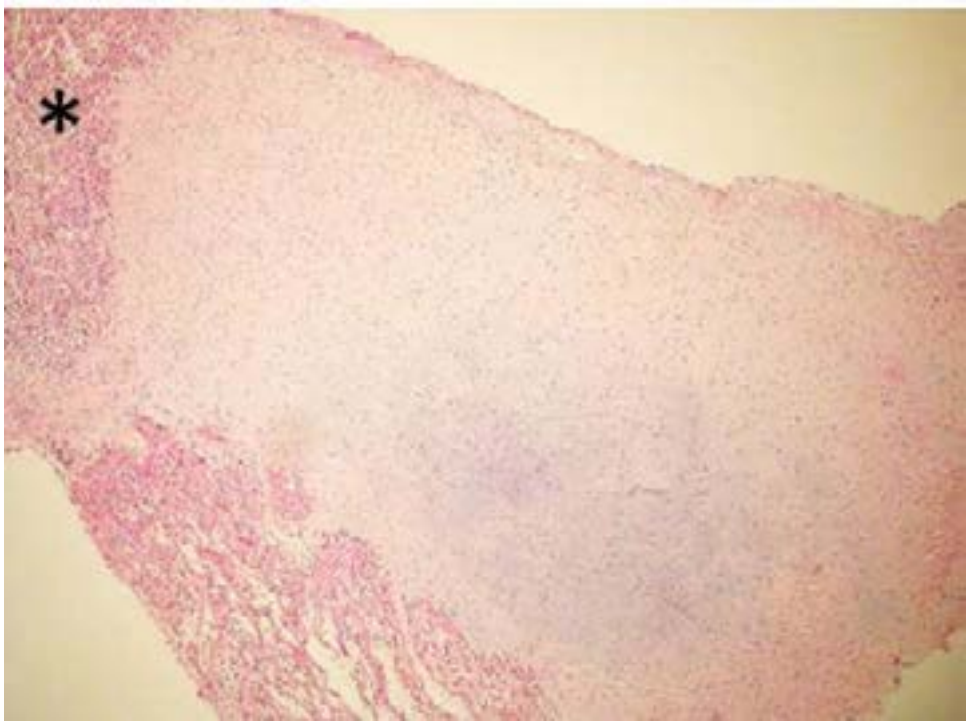

The AV node has a compact portion and a marginal portion of transitional cells (35). The transition zone is located between the wall of the right atrium and the AV node, acting as its "external" layer. The "compact" component has a semi-oval shape. The cells of the compact part of the node are smaller and tapered than the transitional cells. The latter are distributed parallel to each other and are surrounded by a greater amount of connective tissue. They are attributed the function of transmitting electrical information.

The spatial helical arrangement of the myocardium forces the muscle to overlap segments in its spatial conformation. This anatomical situation has a profound correspondence with myocardial movements and with the stimulation that runs through its segments, according to the electrophysiological studies we have performed (Chapter 3) (47-57). The interpretation of the

anatomical relationships between the cardiac fulcrum and the AV node implies the complementarity of the anatomy with the physiology of the continuous helical myocardium, since their contiguity is found at the site where stimulation begins and ends, with the production of the mechanical action of torsion and detorsion in the systolic and suction phases of the ventricles.

The *cardiac fulcrum*, support and insertion of the myocardium to exercise a lever function in its movements, is adjacent to the Aschoff-Tawara AV node. Thus, it constitutes an electromechanical unit located at the beginning and end of the continuous and helical myocardium, that is, at the *fulcrum*. This anatomical and functional arrangement of the myocardium is supported by a rich plexus of specialized filaments located inside the cardiac fulcrum that interact with the mechanical working cardiomyocytes (20).

This interpretation of the research findings in human, bovine, porcine and anuran hearts inevitably lead to therapeutic action (13). What is the explanation in our experience for the better synchrony of pacemakers with the catheter placed in the vicinity of this electromechanical unit?

(73). The AV node is on the base of the muscular septum at the base of implantation of the septal leaflet of the tricuspid valve, in the site of insertion of the interventricular septum with the aorta and the pulmonary artery. In this aspect, the adjacency between the cardiac fulcrum and the beginning of the continuous myocardium in its helical trajectory, in relation to the AV node, demonstrated that stimulation in the right ventricular outflow tract was more effective. In this experience on pacemakers implanted in different points of the right ventricle (apex, para-Hisian, outflow tract), using standard active fixation catheters, the right ventricular outflow tract achieved better electrical synchrony in the left ventricle (19,30,73). The ideal region for pacemaker pacing catheter placement would be high in the right ventricular outflow tract, below the pulmonary valve, and preferably on the septum, but not in the free wall.

Function leads the myocardium to have a point of support like any skeletal muscle both at its origin and at its end. If it did not have this spatial helical anatomical conformation, did not have an insertion at its ends located at the cardiac base and did not remain free at the apex, that is, pendular in the thorax; and furthermore, if it did not present a stimulation that allows its torsion and detorsion, it would not be able to fulfill its extraordinary muscular power.

The adjacency of the cardiac fulcrum to the AV node, surrounded by a rich plexus of neurofilaments (**Figures 80 to 83**), puts us in the anatomical consideration of an electromechanical unit in which stimulation energy and muscular mechanics participate (71). The effectiveness achieved with the placement of the pacing catheter in the vicinity of the right ventricular outflow tract validates the findings of this investigation.

Figure 80. A 3-day-old premature neonate born at 27 weeks. Histological examination shows neurofilaments in the fulcrum adjacent to the atrioventricular node in A (A&E x 100). This finding is confirmed in B at higher magnification (H&E x 200) (immunohistochemistry with S100).

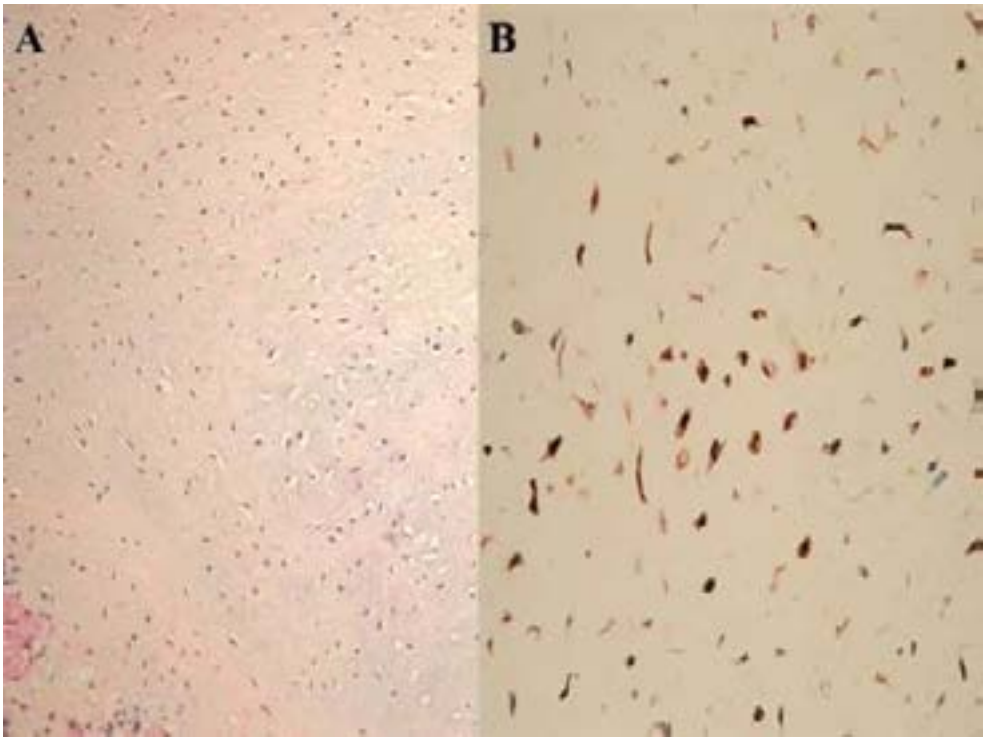

Figure 81. Porcine heart. Fulcrum-conduction cardiomyocytes with nerve plexuses in the spaces. Neurofilament stain (10x)

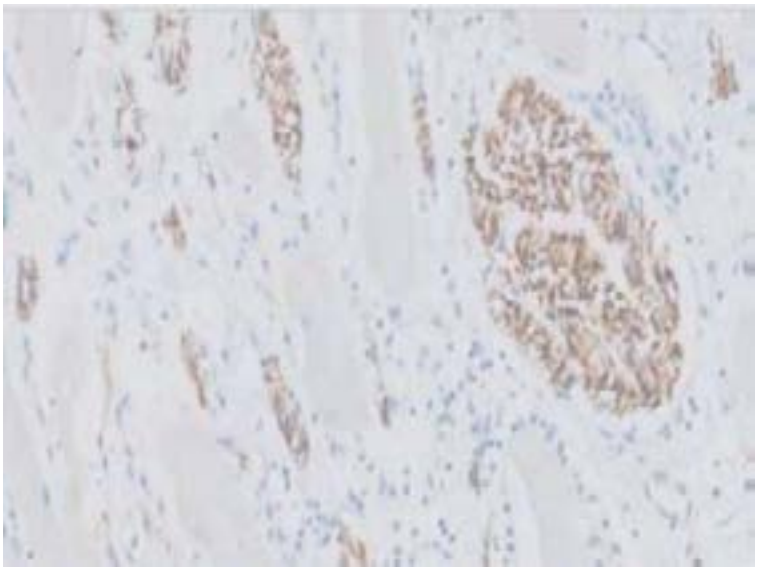

Figure 82. Adult human heart. Conduction cardiomyocytes (Purkinje fibers) and nerve plexuses.

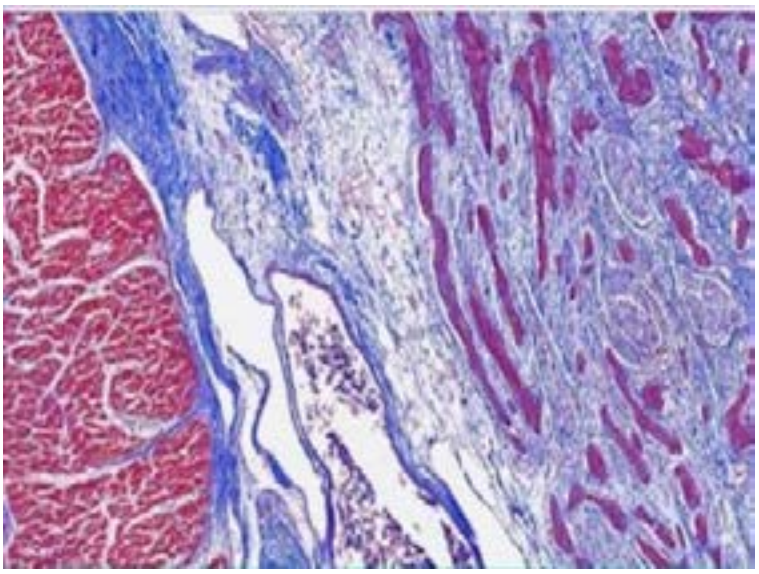

Figure 83. In the human heart, the neurofilament anchoring zone is shown in the fulcrum.

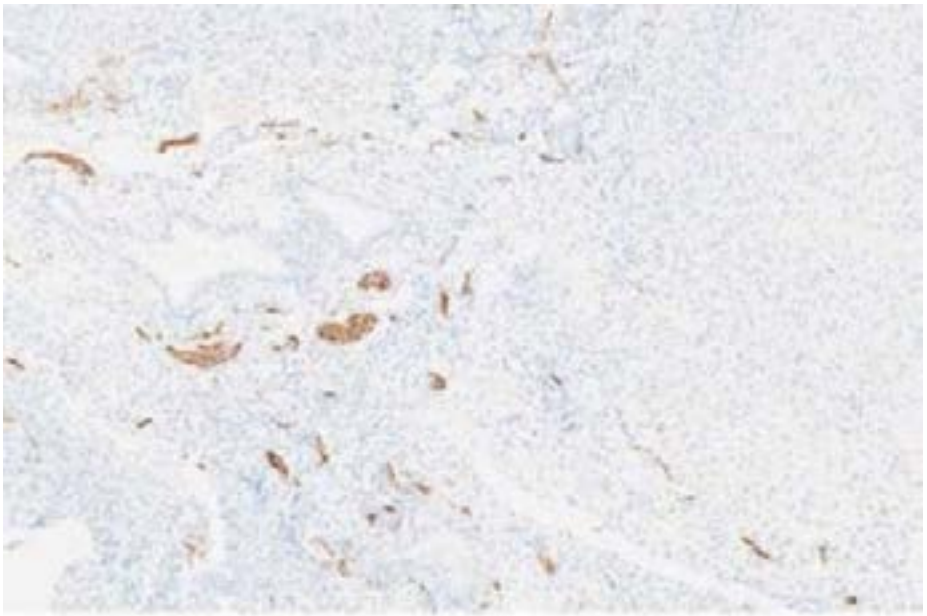

CHAPTER 3

INTERPRETATION OF MYOCARDIAL ACTIVATION IN RELATION TO THE CARDIAC FULCRUM AND THE TORSION MECHANISM

The complexity of biological phenomena implies dynamism, progression, and the simultaneous coexistence of various stages and different structures within an organizational unit. The same occurs in the heart from the perspective of electrical, mechanical, and electromechanical phenomena, with myocardial activation, contraction, and relaxation during systole, suction, and diastole.

Although various aspects of electrical stimulus propagation through the ventricles have long been known, the advent of three-dimensional navigators and electroanatomical mapping has allowed for a much more detailed study of the same in the human heart in completely physiological clinical situations.

There is always an opportunity in nature where functions beyond those known can be integrated with the components that make up a system (5, 7). This is the case of the "pulse center." The heart has historically been studied in its participating components, with a global and homogeneous contraction, simultaneous throughout its entire muscular structure; but not with a clear understanding that the movements in its different phases occur sequentially and overlap, contributing to its function in a complex manner with a tiny time of less than one second per cycle and 100,000 cycles per day. The heart has been studied only partially, surely because relating the complexity of its function to the duration of its cycle implies the difficulty of observing the reality that happens to it.

This situation was noted by William Harvey (1578-1657), who recounts the difficulties in proving his theory of blood circulation: "*I came to think*, [he says] *with Fracastoro*, [Renaissance epidemiologist], *that the movement of the heart could only be known by God*". Due to the rapidity of cardiac movement, Girolamo Fracastoro (Verona, 1478-1553) had expressed this concept in his book "*De sympathía et antipathía rerum*" (Venezia, 1546) (83). It is understandable to consider that the integrity proposed by the general theory of systems will remain relegated as long as adherence to solely analytical models continues, reducing the whole to the sole study of its parts.

Through the development of technology applied to morphology, a comprehensive biological perspective adapted to functional requirements was achieved (23,36,41,63,70). This view of the cardiac organ and its function that we have investigated is in line with general systems theory (8,9,12), a situation that we consider throughout our research.

Our previous publications corresponding to the cardiac fulcrum as a support for the myocardium, its relationship with the Aschoff-Tawara node and the sequential activation of the heart in a clear organizational arrangement to achieve the torsion movement (2,10,18,24,31,32,59), led us to analyze these structures in terms of their potential and functional aspects (4,27,28,42,67). In this way, we arrived at the concept that the heart acts through three fundamental units, which include: activation, electromechanical unit and myocardial torsion, which are interrelated in their anatomy and organization to be able to act in accordance with a highly efficient system.

We have already detailed the anatomical and physiological relationship between the fulcrum and the AV node in previous pages of this article. In this study, we analyzed the anatomical and histological relationship between the cardiac fulcrum and the atrioventricular node in human, porcine, and bovine hearts, as well as the myocardial activation channels that achieve cardiac torsion and detorsion.

In the research results, we find the reference points required to present an organizational pattern that contributes to cardiac function. These are: the anatomical contiguity between the AV node and the cardiac fulcrum; the continuous presence of the filaments that structure the AV node where the myocardium begins—clearly interpreting the formation of an electromechanical unit; and the activation pathway through the myocardium that allows for helical torsion, through the anatomical, anisotropic, and functional spatial location between the descending and ascending segments at the septal level, confirmed by ultrasound and electrophysiological studies. At this point, we must analyze how these elements, which include structures and circuits of energy and mechanical transfer, interact.

The analysis closely corresponds to myocardial movements and the stimulation that runs through its segments, according to the electrophysiological studies we have performed. The interpretation of the anatomical relationships between the cardiac fulcrum and the AV node implies the complementarity of anatomy with the physiology of the continuous helical myocardium, since the contiguity they exhibit is located at the site where stimulation begins and ends, producing the mechanical action of torsion and detorsion in the systolic and suction phases of the ventricles as the different myocardial segments are activated.

a.Cardiac electrical activation

The left ventricular endo and epicardial electrical activation sequence was studied using three-dimensional electroanatomic mapping (3D-EAM) with Carto navigation and mapping system (Biosense Webster, California, USA), enabling three-dimensional anatomical representation, with electrical activation and propagation maps. Isochronic and activation sequence maps were performed, correlating them

with surface ECG. Also, endocardial and epicardial ventricular activation maps were made, achieving detailed high-density recordings in apical, lateral and basal views. The study was performed at Hospital Presidente Perón (Buenos Aires, Argentina), including patients who had signed an informed consent. The research was previously approved by the Institutional Ethics Committee. All patients were in sinus rhythm, with normal QRS and had no verifiable structural cardiac disease by Doppler echocardiography and resting and stress gamma camera studies (**Table 1**).

Table 1. Patient characteristics

Patient	Age (years)	Gender	Studyindication	Other diseases
1	42	F	Isolated atrial fibrillation	NO
2	19	M	Abnormal pathway left epicardial	NO
3	23	M	Abnormal pathway left epicardial	NO
4	29	M	Abnormal pathway left epicardial	NO
5	32	M	Abnormal pathway left epicardial	NO

The 3D-EAM was performed during the course of radiofrequency ablation for arrhythmias owing to probable abnormal occult epicardial pathways. Mapping was carried out at the onset of studies, followed by ablation maneuvers. No complications developed. The presence of abnormal pathways did not interfere with mapping, as during the whole procedure baseline sinus rhythm was preserved with normal QRS complexes, both in duration and morphology, without antegrade preexcitation.
As the muscular structure of the left ventricle is made up of an endocardial layer (descending segment) and an epicardial layer (left and ascending segments), two approaches were used to carry out the mapping. Endocardial access was performed through a conventional atrial transseptal puncture. The epicardial access was obtained by means of a percutaneous approach in the pericardial cavity with an ablation catheter (38). The endo and epicardial mappings were performed consecutively and immediately and were later superimposed, synchronizing them by electrocardiographic timing. Thus, a simultaneous mapping of both surfaces was obtained, with the propagation times of electrical activation through the myocardium measured in milliseconds (ms) (**Figure 84**).

Figure 84. Epicardial mapping. Ref. 1: catheter located in the right atrium; 2: endocavitary catheter. 3: catheter in the pericardial space.

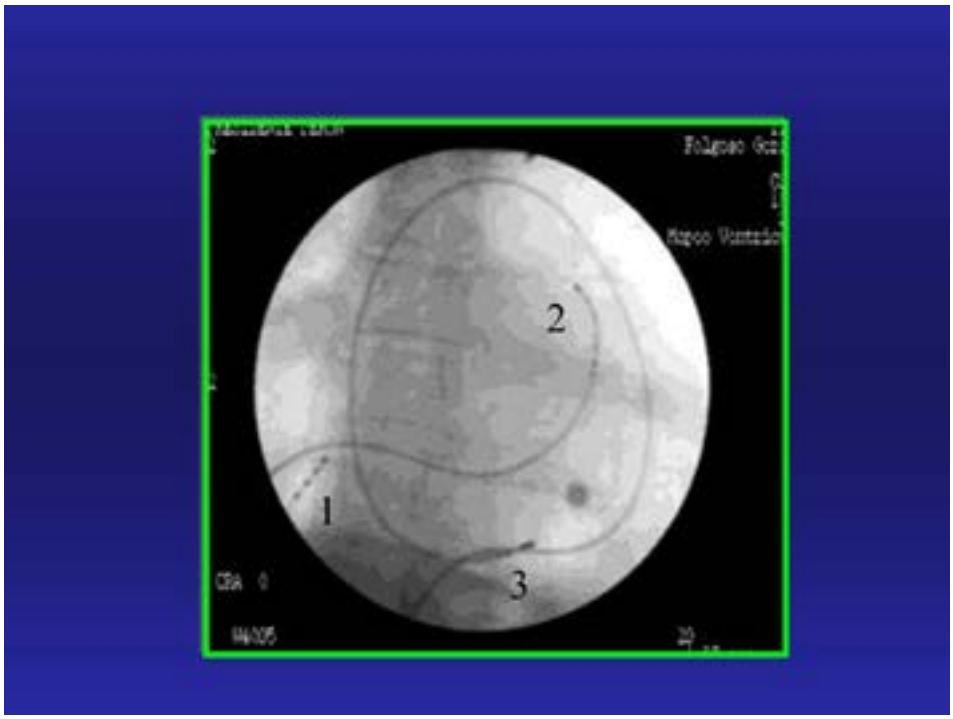

Up to that moment, the theory of the continuous myocardium lacked a fundamental investigation, as there was no documentation on the electrophysiological mechanism supporting the mechanical activation sequence of the helical anatomical model. The advent of clinical 3D-EAM overcame that limitation, as it not only allows the independent recording of different ventricular areas but also of exclusive or integrated endocardial and epicardial areas.

We performed a left ventricular activation mapping of its endocavitary and epicardial surfaces, according to the methodology described above. Mapping was carried out simultaneously with surface ECG, providing a unified temporal reference framework that enabled on the one hand the correlation of both recordings and on the other the synchronized view of the simultaneous activation observed in different electroanatomical conditions (Video 1).
As 3D-EAM corresponded to the left ventricle, the activation wave previously generated in the right ventricle was not obtained. Three-dimensional electroanatomical mapping lasted approximately 20 minutes. There were no complications associated with the procedure or any of the accesses. **Figures 85 to 88** show the propagation of endocardial an epicardial electrical activation. In all the Figures the right projection is observed in the left panel and the simultaneous left anterior oblique projection in the right panel. At each time, the activated zones are detailed in red. The lateral inset represents the activation of the descending and ascending muscle bands that make up the ventricular continuous structure of the myocardium in the cord model, a simplification of the three- dimensional myocardial spatial structure.

Figure 85. Integrated endo-epicardial mapping. The left panel shows the mitral valve annulus (limited by pink dots), the left ventricular (LV) endocardium, the LV septal endocardium and the LV epicardium. The blue vertical bar to the right of the panel indicates total cycle duration and the red zone within it, the activation moment corresponding to the activation graph on the left. The right panel shows the surface ECG. The red dot at peak QRS indicates the point of gated trigger. The green channels correspond to reference electrograms. The dotted vertical line shows QRS onset and the full line the present recording moment. The upper panel represents Torrent Guasp's cord model

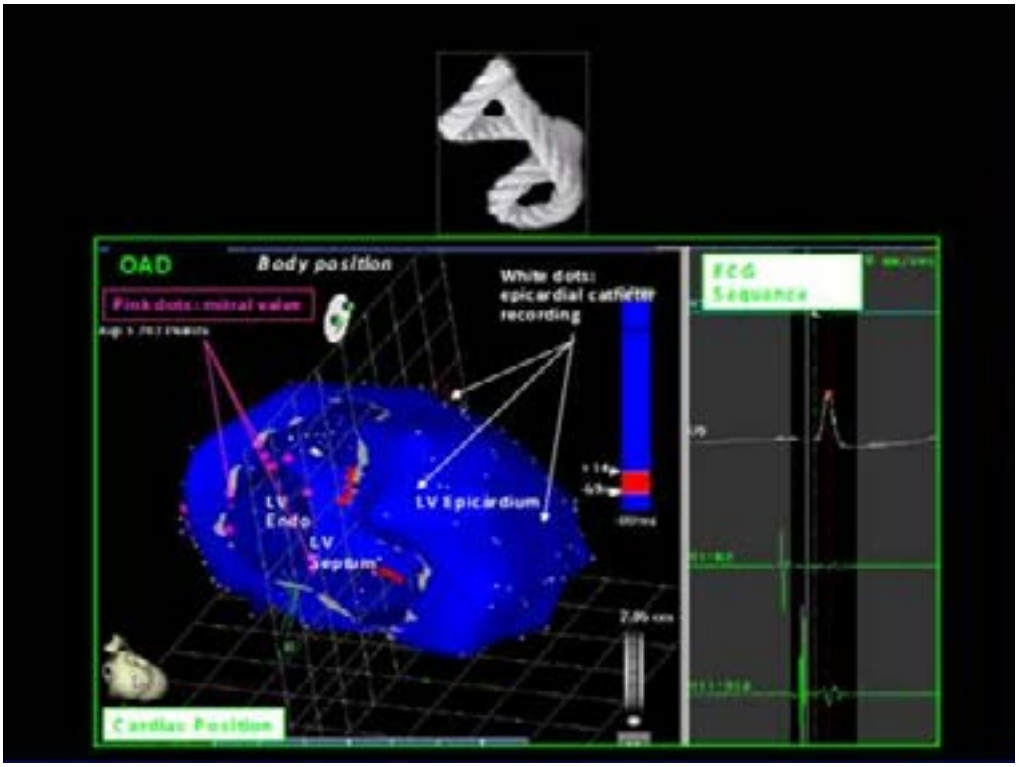

In all figures, the area depolarized at that time is represented in red and those that were previously activated and are in refractory period are represented in blue. Below the cord model, the average electrical propagation time along the myocardium can be seen measured in milliseconds (ms) at the analyzed site (**Tables 2 and 3**).
Left ventricular activation occurs 12.4 ms±1.816 ms after the onset in the interventricular *septum* (Figure 86 A). This contraction is determined by the bundle of His and its conduction fibers that give origin to the Purkinje network. Based on the anatomy that these fibers occupy, the endocardium is the first area of the LV to receive electromechanical activation. At that moment it also propagates to an epicardial area - ascending band- evidencing a transverse activation at a point we call "band crossover" which is produced 25.8±1.483ms after septal stimulation (Figure 86 B, Table 3) and at 38.2±2.135 ms from the onset of cardiac activation. This leads to subendocardial shortening and subepicardial lengthening, resulting in opposite rotations between the ventricular base (counterclockwise) and apex (clockwise). In echocardiographic studies verifying stimulation-function at this time of the cardiac cycle, greater systolic torsion was found in the mid-interventricular septum than in the anterior walls. Synchronously, following the anatomical arrangement of the descending band, the activation propagates longitudinally towards the ventricular apex, reaching it at 58±2.0 ms (Figures 87 A and B, Table 2).

From “band crossover” onwards the activation loses its unidirectional character and becomes slightly more complex. Three simultaneous wave fronts are generated: 1) the distal activation of the descending band towards the apical loop, 2) the depolarization of the ascending band from band crossover towards the apex and 3) the activation of this band from the crossover point towards its final portion in its insertion in the cardiac fulcrum, myocardial support. Figures 87 B, 88 A and B show the continuation and completion of this process. Intracavitary activation ends long before QRS termination (Figure 88). The rest of the QRS corresponds to the late activation of the distal portion of the ascending band, which justifies the persistence of its contraction during the isovolumic diastolic phase. This contraction constitutes the basis of the ventricular suction mechanism (Figure 88), and for this reason, it will be now termed left ventricular protodiastolic phase of myocardial contraction (LVPPMC), as in it there is contraction and no relaxation. A synthesis of the stimulation found in this study is shown with the cord model in figure 89.

Table 2. Activation times of the different cardiac structures (ms) (See explanation in the text of the cited figures).

Site	Patient 1	Patient 2	Patient 3	Patient 4	Patient 5	X	SD
Figure 86 A	10	12	13	15	12	12.4	1.816
Figure 86 B	35	38	37	41	40	38.2	2.135
Figure 87 A	45	47	49	52	49	48.4	2.332
Figure 87 B	55	59	57	61	58	58.0	2.000
Figure 88 A	94	98	98	99	95	96.8	1.939
Figure 88 B	115	118	114	120	116	116.6	2.154

References. ms: milliseconds; X: Mean; SD: Standard deviation.

Table 3. Radial propagation time (ms)

Time	Pat.1	Pat.2	Pat. 3	Pat. 4	Pat. 5	X	SD
Radial time from descending to ascending band	25	26	24	26	28	25.8	1.483

References. Pat: Patient; ms: milliseconds; X: Mean; SD: Standard deviation.

Figure 86. A. A. Onset of left ventricular activation. The left panel shows interventricular septum depolarization, corresponding to the descending band. In the right panel, the ventricular epicardium (ascending band), which has not been activated yet. B; Simultaneous band activation. Activation progresses in the left ventricular septum through the descending band (longitudinal activation) and propagates simultaneously to the epicardium (transverse activation) activating the ascending band.

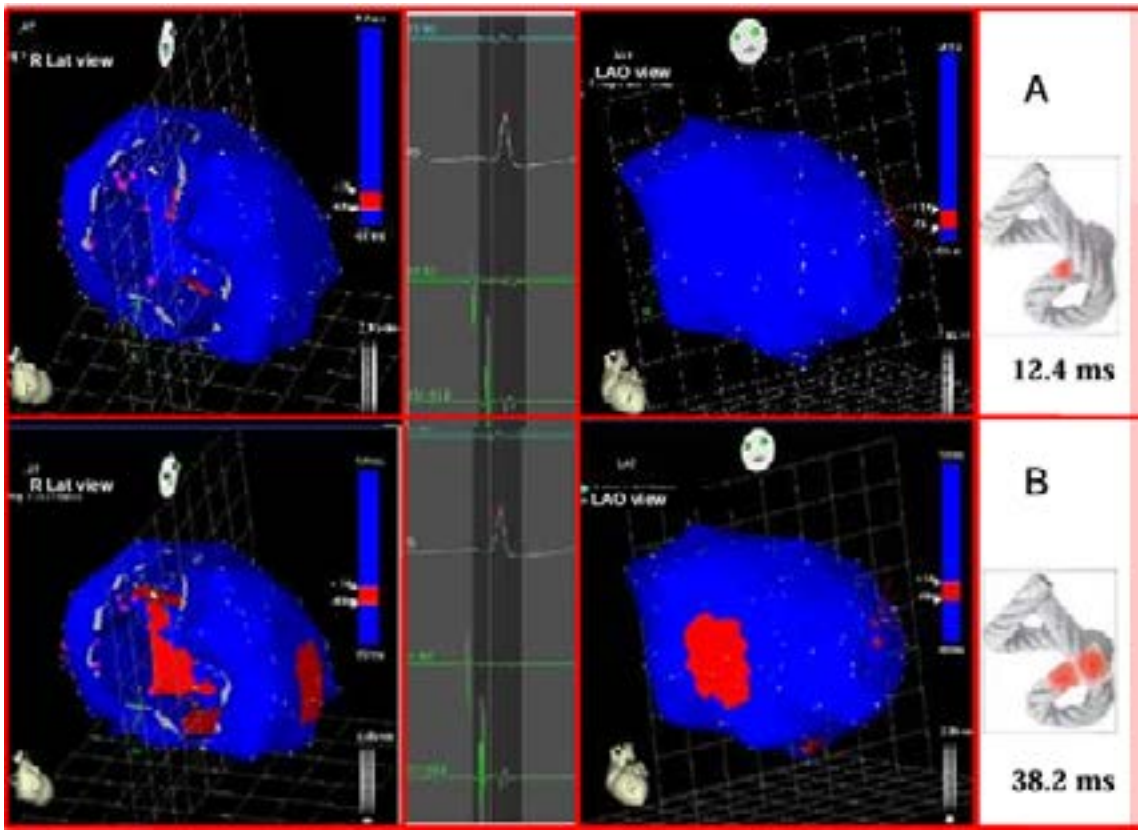

Figure 87. A. Bidirectional apex and ascending band activation. The final activation of the septum is observed, progressing towards the apex, synchronously with the epicardial activation in the same direction. At the same time the epicardial activation is directed towards the base of the left ventricle. B: Activation progression. Activation progresses in the same directions of the previous figure.

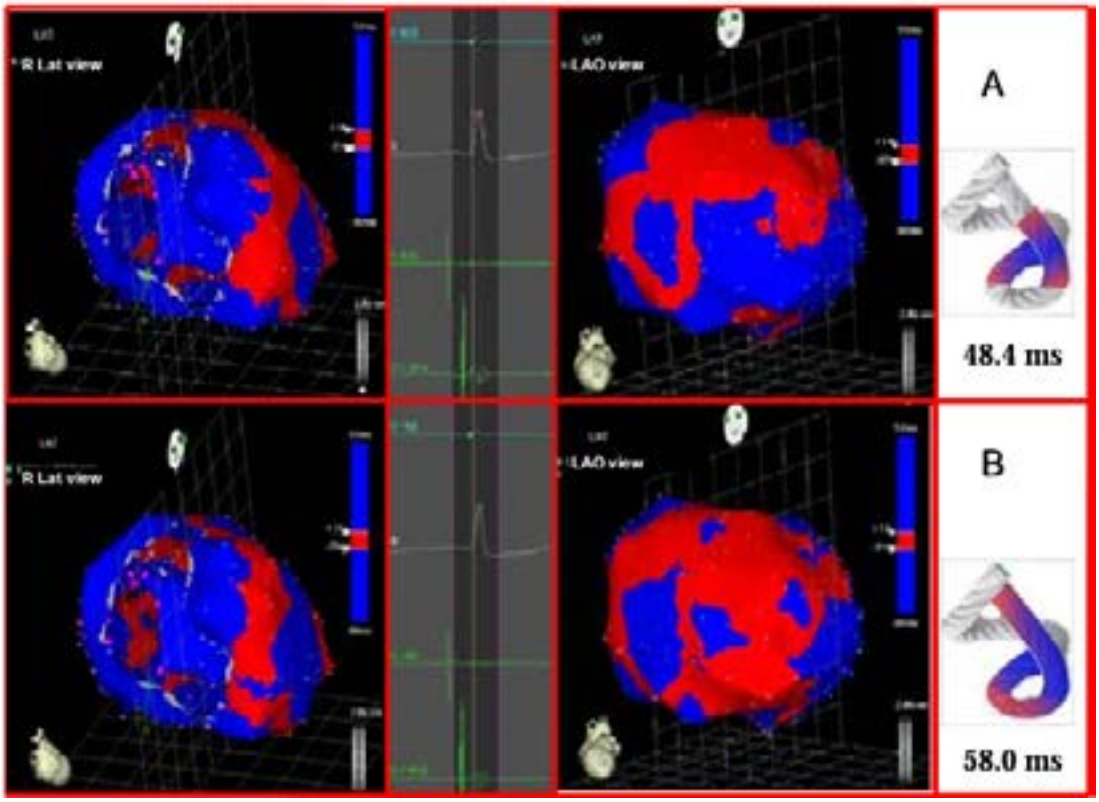

Figure 88. A: Late ascending band activation. At this moment, which corresponds to approximately 60% of QRS duration, the intracavitary activation (descending band) has already been completed. The distal portion of the ascending (epicardial) band is depolarized later. This phenomenon correlates with the persistence of this bands's contraction in the initial phase of diastole. B: Final activation. In the right panel, the left anterior oblique projection was modified to a left posterolateral projection, evidencing the very late activation of the distal portion of the ascending band.

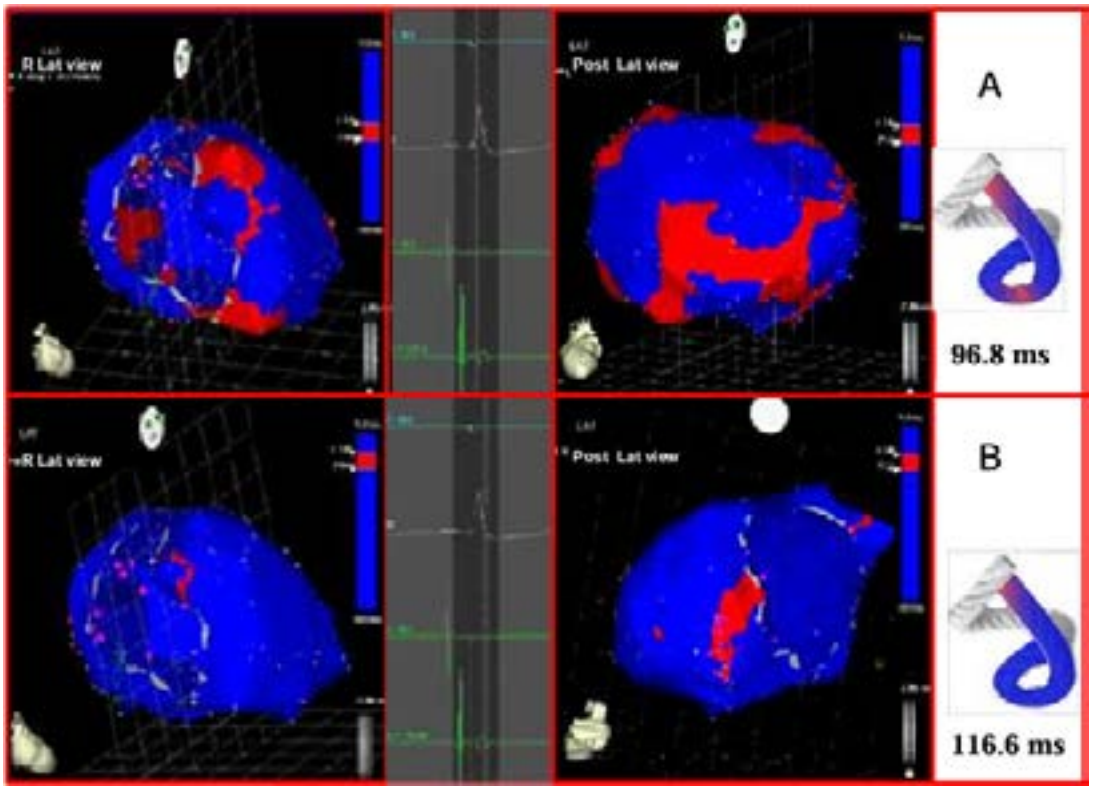

Figure 89. Cord model. Upper panel: Activation sequence (A-F) in the continuous myocardium according to our investigation. The figure shows the propagation times. The 25.8 milliseconds in B indicate the delay in the stimulation to pass from the descending band in A to the ascending band in B. References: In red: depolarization; in blue: already activated zones. Lower panel: unidirectional excitation propagation (in red) in the continuous myocardium according to Torrent Guasp's theory (A-D).

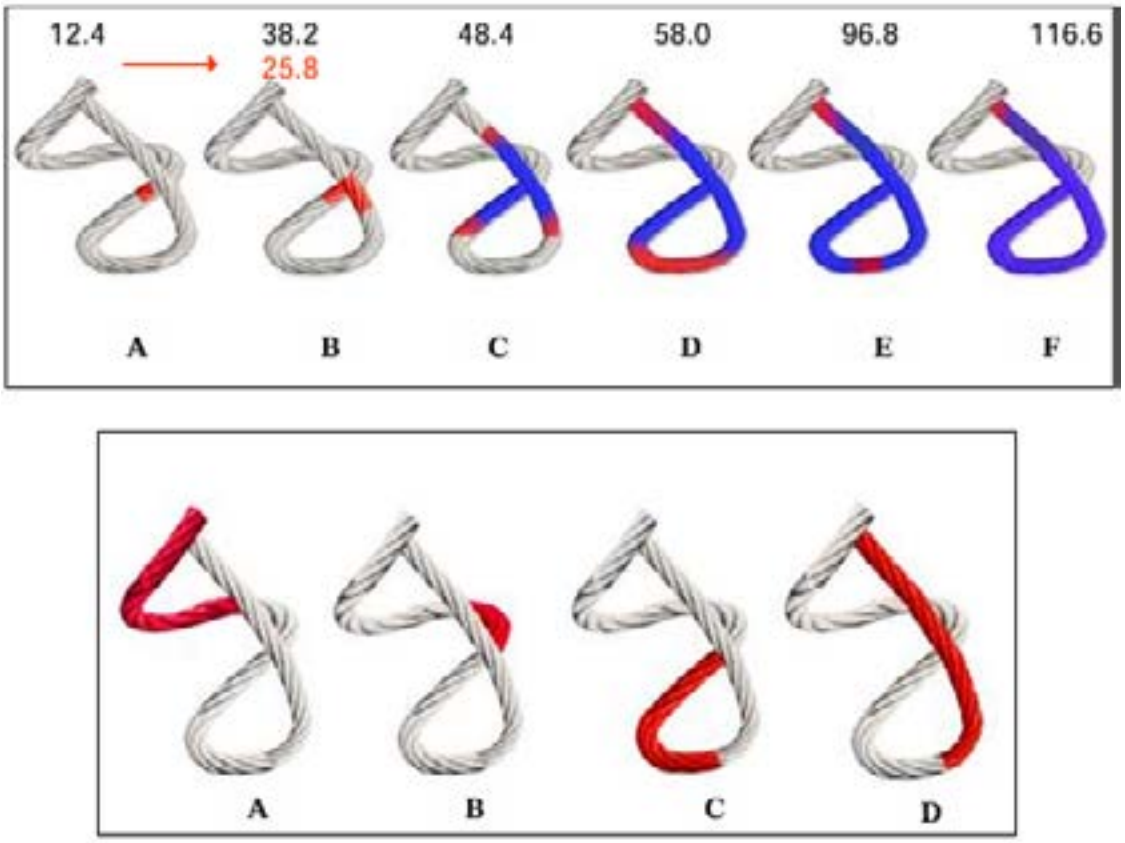

The right ventricle initiates its systolic activity, in our research, 12.4 ms before the left ventricle. The opening of the pulmonary valve begins as soon as its intraventricular pressure rises to 8-10 mm Hg. The right ventricular inflow tract contracts very early. This onset of right ventricular ejection precedes left ventricular systole. Only at an average of 38.2 ms in our research, after the beginning of the cardiac cycle with right ventricular contraction, are the ascending and descending segments stimulated, which would imply left ventricular ejection at that moment when the aortic valve opens. This difference between the early opening of the pulmonary valve relative to the aortic valve of 40 ms is logical, since with both ventricles ejecting and filling simultaneously, circulation would be practically interrupted, lacking the necessary continuity, falling to levels even lower than the gradients exhibited by normal circulatory return.

The two active functions of ejection and suction, synchronized between both ventricles, would correspond to circulatory continuity. This raises the question: how is the early opening of the pulmonary valve relative to the aortic valve based? The ventricles take advantage of the asynchronous impulse of approximately 40 ms, or 5% of the 800 ms duration of the cardiac cycle, so that one of them, the right ventricle, collaborates in the loading of the other, the left, through the complementarity between ejection and suction. Correlating this early opening of approximately 40 ms of the pulmonary valve relative to the aortic valve found in our research in humans, the same has also been observed in fish. Thus, in teleosts (Cretaceous period), which have four cardiac chambers in line (sinus venosus, atrium, ventricle and bulbus arteriosus), the same delay of 40 ms has been found in the deflection of the myocardium after the discharge of the spike, between the proximal and distal ventricle at the level of the bulb, analogous to the right and left ventricles of mammals (**Figure 90**) (80). This correlation implies an evolutionary biological matrix that transcends species. In this estimated interval of at least 38.2 ms on average in our investigations, between the openings of the pulmonary valve and the aortic valve, the last phase of filling of this ventricle occurs in the left ventricle (diastolic period 3).

Figure 90. The diagram of the circulatory system of a teleost fish shows the delay in obtaining myocardial deflection from the proximal ventricle (right ventricle) to the distal and bulbus (left ventricle). This 40 ms time is analogous to what we found in our electrophysiological research in humans between the opening of the pulmonary valve and the aortic valve. The diagram represents the cardiac chambers of a teleost fish, which are located in a line: sinus venosus (SV), atrium (A), ventricle (V), and bulbus (B).

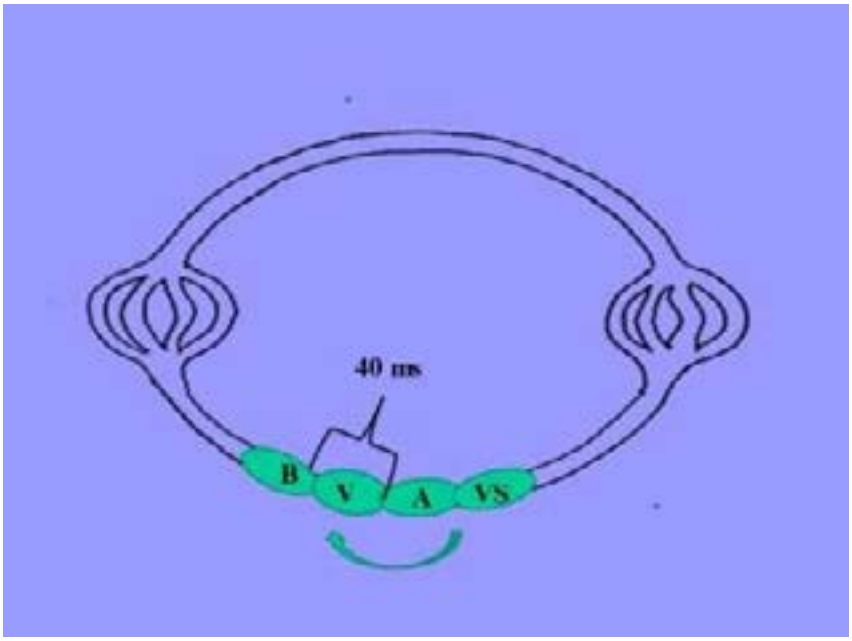

b.Myocardial torsion

As noted, left ventricular activation begins in the endocardial descending band, which is depolarized longitudinally and transversally almost simultaneously. At the crossover point of both bands, the activation propagates from the endocardium to the epicardium (transverse propagation), that is, from the descending to the ascending band. From this point onwards, the ascending band depolarizes in two directions: towards the apex and towards the base, at the same time that the descending band completes its activation towards the apex (Figure 87). Thus, two essential phenomena occur:

1 - As the apical loop depolarizes from band crossover with two simultaneous wavefronts (from the descending and the ascending band) it generates their synchronized contraction.

2- The activation of the ascending band propagates from band crossover in two opposite directions: towards the apex and towards the base (Figure 87). The resulting mechanical contraction will also have a divergent direction, giving origin to the clockwise (apex) and counterclockwise (basal) rotations. The helical myocardial arrangement forces the muscle to overlap segments in its spatial configuration. According to the electrophysiological studies we performed, this anatomical situation has great correspondence with myocardial movements and the stimulation that runs along its segments (88),In a cardiac cross-section (**Figure 91**) below the atrioventricular valves, we can observe that the descending segment is located internally surrounded by the ascending segment in the free wall of the left ventricle (73). The ascending and descending segments undergo opposite movements, both in systole and diastole, to achieve the expulsion and suction of ventricular blood contents, generating friction between their surfaces, a topic we have discussed in other publications when finding hyaluronic acid, with a lubricating function, in abundance both in the myocardium and in The besius vessels in studies performed in anurans, bovines and humans (**Figures 92 to 94**) (62,69). The histology in the box of Figure 91 clearly shows the different orientation of the fibers of the descending segment in relation to the ascending segment, which explains the opposite movements they present. The arrangement of myocardial fibers in the epicardium and endocardium, whose 180º angulation change causes the epicardial fibers to be arranged in the opposite orientation to the endocardial ones. Given the different anisotropic orientations of the fibers, this area corresponds to the beginning of the opposite movement that produces myocardial torsion. The constitution of the septum with the contiguity between the descending and ascending segments allows the continuity of activation between them with opposite movements and the consequent myocardial torsion. The interventricular septum has a predominant value in the function of the myocardium since its location is essential in biventricular interdependence (33).

Figura 91. Cross-section of both ventricles (Human heart). References: 1. Interband fibers; 2. Right paraepicardial bundle; 3. Right paraendocardial bundle; 4. Anterior septal band; 5. Posterior septal band; 6. Intraseptal band; 7. Descending segment; 8. Ascending segment. The black arrows indicate the direction of movement of each segment in systole. The yellow arrow points to the plane of friction between both segments; counterclockwise (levogirous); clockwise (dextrogirous. The box shows the septum with the different segments that form it. In the lower corner, a microscopic view (right) of the interventricular septum middle segment in the human heart can be seen, clearly showing the absence of circumferential transition fibers between the fibers of the descending (right) and ascending (left) segments of the continuous myocardium. Also note how there is no fascia or anatomical structure interspersed between the two fiber bundles. Similarly, the macroscopic section (left), shows how the abrupt transition of the fiber angle change draws a line that can be seen with the naked eye and, in echocardiographic images, gives rise to the well-known midseptal linear image, generated by the acoustic interface that generates the abrupt change in angle in this area of the septum.

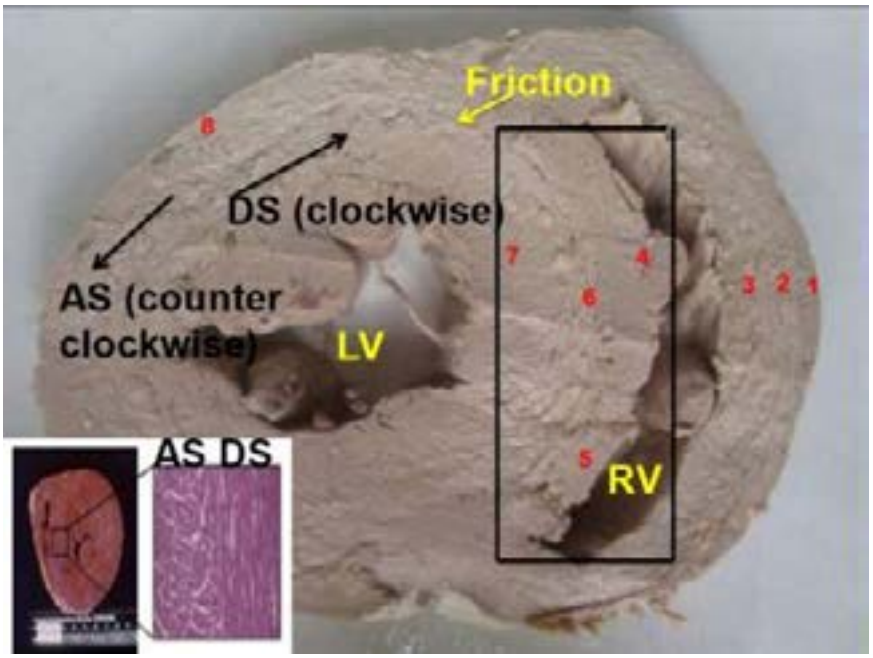

Figura 92. Histology of anuran (Rhinella arenarum) myocardium stained with Alcian Blue. A: 10x magnification; B: 40x magnification. Ref. 1: cardiomyocytes; HA: hyaluronic acid.

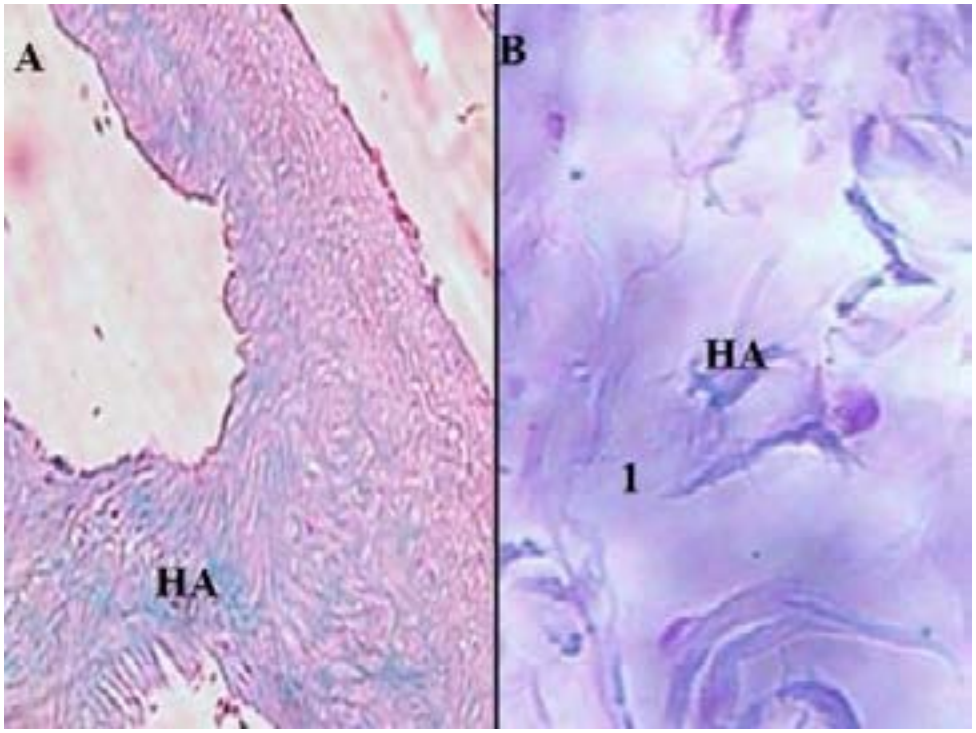

Figure 93. Contracted transverse vein with Alcian blue-positive edematous perivenous interstitium. Note the Alcian blue-stained hyaluronic acid (HA) in the interstitium between the cardiomyocytes (15x) (bovine heart).

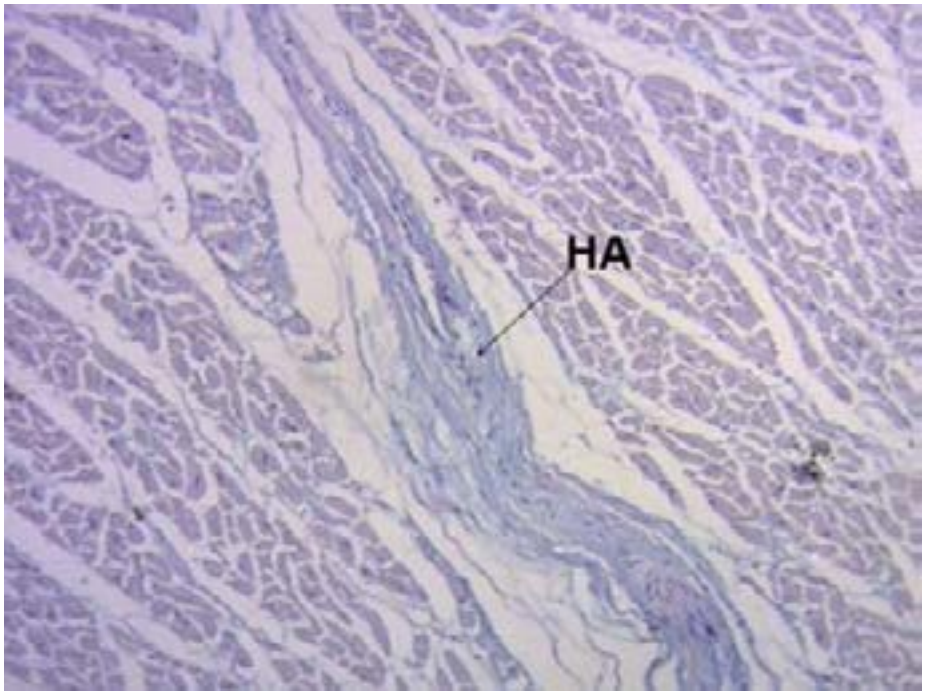

Figure 94. Interstitium between cardiomyocytes showing hyaluronic acid (HA) stained light blue with Alcian blue (15x) (adult human heart).

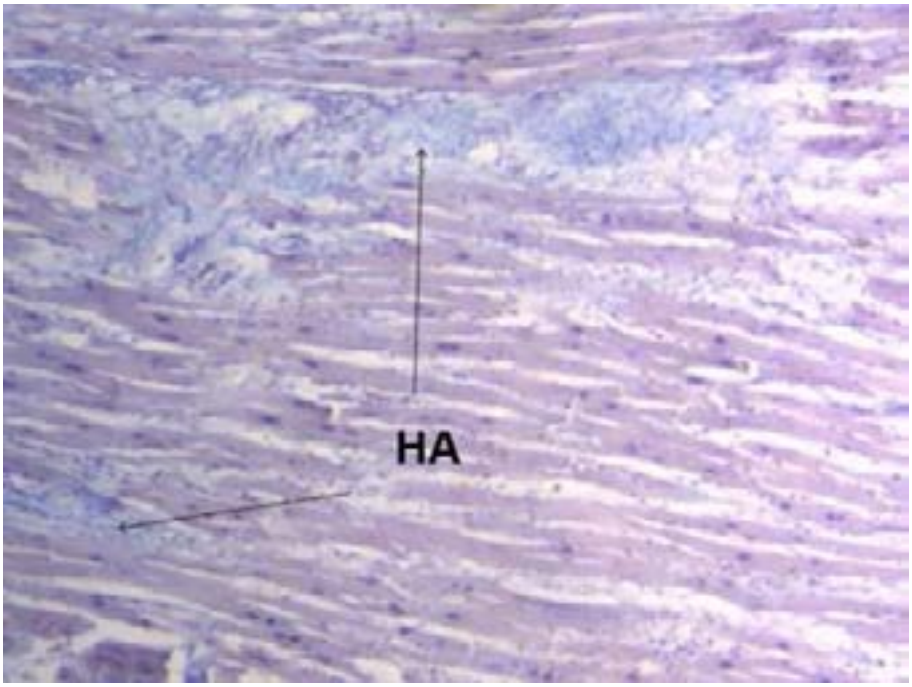

An important detail derived from tractographic images is their correspondence with the changes in angulation observed in the two-dimensional sections published by Streeter or with the rough arrangement of the band bundles in the anatomical sections of the recomposed hearts once dissected, highlighting the abrupt change in angulation present in the interventricular septum, due to the absence of transition of fibers with a circumferential course, since the septum is a structure that results from the apposition of the descending and ascending segments of the continuous myocardium (40).

The research aspect on the stimulation sequence allowed to determine the electrophysiological propagation in the continuous myocardium and also led to deductions about ventricular torsion and the suction effect in LVPPMC (60). The orientation of the fibers in the continuous myocardium and its activation imply a concatenation of muscular movements in cardiac mechanics. These occur giving rise to four phases: narrowing, shortening-torsion, lengthening- detorsion and widening, which allow it to

perform its functions of systole, suction and diastole. The fundamental movements in which the different segments of the continuous myocardium participate in systole and suction are shown in **Table 4**.

Table 4. Segment function

Segment	Movement
Right	Narrowing (systole)
Left	Narrowing (systole)
Descending	Shortening-torsion (systole)
Ascending	Shortening-torsion (systole)
Ascending (terminall portion)	Lengthening-detorsion (PPMC)

This sequential activation correlates with fundamental phenomena that are well known today, such as the opposing clockwise and counterclockwise torsion of the apex and base of the left ventricle, which are responsible for its mechanical efficiency (Video 2). In order to try to explain the mechanism of this muscular torsion, this research aimed to analyze the sequence of ventricular electrical activation by means of the simultaneous endo-epicardial MET of the segments from their beginning in the anatomical and functional contiguity between the AV node and the cardiac fulcrum (**Figure 95**).

Figure 95. Helical myocardium in the cord model that simplifies the spatial structure. It shows the different segments that comprise it. In blue: basal loop. In red: apical loop. PA: pulmonary artery; A: Aorta; r: stimulus reception; e: stimulus emission. The three anatomical and functional units that allow integration between the AV node, the cardiac fulcrum, and myocardial torsion are detailed. The black circle details the site we have called band crossover. Given the different anisotropic orientations of the fibers, this area corresponds to the beginning of the helical opposite movement that produces myocardial torsion. The spatial arrangement of the continuous myocardium can be seen in the upper corner.

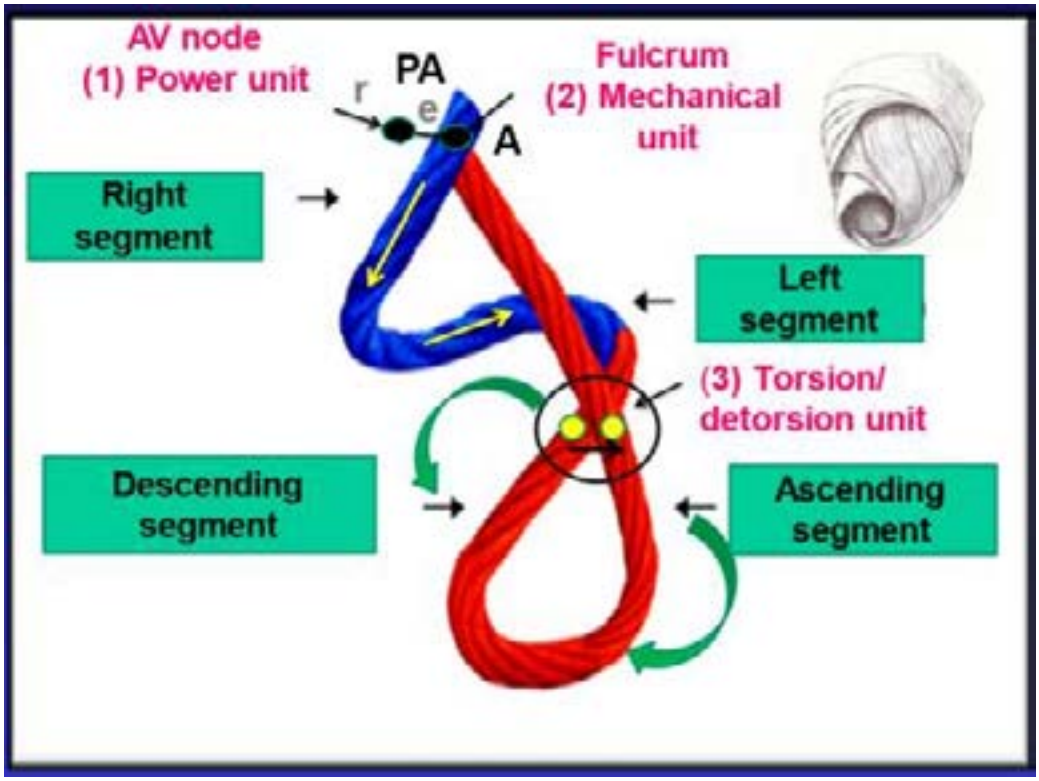

In the narrowing phase there is a consecutive contraction of the right (free wall of the right ventricle) and left (edge of the mitral orifice) segments, which constitute the basal loop. According to Armour (1970) (1), this contraction constitutes an external cover within which the apical loop will contract. In reality, the crescentic free wall of the right ventricle is located “ad latere” of the rest of the ventricular mass (septum and left ventricle), since the left segment constitutes part of the posterior epicardial wall of the left ventricle in its upper portion, surrounding the mitral annulus, while the rest of it is covered externally by the ascending segment.

In this layer (basal loop) the stimulation goes from subepicardium to subendocardium. Then, it stimulates the descending segment and at 25.8 ms average in our research the ascending segment is activated. The end of the stimulation in the myocardium occurs at the level of the terminal part of the ascending segment, close to its insertion into the cardiac fulcrum, during the first 80-100 ms of diástole, in the period traditionally referred to as the diastolic isovolumetric phase and wich we have more properly called PPMC (68).

Since Harvey and later with Einthoven's electrocardiography, both the electrical activation and mechanical contraction of the heart were considered to be linear and homogeneous processes. Thus, contraction would occur "en bloc" during systole and relaxation would occur uniformly during diastole. At this stage of current knowledge of the helical myocardium, these concepts do not explain cardiac function, whose movements are sequential (3). In this regard, the same occurs with cellular stimulation, which is explained in the diagram in **Figure 96**.

Figure 96. We have already analyzed that the myocardium contracts sequentially and not in a block manner. This stepwise propagation through its segments is repeated at the cellular level. Thus, the figure shows that excitable cells are then activated and subsequently become refractory, while cells that were in this last state become excited again to transmit the stimulus.

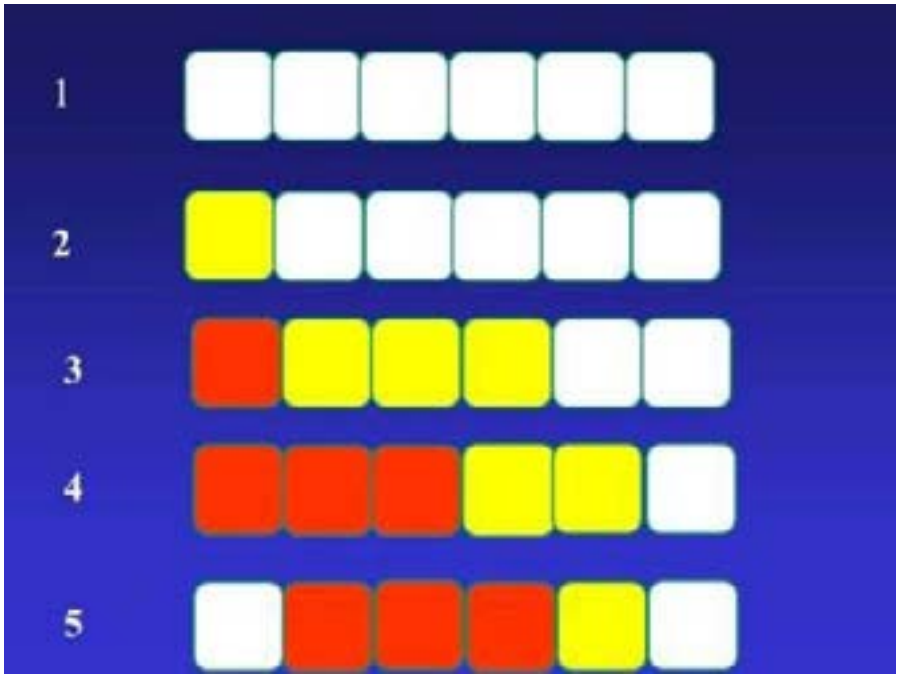

White: excitable cell
Yellow: cell with stimulus conduction.
Red: cell in a refractory state.
Line 1: Cells in a state of excitability
Line 2: a cell initiates stimulus conduction
Line 3: the stimulus propagates to neighboring cells, leaving the initial cell in a refractory state
Line 4: the stimulation propagates through contiguity with other cells.
Line 5: After a certain time, the first cell to conduct becomes excitable again.

Although various aspects of electrical stimulus propagation in the ventricle have long been understood, the advent of three-dimensional navigators and electroanatomical mapping has enabled a much more detailed study of this process in the human heart under completely physiological clinical situations. This research allows us to elucidate the activation sequence of contractile areas and their entry into cardiac dynamics in relation to the path of the excitation wave with a coordinated pattern consistent with the helical structure of the continuous myocardium.

Research conducted with MET explains the torsion phase of the heart, defined as the opposing rotational movement of the base and apex. Activation, for this purpose, at the intersection of the descending and ascending segments propagates from the endocardium to the epicardium (transverse propagation), that is, from the descending segment to the ascending segment. This research on the transmission of impulses through the myocardium led to the investigations presented here, which correlate the structure of the continuous and helical myocardium with the propagation of stimulation.

Our analysis implies that diffusion occurs simultaneously longitudinally and transversely between the descending and ascending segments. We must find a relationship between the activation action and the mechanical product. The explanation

is provided by the simultaneous longitudinal and transverse electrical conduction pathways.

The ventricular narrowing phase (systolic isovolumic) at the beginning of systole is produced by the contraction of the right and left segments of the basal loop. The superimposed shortening phase is due to the descent of the base, which occurs simultaneously with myocardial torsion. It originates longitudinally when the annulus contracts before the apex. The fact that the latter does not move is due to the mechanism of the base descending in systole and ascending in diastole.

The pressure generated to expel the largest amount of blood at the beginning of ejection, in a period that occupies only 20% of the systolic phase, is made possible by the torsional movement.

Although there is a progression in electrical conduction along the continuous myocardium, this isolated activation does not explain the generation of a force capable of ejecting ventricular contents at a speed of 200 cm/s at low energy expenditure. What was found in this investigation: the transverse propagation from the descending segment to the ascending one plays a fundamental role in ventricular torsion, allowing opposing forces on its longitudinal axis to generate the intraventricular pressure necessary to achieve the abrupt expulsion of blood. In this way, a torsion mechanism similar to "wringing out a towel" would be produced, as described by Giovanni Borelli and Richard Lower (73).

c. The three electromechanical units of the heart. Conclusions

During this investigation, in both human and bovine hearts, the histological study revealed that the fulcrum (the beginning and end of the continuous myocardium) is adjacent to the AV node, creating a space rich in neurofilament plexuses. A crucial finding is that neurofilaments also occupy the cardiac fulcrum, constituting an electromechanical unit (71,77,78).

We mapped left ventricular activation on its endocavitary and epicardial surfaces according to the methodology described above. The mapping was performed simultaneously with the surface ECG. This provided a unified temporal reference frame, allowing both recordings to be correlated and, on the one hand, to obtain a synchronized view of the simultaneous activation observed in various electroanatomical incidents.

This study found a relationship between myocardial stimulation and its mechanical product. The mechanical consequence of the cardiac structure is the initiation of stimulation in the anatomical and functional unit between the AV node and the cardiac fulcrum, and its continuity in myocardial activation up to the simultaneous activation zone with movements between the descending and ascending segments, which generates torsion of the left ventricular myocardium, due to opposite rotation between the base and the apex, with simultaneous shortening of both ventricles.

Acknowledgments

I would like to thank all those who in some way enriched the project, allowing its development: María Elena Bastarrica, Francesc Carreras Costa, Marta Cohen, Pedro Cossio, Benjamín Elencwajg, Oscar Fariña, Miguel Angel García Fernández, Víctor González, Mayra Patricia Hernández López, Efraín Herrero, Noemí Lago, Néstor López Cabanillas, Jorge Alejandro Lowenstein, Diego Lowenstein Haber, Darío Martino, Vicente Mora Llabata, Jesús Valle Cabezas.

Video 1. Cardiac electrical activation. The left ventricular endo and epicardial electrical activation sequence was studied using three-dimensional electroanatomical mapping with a navigation system and Carto mapping, enabling three-dimensional anatomical representation, with activation and electrical propagation maps.

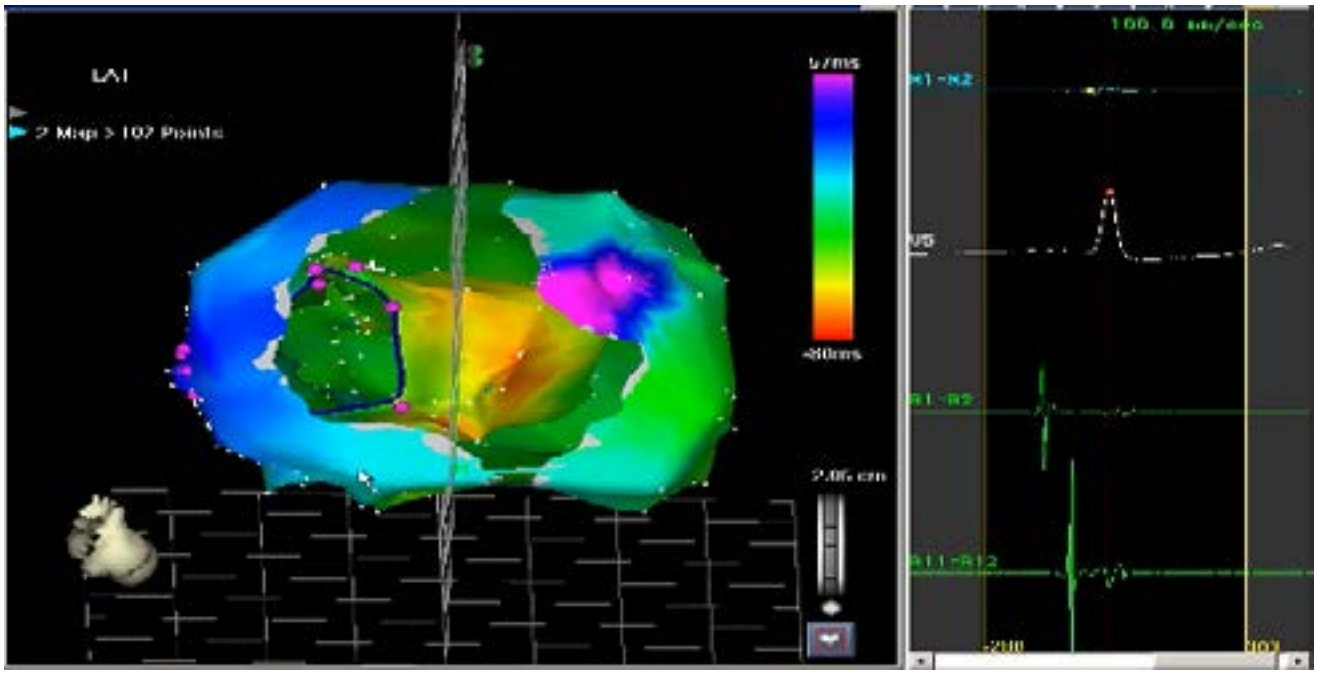

Video 2. Ventricular torsion-detorsion. Video seen perpendicular to the apex in a human heart. The torsion movement is observed and at the end of the systole, strictly at the tip, an umbilication of the apex that corresponds to the protodiastolic suction phase is observed.



REFERENCES

1. Armour JA, Randall WC. Structural basis for cardiac function. Am J Physiol 1970;218:1517-23.

2. Arvidsson M, Töger J, Carlsson M, Steding-Ehrenborg K, Pedrizzetti G, Heiberg E, Arheden H.Left and right ventricular hemodynamic forces in healthy volunteers and elite athletes assessed with 4D flow magnetic resonance imaging. Am J Physiol Heart Circ Physiol 2017;312:H314-H328. doi:10.1152/ajpheart.00583.2016.

3. Ballester-Rodés M, A, Flotats A,Torrent-Guasp F, Carrió-Gasset I, Ballester-Alomar M, Carreras F, Ferreira A, Narula J. The sequence of regional ventricular motion. Eur J Cardiothorac Surg 2006;29:139-44.

4. Ballester M, Ferreira A, Carreras F. The myocardial band. Heart Fail Clin. 2008;4:261-272. doi: 10.1016/j.hfc.2008.02.011.

5. Bateson G. Mind and nature: a necessary unity. Dutton, New York, 1979.

6. Beaumont A, Grace F, Richards J, Hough J, Oxborough D, Sculthorpe N. Left Ventricular Speckle Tracking Derived Cardiac Strain and Cardiac Twist Mechanics in Athletes: A Systematic Review and Meta-Analysis of Controlled Studies. Sports Med 2017; 47:1145-70.

7. Bertalanffy von L. Teoría general de los sistemas. Alianza, Buenos Aires, 1978.

8. Best A, Egerbacher M, Swaine S, Pérez W, Alibhai A, Rutland P, Kubale V,. El-Gendy S, Alsafy M, Baiker K, Sturrock C, Catrin R. Anatomy, histology, development and functions of Ossa cordis: A review. Anat Histol Embryol 2022; 00:1–13. DOI: 10.1111/ahe.12861

9. Buckberg GD, Coghlan HC, Torrent Guasp F. The structure and function of the helical heart and its buttress wrapping. V. Anatomic and physiologic considerations in the healthy and failing heart. Sem Thorac Cardiovasc Surg 2001;13:358-85.

10. Carreras F, Ballester M, Pujadas S, Leta R, Pons-Lladó G. Morphological and functional evidences of the helical heart from non-invasive cardiac imaging. Eur J Cardiothoracic Surg 2006;29(Suppl 1):S50-5.

11. Carreras F, Garcia-Barnes J, Gil D, Pujadas S, Li CH, Suarez-Arias R, Leta R, Alomar X, Ballester M, Pons Llado G. Left ventricular torsion and longitudinal shortening: two fundamental components of myocardial mechanics assessed by tagged cine-MRI in normal subjects. Int J Cardiovasc Imaging 2012; 28:273-84.

12. Cosín-Aguilar J, Hernándiz Martínez A, Tuzón Segarra MT, Agüero Ramón-Llin J, Torrent Guasp F. Estudio experimental de la llamada fase de relajación isovolumétrica del ventrículo izquierdo. Rev Esp Cardiol 2009;62:392-9.

13. Elencwajg B, López-Cabanillas N, Cardinali EL, Barisani JL, Trainini J, Fischer A, Worley S. The Jurdham procedure endocardial left ventricular lead insertion via a femoral transseptal sheath for cardiac resynchronization therapy pectoral device implantation. Heart Rhythm 2012;9:1798-1804.

14. Franklin KJ. The Work of Richard Lower (1631-1691). Proc R Soc Med 1931;25:113-118.

15. Gourdie RG, Mima T, Thompson RP, Mikawa T. Terminal diversification of the myocyte lineage generates Purkinje fibers of the cardiac conduction system. Development 1995;121:1423–31.

16. Hayabuchi Y, Sakata M, Kagami S. Assessment of the helical ventricular myocardial band using standard echocardiography. Echocardiography 2015;32:310-8.

17. Helle-Valle T, Crosby J, Edvardsen T, Lvseggen E, Amundsen BH, Smith HJ, Rosen BD, Lima JA, Torp H, Ihlen H, Smiseth OA. New noninvasive method for assessment of left ventricular rotation: speckle tracking echocardiography. Circulation 2005;112:3149-56.

18. Henson RE, Song SK, Pastorek JS, Ackerman JH, Lorenz CH. Left ventricular torsion is equal mice and humans. Am J Physiol Heart Circu Physiol 2000; 278:H1117-H1123.

19. Herreros J, Trainini JC, Bernal JM, Gutierrez F, Cabo J, Chachques JC. Tratamiento de la insuficiencia cardíaca: nuevas estrategias terapéuticas. Cir Cardiovasc 2011;18:113-20.

20. Hucker WJ, McCain ML, Laughner JI, Iaizzo PA, Efimov IR. Connexin 43 expression delineates two discrete pathways in the human atrioventricular junction. Anat Rec (Hoboken) 2008;291:204–15. [PubMed: 18085635].

21. Jacob F. "El juego de lo posible". Grijalbo Ed., Barcelona, 1982.

22. Jondeau G, Dorent R, Bors V, Dib JC, Dubourg O, Benzidia R, Gandjbakhch Y, Bourdarias JP. Dynamic Cardiomyoplasty: Effect of discontinuing latissimus dorsi muscle stimulation on left ventricular systolic and diastolic performance and exercise capacity. J Am Coll Cardiol 1995;26:129-34.

23. Karamchandani JR, Nielsen TO, van de Rijn M, West RB. Sox10 and S100 in the diagnosis of soft-tissue neoplasms. Appl Immunohistochem. Mol Morphol 2012;20:445-50.

24. Maksuti E, Carlsson M, Arheden H, Kovács S, Broomé M, Ugander M. Hydraulic forces contribute to left ventricular diastolic filling. Scientif reports 2017;7:43505. doi:10.1038/srep43505.

25. Moittié S, Baiker K, Strong V, Cousins E, White K, Liptovszky M, Redrobe S, Alibhai A, Sturrock C, Rutland C. Discovery of os cordis in the cardiac skeleton of chimpanzees (Pan troglodytes). Sci Rep 2020;10:9417. https://doi.org/10.1038/s41598-020-66345-7

26. Mora Llabata V, Roldán Torresa I, Saurí Ortiza A, Fernández Galera R, Monteagudo Viana M, Romero Dorta E, Cosín Aguilar JA, Trainini J, Lowenstein J. Correspondence of myocardial strain with Torrent-Guasp's theory. Contributions of new echocardiographic parameters. Rev Arg de Cardiol 2016;84:541-9.

27. Mora V, Roldán I. Romero E, Saurí A, Romero D, Perez-Gozabo J, Ugalde N, Bertolín J, Rodríguez-Israel M, Perez-Olivares Delgado C, Lowenstein J. Myocardial contraction during the diastolic isovolumetric period: analysis of longitudinal strain by means of speckle tracking echocardiography. J Cardiovasc Dev Dis 2018;5:41. doi:10.3390/jcdd5030041

28. Mora V, Roldán I, Bertolín J, Faga V, Pérez-Gil M, Saad A, Serrats R, Callizo R, Arbucci R, Lowenstein J. Influence of ventricular wringing in the preservation of left ventricle ejection fraction in cardiac amyloidosis. J Am Soc Echocardiog 2021;34:767-74.

29. Nakatani S. Left ventricular rotation and twist: why should we learn? J Cardiovasc Ultrasound 2011;19:1-6.

30. Ortega D, Logarzo E, Barja L, Paolucci A, Mangani N, Mazzetti E, Bonomini MP. Novel implant technique for septal pacing. A noninvasive approach to nonselective his bundle pacing. Journal of Electrocardiology 2020;63: 35–40.

31. Pedrizzetti G, Arvidsson PM, Töger J, Borgquist R, Domenichini F, Arheden H, Heiberg E. On estimating intraventricular hemodymamic forces from endocardial dynamics: A comparative study with 4D flow MRI. J Biomech 2017; 60:203-10. http://dx.doi.org/10.1016/j.biomech.2017.06.046

32. Poveda F, Gil D, Martí E, Andaluz A, Ballester M, Carreras F. Estudio tractográfico de la anatomía helicoidal del miocardio ventricular mediante resonancia magnética por tensor de difusión. Rev Esp Cardiol 2013;66:78290.

33. Rodríguez-Padilla J, Petras A, Magat J, Bayer J, Bihan-Poudec Y, El Hamrani D, Ramlugun G, Neic A, Augustin CM, Vaillant F, Constantin M, Benoist D, Pourtau L, Dubes V, Rogier J, Labrousse L, Bernus O, Quesson B, Haïssaguerre M, Gsell M, Plank G, Ozenne V, Vigmond E. Impact of intraventricular septal fiber orientation on cardiac electromechanical function. Am J Physiol Heart Circ Physiol 2022;322:H936-H952.

34. Rushmer RF, Crystal DK, Wagner C. The functional anatomy of ventricular contraction. Circ Res. 1953; 1:162-70.

35. Rushmer RF. Initial ventricular impulse. A potential key to cardiac evaluation. Circulation 1964; 29:268-83.

36. Rushmer RF. Structure and Function of the Cardiovascular System. Philadelphia, Saunders Company, 1972.

37. Sánchez-Quintana D, Yen Ho S. Anatomía de los nodos cardíacos y del sistema de conducción específico auriculoventricular [Anatomy of cardiac nodes and atrioventricular specialized conduction system]. Rev Esp Cardiol 2003;56:1085-92. doi: 10.1016/s0300-8932(03)77019-5. PMID: 14622540

38. Shehata ML, Cheng S, Osman NF, Bluemke DA, Lima JA. Myocardial tissue tagging with cardiovascular magnetic resonance. J Cardiovasc Magn Reson 2009;11:55.

39. Sosa Olavarría A, Martí Peña A, Martínez A, Zambrana Camacho J, Ulloa Virgen J, Zurita Peralta J, Alcedo A, Pérez-Canto G, Vázquez E, Yassef Antúnez- Montes O, Moncayo R, Belgoff S. Fulcro cardíaco de Trainini en el corazón fetal. Rev Peru Ginecol Obstet. 2023;69(4) 1-8. DOI: https://doi.org/10.31403/rpgo.v69i2579

40. Torrent Guasp F. Nuevos conceptos sobre la estructura miocárdica ventricular. En Torrent Guasp F, editor. Estructura y mecánica del corazón. Barcelona: Grass Ed, 1987, pp 35-97.

41. Torrent Guasp F. Estructura y función del corazón. Rev Esp Cardiol 1998;51:91-102.

42. Torrent Guasp F, Buckberg G, Carmine C, Cox J, Coghlan H, Gharib M. The structure and function of the helical heart and its buttress wrapping. I. The normal macroscopic structure of the heart. Seminars in Thorac and Cardiovasc Surg 2001;13:301-19.

43. Trainini JC, Elencwajg B, López Cabanillas N, Herreros J, Lago N, Lowenstein J. Electrical Propagation in the Mechanisms of Torsion and Suction in a Three-phase. Rev Argent Cardiol 2015;83:416-28.

44. Trainini JC, Elencwajg B, López Cabanillas N, Herreros J, Lago N, Lowenstein J, Trainini A. Stimuli propagation, muscle torsión and cardiac suction effect through electrophysiological research. In "Basis of the New Cardiac Mechanics. The Suction Pump", Trainini JC and col. Lumen, Bs. As, 2015, pp 39-61.

45. Trainini JC, Elencwajg B, López-Cabanillas N, Herreros J, Lago N. Lowenstein JA. Propagación eléctrica en los mecanismos de torsión y succión en un corazón de tres tiempos. Rev Argent Cardiol 2015;83:420-8.

46. Trainini JC, Herreros J, Elencwajg B, López-Cabanillas N, Lago N, Lowenstein JA, Trainini A. "Fundamentos de la Nueva Mecánica Cardíaca. La Bomba de Succión". Ed UCAM; Murcia, España, 2015.

47. Trainini JC, Elencwajg B, López-Cabanillas N, Herreros J, Lago N. Electrophysiological Basis of Torsión and Suction in the Continuous Cardiac Band Model. Anat Physiol 2015;5:S4-001. http://dx.doi.org/10.4172/21610940. S4-001

48. Trainini JC, Elencwajg B, López-Cabanillas N, Herreros J, Lago N. Ventricular torsion and cardiac suction effect. The electrophysiological analysis of the cardiac muscle". J Clin Exp Cardiolog 2015, 6:10.

49. Trainini JC, Elencwajg B, López-Cabanillas N, Herreros J, Lago N, Lowenstein J, Trainini A. Activación electrofisiológica y tiempos de propagación en la banda muscular ventricular. Primer estudio mundial en seres humanos. Rev. Arg. Cardiol 2016;84:475-8.

50. Trainini JC, Herreros J, Elencwajg B, Trainini A, Lago N, López Cabanillas N, Lowenstein JM. Disección del miocardio. Rev Argent Cardiol 2017;85:44-50.

51. Trainini JC, Herreros J, Cossio P. Epistolario entre Pedro Cossio (1900-1986), Luis Becú (1927-1997) y Francisco Torrent Guasp (1931-2005). Rev Argent Cardiol 2017;85:264-7.

52. Trainini JC, Elencwajg B, López-Cabanillas N, Herreros J, Lowenstein J Bustamante-Munguira J, García Fernández MA, Trainini A. Ventricular torsion and cardiac suction effect: The electrophysiological analysis of the cardiac band muscle. Interventional Cardiol 2017; 9: 45-51.

53. Trainini J, Elencwajg B, Herreros J. Activation Times in the Ventricular Myocardial Band. J Cardiol & Cardiovasc Ther 2017; 4: 555638. DOI:10.19080/JOCCT.2017.04.555638

54. Trainini JC, Elencwajg B, Herreros J. New Physiological Concept of the Heart. Ann Transplant Res. 2017; 1: 1001.

55. Trainini J, Herreros J, Trainini A, García-Jimenez E, Cabo J, Valle-Cabezas J. Left ventricular suction in right ventricular dysfunction (abstract). XXIII Congreso SEIQ, Madrid, España, 2017. BJS, vol 105, s2.

56. Trainini JC, Herreros J, Beraudo M, Trainini A, Cabo J, Bustamante J, Martínez Almagro Andrés, Wernicke M. Fulcro Cardíaco. Inserción de la banda miocárdica (abstract). XXIV Congreso SEIQ, Bilbao, España, 2018.

57. Trainini JC, Elencwajg B , López Cabanillas N, Herreros J, Lago N, Lowenstein J, Bustamante Munguira J,Trainini A. Stimulus Propagation and Left Ventricular Torsion. Advancements in Cardiovascular Research. Volume 1 - Issue 2, 2018. doi: 10.32474/ACR.2018.01.000109

58. Trainini JC, Herreros J. "El explorador del corazón. Biografía de Francisco Torrent Guasp". Ed Biblos, Buenos Aires, 2019.

59. Trainini JC, Trainini A, Valle Cabezas J, Cabo J. Left Ventricular Suction in Right Ventricular Dysfunction. EC Cardiology 2019;6: 572-7.

60. Trainini JC, Lowenstein J, Beraudo M, Trainini A, Mora Llabata V, Wernicke M. "Myocardial Torsion". Ed Biblos, Buenos Aires; Argentina, 2019.

61. Trainini JC, Mora V, Lowenstein J, Beraudo M, Wernicke M, Trainini A. La teoria de la banda miocárdica Nuevos descubrimientos que apoyan el complejo mecanismo de torsión miocárdica. Revista de Ecocardiografía Práctica y Otras Técnicas de Imagen Cardíaca 2020;3:14-18. doi: 10.37615/retic.v3n1a4

62. Trainini JC, Wernicke M, Beraudo M, Lowenstein J, Trainini A, Bastarrica ME. Hyaluronic acid in the heart. J Trends Biomedical Research 2021; 4: 1. doi: 510.15761/JTBR.1000122.

63. Trainini J, Beraudo M , Wernicke M, Trainini A, Lowenstein J, Bastarrica ME. Myocardial Torsion and Cardiac Fulcrum . J Morphol Anat 2021;S1:001.

64. Trainini J, Beraudo M, Wernicke M, Trainini A, Lowenstein J, Bastarrica M E, Lowenstein. Cardiac Fulcrum. Cardiovasc Surg Int 2021;2:CSI-02-1011.

65. Trainini JC, Lowenstein J, Beraudo M, Wernicke M, Trainini A, Llabata MV, Carreras CF. Myocardial torsion and cardiac fulcrum (Torsion myocardique et pivot cardiaque). Morphologie, 2021;105 :15-23. https://doi.org/10.1016/j.morpho.2020.06.010

66. Trainini JC, Beraudo M, Wernicke M, Trainini A. Haber Lowenstein D, Bastarrica M, Martino DC, Lowenstein myocardial http://dx.doi.org/10.7775/rac.v89.i3.20407 support. Rev Argent Cardiol 2021; 89: 217-23.

67. Trainini JC, Beraudo M, Wernicke M, Carreras-Costa F, Trainini A, M, Mora Llabata V, Cabezas Valle J, Lowenstein Haber D, Bastarrica ME, Lowenstein JA. Evidence that the myocardium is a continuous helical muscle with one insertion. REC: CardioClinics 2022;57:194-202. https://doi.org/10.1016/j.rccl.2022.01.006

68. Trainini J, Lowenstein J, Beraudo M, Wernicke M, Mora Llabata V, Lowenstein-Haber D, Trainini A, Carreras-Costa F, Valle Cabezas J, Bastarrica ME. Cardiac Helical Function. Fulcrum and Torsion. Japan Journal of Clinical & Medical Research. 2022, SRC/JJCMR-139. Doi: doi.org/10.47363/JJCMR/2022(2)136

69. Trainini J, Beraudo M, Wernicke M, Carreras Costa F, Trainini A, Mora Llabata V,Valle Cabezas J, Lowenstein Haber D, Bastarrica ME, Lowenstein J. The hyaluronic acid in intramyocardial sliding. REC: CardioClinics 2022. https://doi.org710.1016/j.rccl.2022.07.008

70. Trainini J, Lowenstein J, Beraudo M, Mora Llabata V, Carreras-Costa F, Valle Cabezas J, Wernicke M, Elencwajg B, Trainini A, Lowenstein Haber D, Bastarrica ME. "El corazón helicoidal. Fulcro y Torsion". UNDAV Ed, Buenos Aires; Argentina, 2022.

71. Trainini J, Wernicke M , Beraudo M , Cohen M, Traininil A, Bastarrica ME, Elencwajg B, Lowenstein J, Ventura A. Cardiac Fulcrum, its Relationship with the

Atrioventricular Node. Rev Argent Cardiol 2023;91:429-435. http://dx.doi.org/10.7775/rac.v91.i6.20722

72. Trainini J, Beraudo M, Wernicke M, Trainini A, Haber Lowenstein D, Bastarrica ME, Martino DC, Lowenstein J. Myocardial support. Cardiac and Cardiovascular Research (2023) Volume 4 Issue 2, 8 pages doi: 10.54517/ccr.v4i2.1919

73. Trainini J, Lowenstein J, Beraudo M, Valle Cabezas J, Wernicke M, Trainini A, Bastarrica ME, Carreras Costa F, Elencwajg B, Mora Llabata V, Lowenstein Haber D, Cohen M. "Anatomy and organization of the helical heart". UNDAV Ed., Buenos Aires, 2023.

74. Trainini J, Wernicke M, Beraudo M ,Trainini A. The Fulcrum of the Human Heart (Cardiac fulcrum). J Cardiol Cardiovasc Med. 2024; 9: 001-005. DOI: 10.29328/journal.jccm.1001171

75. Trainini J, Wernicke M, Beraudo M, Trainini A. The fulcrum of the human heart (Cardiac fulcrum). World Journal of Biology Pharmacy and Health Sciences, 2024, 17(01), 049–056 Article DOI: https://doi.org/10.30574/wjbphs.2024.17.1.0531

76. Trainini Jorge, Beraudo Mario, Wernicke Mario, Efraín Herrero, Trainini Alejandro. The Cardiac Fulcrum Comments. AJ Biomed Sci & Res. 2024 23(4) AJBSR. MS.ID.003092, DOI: 10.34297/AJBSR.2024.23.003092

77. Trainini Jorge, Beraudo Mario, Wernicke Mario, Trainini Alejandro, Lowenstein Jorge, Valle Cabezas J, Elencwajg B, Fariña O, Cohen Marta, Bastarrica ME, Hernández López M, Lowenstein-Haber D, Carreras Costa F, Herrero E, Mora Llabata V. Fundamental Conclusions on Research into the Anatomy and Organization of the Helical Heart. Am J Biomed Sci & Res. 2024 23(5) AJBSR. MS.ID.003125, DOI: 10.34297/ AJBSR.2024.23.003125

78. Trainini J, Beraudo M, Wernicke M, Trainini A, Cohen M, Elencwajg B, Fariña O, Valle Cabezas J, Bastarrica ME, Lowenstein Haber D, Carreras Costa F, Mora Llabata V, Lowenstein J. Relationship of the cardiac fulcrum and the AV node with ventricular torsion. Am J Biomed Sci & Res. 2024 24(2) AJBSR.MS.ID.003180, DOI: 10.34297/AJBSR.2024.24.003180

79. Trainini J, Beraudo M, Wernicke M, Herrero E and Trainini A. (2024), The Cardiac Fulcrum Comments. International Journal of Cardiovascular Medicine, 3(5); DOI:10.31579/2834-796X/076

80. Trainini J. "En busca del fulcro cardíaco. El hallazgo del soporte del corazón". Ed. Biblos, Buenos Aires, Argentina, 2024.

81. Trainini J, Beraudo M, Wernicke M, Herrero E, Trainini A, Fariña O, Valle Cabezas J, Lowenstein J, López Santoro R. Propiedades del Fulcro Cardíaco. Rev Argent Cardiol 2025;93:43-49. https://doi.org/10.7775/rac.es.v93.i1.20862

82. Trainini J, Beraudo M, Wernicke M, Freire G, Trainini A, López Hernández MP, Bastarrica ME, Fariña O, Valle Cabezas J, Lowenstein J. Helical Heart Suction in Heart Failure with Preserved Ejection Fraction. Am J Biomed Sci & Res. 2025 25(6) AJBSR.MS.ID.003388, DOI: 10.34297/AJBSR.2025.25.003388

83. Trainini J, Trainini A. "La Circulación de la Sangre". Ed. Biblos, Buenos Aires, 2025.

84. Trainini Jorge, Beraudo Mario, Trainini Alejandro, Wernicke Mario, Valle Cabezas Jesús, Lowenstein Jorge, Bastarrica María Elena, Herrero Efraín, Fariña Oscar, Carreras Francesc. Why is the heart helical? The Journal of Anatomy . The Journal of Anatomy, 2025, Volume 10, Issue 1, Pages: 1-17. DOI: 10.52338/tjoa.2025.4670

85. Trainini J, Elencwajg B, Lowenstein J, Beraudo M, Trainini A, Wernicke M, Mora Llabata V, Valle Cabezas J, Bastarrica ME, Ventura A, Herrero E, Carreras F. The cardiac suction pump. Am J Biomed Sci & Res. 2025 26(6) AJBSR. MS.ID.003511, DOI: 10.34297/AJBSR.2025.26.003511

86. Trainini J, Lowenstein J, Elencwajg B, Beraudo M, Trainini A, Wernicke M, Mora Llabata V, Carreras F, Valle Cabezas J, Herrero E, Fariña O. Fulcrum and Function of the Helical Heart: State of Research. Am J Biomed Sci & Res. 2025 27(2):417-434. AJBSR.MS.ID.00350, DOI: 10.34297/AJBSR.2025.27.003550

87. Trainini J, Beraudo M, Trainini A, Wernicke M, Lowenstein J, Herrero E, Hernández López MP. Protodiastolic Phase of Myocardilal Contraction. Am J Biomed Sci & Res. 2025 27(4) AJBSR.MS.ID.003590, DOI: 10.34297/AJBSR.2025.27.003590 Pages:746-754

88. Valle J, Herreros J, Trainini J, García-Jimenez E, Talents M, González V Three-dimensional definition of Torrent Guasp´s ventricular muscle band and its correlation with electric activation of the left ventricle (abstract). XXIII Congreso SEIQ, Madrid, España, 2017. BJS, vol 105, s2.

89. Whitehead AN. "Nature and life". Cambridge University Press, Londres, 1934.